

Supporting Information for the article:

New synthetic conjugates of ursodeoxycholic acid inhibit cystogenesis in experimental models of polycystic liver disease

Francisco J. Caballero-Camino,^{1,2} Ivan Rivilla,¹ Elisa Herraez,^{3,4} Oscar Briz,^{3,4} Alvaro Santos-Laso,² Laura Izquierdo-Sanchez,^{2,4} Pui Y. Lee-Law,² Pedro M. Rodrigues,² Munoz-Garrido P,² Sujeong Jin,⁵ Estanislao Peixoto,⁵ Seth Richard,⁵ Sergio A. Gradilone,⁵ Maria J. Perugorria,^{2,4} Manel Esteller,^{6,7,8,9} Luis Bujanda,^{2,4} Jose J.G. Marin,^{3,4} Jesus M. Banales,^{2,4,10,§} Fernando P. Cossio.^{1,§}

¹Department of Organic Chemistry I, Center of Innovation in Advanced Chemistry (ORFEO-CINQA), University of the Basque Country/Euskal Herriko Unibertsitatea (UPV/EHU), Donostia International Physics Center (DIPC), Donostia-San Sebastian, Spain; ²Department of Liver and Gastrointestinal Diseases, Biodonostia Health Research Institute – Donostia University Hospital –, UPV/EHU, Donostia-San Sebastian, Spain; ³Experimental Hepatology and Drug Targeting (HEVEFARM), Biomedical Research Institute of Salamanca (IBSAL), University of Salamanca, Salamanca, Spain; ⁴National Institute for the Study of Liver and Gastrointestinal Diseases (CIBERehd), Carlos III National Institute of Health, Madrid, Spain; ⁵The Hormel Institute, University of Minnesota, Austin; Masonic Cancer Center, University of Minnesota, Minneapolis, Minnesota; ⁶Josep Carreras Leukaemia Research Institute (IJC), Badalona, Barcelona, Catalonia, Spain; ⁷Centro de Investigacion Biomedica en Red Cancer (CIBERONC), 28029 Madrid, Spain; ⁸Institucio Catalana de Recerca i Estudis Avançats (ICREA), Barcelona, Catalonia, Spain; ⁹Physiological Sciences Department, School of Medicine and Health Sciences, University of Barcelona (UB), Barcelona, Catalonia, Spain. ¹⁰IKERBASQUE, Basque Foundation for Science, Bilbao, Spain.

§Both authors share co-seniorship.

Materials and Methods

HDAC activity assays

The HDAC activity assays were performed using acetylated peptide substrates labeled with 7-amino-4-methylcoumarin (AMC) at Reaction Biology Corporation (Pennsylvania, USA). All the enzymes and substrates used are summarized in Supplementary table S9. The assays were performed in a solution buffer (50 mM Tris-HCl, pH 8.0; 137 mM NaCl; 2.7 mM KCl; 1 mM MgCl₂; supplemented with 1 mg/ml of BSA for dilution; BioMol Cat. # KI-143).

Briefly, 50 μ L of peptide substrate and an optimal concentration of the corresponding enzyme (see supplementary table S9) were incubated in the assay buffer at a final DMSO concentration of 1% in the presence of increased concentrations of inhibitors at 30°C for 2 h. The reactions were carried out in 96-well fluorimeter microplates in a final reaction volume of 50 μ L. After the deacetylation reaction, Fluor-de-Lys-Developer (BioMol Cat. # KI-105) was added to each well to digest the deacetylated substrate according to manufacturer instructions, thereby producing the fluorescent signal. The reaction was carried out for 45 min at 30°C with 5% CO₂. Then, the fluorescence signal was measured using an excitation wavelength of 360 nm and an emission wavelength at 460 nm in a fluorimeter (GeminiXS, Molecular Devices, Sunnyvale, CA). All the experiments were performed in triplicate. The IC₅₀ values were calculated by fitting the experimental data with Graphpad Prism 6 software using the equation log(inhibitor) vs. normalized response with variable slope. DMSO was used as a negative control; Trichostatin A (Biomol Cat. # GR-309) was used as a positive control inhibitor.

Cells and culture conditions

Primary cultures of normal and cystic human cholangiocytes, previously isolated and characterized by our group,(1) were seeded at the required cell density for each experimental condition on collagen type I coated plates at 0.05 mg/mL (Corning, NY, USA) in complete media (DMEM/F12 1% (Gibco-Invitrogen), FBS 5% (Gibco-Invitrogen), MEM-non-essential amino acids 1% (Lonza), Lipid

mixture 1% (Sigma-Aldrich), MEM vitamin solution 1% (Gibco-Invitrogen), Penicillin/Streptomycin 1% (Gibco-Invitrogen), Soyben Trypsin Inhibitor 0.05 mg/mL (Gibco-Invitrogen), Insulin Transferrin Selenium 1% (Gibco-Invitrogen), Bovine Pituitary Extract 30 µg/mL (Gibco-Invitrogen), Dexamethasone 393 ng/mL (Sigma-Aldrich), T3 (3, 3' 5-triiodo-L-thyronine) 3.4 µg/mL (Sigma-Aldrich), Epidermal Growth Factor (EGF) 25 ng/mL (Gibco-Invitrogen), Forskolin 4.11 mg/mL (Ascent-Scientific). For transport assays, Alexander or PCL/PRF/5 (human HCC), HEK293T (human embryonic kidney) HepG2 (human hepatoblastoma) and CHO-K1 (Chinese hamster ovary) cells were obtained from the American Type Culture Collection (LGC Standards, Barcelona, Spain) and TFK1 (human cholangiocarcinoma) were obtained from the German Collection of Microorganisms and Cell Cultures (DSMZ, Braunschweig, Germany). All cell lines were cultured as recommended by the suppliers.

3D culturing of cystic cholangiocytes

Bile cysts directly isolated from PCK rats were 3D-cultured within a collagen type I matrix of 1.8 mg/ml derived from rat tail (Corning, NY, USA) and incubated under appropriate culture conditions, as we previously reported.(2) The cyst growth was monitored in HDAC6i-UDCA #1 treated and control groups for 48 h by the acquisition of images every 24 h. Circumferential areas were measured with ImageJ software (NIH, Bethesda, MD).

Experimental overexpression of human transporters in cells and transport assays

The open reading frame ORF of: apical sodium-dependent bile salt transporter (ASBT, *SLC10A2*); Na⁺-taurocholate cotransporting polypeptide (NTCP, *SLC10A1* gene); organic anionic transporting polypeptides OATP1A2 (*SLC01A2*), OATP1B1 (*SLC01B1*), OATP1B3 (*SLC01B3*) and OATP2B1 (*SLC02B1*); and organic cation transporters OCT1 (*SLC22A1*) and (OCT3, *SLC22A3*) were amplified from total RNA isolated from liver by RT followed by high-fidelity PCR using AccuPrime Pfx DNA polymerase (Life Technologies) and specific primers (Supplementary Table S10). cDNAs were cloned into a pWPI

lentiviral vector to obtain transfer vectors encoding both transporters and eGFP as a reporter gene. Using pWPI plasmid, “empty viruses” were generated and used as a negative control. Lentiviral vectors were produced in HEK293T cells and used to transduced target cells (CHO or HepG2 cells) as described.(3) Monoclonal cells stably expressing each transporter were selected by double subcloning using the limiting dilution method. TFK-1 cells overexpressing the apical sodium-dependent bile acid transporter (ASBT, *SLC10A2*) and HepG2 cells overexpressing the organic cation transporters 1 (OCT1, *SLC22A1*) were obtained in the same manner.(3, 4)

For transport competition assays, cells were seeded onto 24-well plates at subconfluence. After 24 h, cells were incubated with “uptake” medium (96 mM NaCl, 5.3 mM KCl, 1.1 mM KH₂PO₄, 0.8 mM MgSO₄, 1.8 mM CaCl₂, 11 mM glucose, and 50 mM HEPES/Tris, pH 7.40) containing 100 μM UDCA-HDAC6i #1 for 1 h at 37°C. Rifamycin SV (OATP1A2), mifepristone (OATP2B1), quinine (OCT1 and OCT3), and taurocholic acid (ASBT, NTCP, OATP1B1 and OATP1B3) were used as inhibitors or competitors. For time course experiments, cells were seeded onto 6-well plates at subconfluence. After 24 h, cells were incubated with “uptake” medium containing 100 μM UDCA-HDAC6i #1 for the corresponding time at 37°C or 4°C. Transport fluxes were stopped by rinsing the cultures 4 times with 1 mL of ice-cold medium, and then, cells were lysed using pure water. UDCA-HDAC6i #1 concentration was determined by high performance liquid chromatography-tandem mass spectrometry (HPLC-MS/MS) (6410 Triple Quad LC/MS, Agilent Technologies, Santa Clara, CA). Chromatographic separation was carried out in isocratic mode in a Zorbax Eclipse XDB-C18 column (30 mm x 2.1 mm, 3.5 μm) and kept at 35°C. Flow rate was 300 μL/min and mobile phase was 64:36 methanol/water, both containing 5 mM ammonium acetate and 0.1% formic acid. Electrospray ionization (ESI) in negative mode was used, with the following conditions: gas temperature 350°C, gas flow 8 L/min, nebulizer 30 psi, capillary voltage 2500 V. MS/MS acquisition was performed in multiple reaction monitoring (MRM) mode using the specific *m/z* transitions 539.4-539.4 *m/z* for UDCA-HDAC6i #1, and 498.4-80.2 *m/z* for TUDCA. The results were corrected by protein content.(5)

Quantitative polymerase chain reaction (qPCR)

Total RNA was extracted from human cholangiocytes cell cultures with TriReagent (Sigma, Misuri, USA) following manufacturer's instructions. Messenger RNA was transcribed to cDNA via reverse transcription with iScript™ cDNA Synthesis Kit (Bio-Rad) and expression levels of particular genes were measured by qPCR using iQ™ SYBR® Green Supermix (Bio-Rad). *RPL22* gene was used as a normalizing control. All the primer sequences are summarized in Supplementary Table S11.

Immunoblotting

Protein extracts were obtained from cell lysates or frozen tissue homogenized with RIPA. Protein expression, acetylation and phosphorylation levels were measured by immunoblotting using either 30 µg of cell culture protein extract or 40 µg of PCK rat liver or kidney tissue. Samples were separated by electrophoresis in 10% SDS-PAGE acrylamide gels and electro-transferred onto nitrocellulose membranes (BioRad, Hercules, CA). After blocking with either 2.5% BSA or 2.5% skimmed milk powder, membranes were incubated overnight with primary antibodies (Supplementary Table S12). Membranes were then washed with TBS (1% Tween 20) and incubated for 1 h at room temperature with Horseradish peroxidase-conjugated secondary antibodies (Cell Signaling, 1:5,000). Afterwards, membranes were washed with TBS to remove unbound secondary antibody, incubated with Novex® ECL HRP Chemiluminescent Substrate Reagent Kit (Invitrogen) and visualized in an iBright Imaging System (Thermo Fisher Scientific). To determine relative expression or post-translational modification levels, obtained images were analyzed with ImageJ software (NIH, Bethesda, MD, <https://imagej.nih.gov/ij/>).

Primary cilia analysis

For *in vitro* analysis of ciliary length, cholangiocyte cultures in glass cover slips were washed and fixed with ice cold (-20°C) methanol for 10 min. Cells were blocked at room temperature for 1 h, as previously described,(6) and incubated overnight at 4°C with acetylated α -tubulin antibody (1:1000; Sigma, USA).

Afterwards, cells were incubated for 2 h at room temperature with Alexa Fluor 488 secondary antibody (Life Technologies, USA). Next, coverslips were mounted on slides using Prolong Gold Antifade with Dapi (Invitrogen; Carlsbad, CA, USA). Images were obtained at 60X with a laser scanning confocal microscopy (NIKON C1si Confocal Spectral Imaging System, NIKON Instruments Co., Melville, NY, USA), and the fields were zoomed 4X. Scale bars were added with EZ-C1 3.90 Freeviewer. Finally, images were analyzed for individual cilia length using ImageJ software.

For immunofluorescence analysis of primary cilia in liver, tissue slides were incubated overnight at 4°C with anti- α -tubulin (1:200, Sigma, USA) antibodies. Afterwards, slides were incubated with Alexa Fluor 594 conjugated goat secondary antibodies. The nuclei were visualized with DAPI and the immunostainings were viewed and documented using a Ziess Axio Observer with Apotome. Cysts were randomly selected from untreated (n=6) and treated rats (n=9) and ciliary frequency and length were measured.

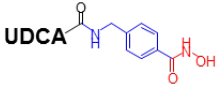
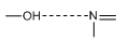
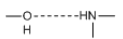
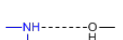
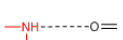
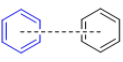
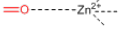
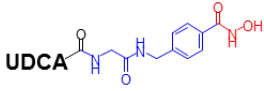
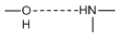
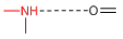
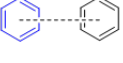
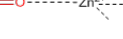
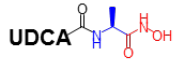
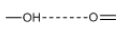
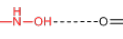
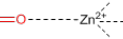
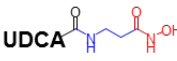
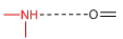
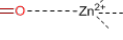
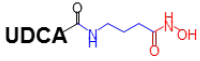
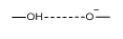
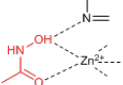
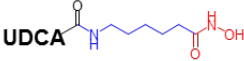
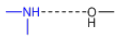
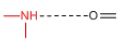
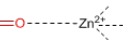
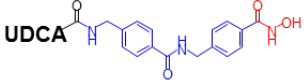
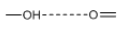

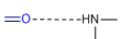
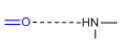
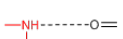
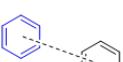

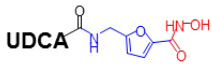
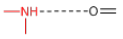
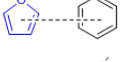

Immunohistochemistry

Hydrated tissue slides were incubated with a solution containing 3% hydrogen peroxide in methanol for 15 minutes. Next, antigen retrieval and the Avidin/Biotin blocking kit (Vector laboratories, USA) were performed. The corresponding primary antibodies anti-CK19 (1:50; ARP 03-61029, American Research Products, USA), OCT1 (1:50; LS-C31870, LSBio, USA), or OCT3 (1:50; ab183071, Abcam, United Kingdom) were added and incubated overnight at 4°C. After washing with PBS 1X, the corresponding biotinylated secondary antibody was added and incubated at room temperature for 2 h. For staining, Vectastain ABC Reagent (Vector laboratories, USA) followed by 3,3-diaminobenzidine (DAB) peroxidase substrate Kit (Vector laboratories, USA) were used. Finally, Harris Haematoxylin (Merck Millipore) was used for counterstaining, and slides were dehydrated and mounted for microscopic analysis.

Cell proliferation

Cystic cholangiocytes in culture were stained with CellTrace™ CFSE Cell Proliferation Kit (Invitrogen) according to manufacturer's protocol and seeded them at a density of 3×10^4 cells/well in complete media under collagen type I coated 12-well plates. After overnight incubation at 37°C and 5% CO₂, cells were incubated with 10 μM or 100 μM UDCA, 2 μM or 10 μM UDCA-HDAC6i #1, 10 μM (8), or 10 μM UDCA together with 10 μM (8) in complete media (0.1% DMSO) and were maintained for 48 h at appropriate incubation conditions. Finally, cells were trypsinized and fluorescence intensities of individual cells were measured by flow cytometry using a Guava® easyCyte 8HT (Merck Millipore). Relative proliferation rates were calculated by establishing a fluorescence threshold based on the fluorescence of control group cells, and calculating the proportion of cells above and below the fluorescence threshold in all treatment conditions.

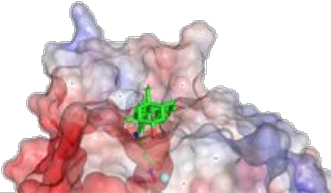
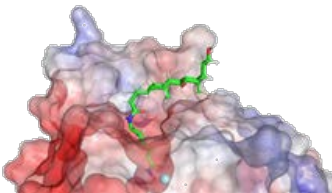
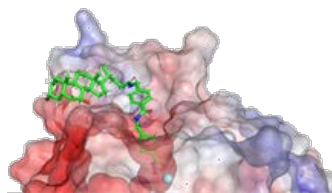
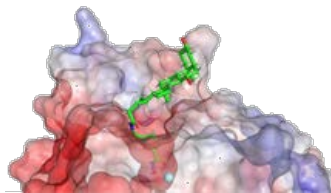
Supplementary Table S1. Main protein-ligand interactions characterized in the docking model. (**UDCA**, ursodeoxycholic acid)

| Compound | Interaction | Compound | Interaction |
|---|---|---|---|
|  <p>UDCA-HDAC6i #1 -8.3 kcal/mol</p> |  His560  Trp496  Ser568  Gly619  Phe620  |  <p>UDCA-HDAC6i #2 -7.9 kcal/mol</p> |  Trp496  Gly619  Phe620  |
|  <p>UDCA-HDAC6i #3 -3.9 kcal/mol</p> |  Leu749  Gly619  |  <p>UDCA-HDAC6i #4 -4.8 kcal/mol</p> |  Gly619  |
|  <p>UDCA-HDAC6i #5 -3.9 kcal/mol</p> |  Asp675  His610 |  <p>UDCA-HDAC6i #6 -4.2 kcal/mol</p> |  Ser568  Gly619  |
|  <p>UDCA-HDAC6i #9 -9.4 kcal/mol</p> |  Ser564  Asp567  Asn494  Trp496  Gly619  Phe620  |  <p>UDCA-HDAC6i #10 -4.7 kcal/mol</p> |  Gly619  Phe620  |

Supplementary Table S2A. Contribution of different molecular descriptors to the total binding affinities. (ΔG in kcal/mol)

| | UDCA-HDAC6i #1 | | | UDCA-HDAC6i #2 | | | UDCA-HDAC6i #3 | | | UDCA-HDAC6i #4 | | |
|--------------------------|-----------------|--------------|------------------|-----------------|--------------|------------------|-----------------|--------------|------------------|-----------------|--------------|------------------|
| | $\Delta G=-8.3$ | | | $\Delta G=-7.9$ | | | $\Delta G=-3.9$ | | | $\Delta G=-4.8$ | | |
| | Total | UDCA | Spacer-chelating | Total | UDCA | Spacer-chelating | Total | UDCA | Spacer-chelating | Total | UDCA | Spacer-chelating |
| XP GScore | -8.3 | -3.4 | -6.0 | -7.9 | -1.7 | -5.3 | -3.9 | -3.3 | -1.2 | -4.8 | -0.6 | -2.2 |
| Lipophilic EvdW | -4.5 | -1.91 | -2.72 | -4.38 | -1.68 | -2.7 | -2.18 | -1.66 | -0.53 | -2.57 | -1.48 | -1.13 |
| PhobEn | -0.66 | 0 | -0.73 | -0.39 | 0 | -0.39 | 0 | 0 | 0 | 0 | 0 | 0 |
| PhobEnHB | 0 | 0 | 0 | 0 | 0 | 0 | 0 | 0 | 0 | 0 | 0 | 0 |
| PhobEnPairHB | 0 | 0 | 0 | 0 | 0 | 0 | 0 | 0 | 0 | 0 | 0 | 0 |
| HBond | -2.25 | -1.18 | -1.67 | -2.17 | -0.7 | -1.59 | -1.66 | -1.18 | -1.01 | -1.81 | -0.48 | -1.81 |
| Electro | -1.43 | -0.63 | -0.81 | -1.25 | -0.37 | -0.84 | -1.14 | -0.37 | -0.87 | -0.85 | -0.08 | -0.8 |
| Sitemap | 0 | 0 | 0 | -0.14 | -0.09 | -0.04 | -0.33 | -0.33 | 0 | -0.28 | -0.28 | 0 |
| PiCat | 0 | 0 | 0 | 0 | 0 | 0 | 0 | 0 | 0 | 0 | 0 | 0 |
| CIBr | 0 | 0 | 0 | 0 | 0 | 0 | 0 | 0 | 0 | 0 | 0 | 0 |
| LowMW | 0 | 0 | 0 | 0 | 0 | 0 | 0 | 0 | 0 | 0 | 0 | 0 |
| Penalties | 0 | 0 | 0 | 0 | 0 | 0 | 0.96 | 0 | 1.26 | 0 | 0 | 0 |
| HBPenal | 0 | 0 | 0 | 0 | 0 | 0 | 0 | 0 | 0 | 0 | 0 | 0 |
| ExposPenal | 0.22 | 0.31 | 0 | 0.17 | 0.16 | 0.01 | 0.19 | 0.19 | 0 | 0.33 | 1.7 | 0 |
| RotPenal | 0.27 | 0.22 | 0 | 0.25 | 0.22 | 0 | 0.3 | 0.22 | 0 | 0.34 | 0.22 | 0 |
| EpikState Penalty | 0.01 | 0.01 | 0.01 | 0.01 | 0.01 | 0.01 | 0.01 | 0.01 | 0.01 | 0 | 0 | 0 |
| Corrected Gscore | -9.1 | -3.18 | -5.92 | -7.99 | -2.45 | -5.54 | -4.26 | -3.12 | -1.14 | -4.14 | -0.4 | -3.74 |

Supplementary Table S2B. Contribution of different molecular descriptors to the total binding affinities. (ΔG in kcal/mol)

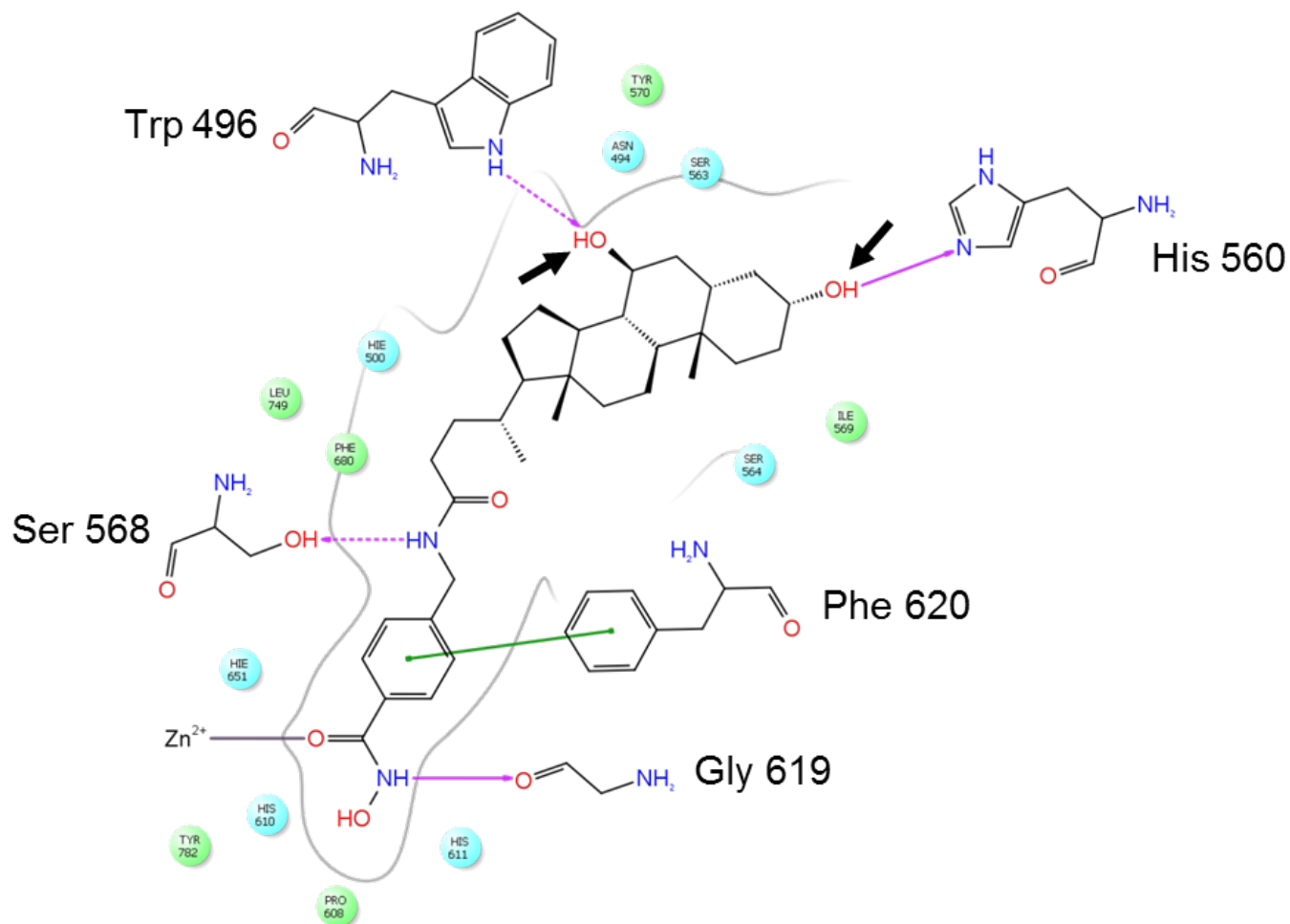
| | UDCA-HDAC6i #5 | | | UDCA-HDAC6i #6 | | | UDCA-HDAC6i #9 | | | UDCA-HDAC6i #10 | | |
|--------------------------|---|--------------|------------------|--|--------------|------------------|---|--------------|------------------|---|--------------|------------------|
| | $\Delta G=-3.9$ | | | $\Delta G=-4.2$ | | | $\Delta G=-9.4$ | | | $\Delta G=-4.7$ | | |
| |  | | |  | | |  | | |  | | |
| | Total | UDCA | Spacer-chelating | Total | UDCA | Spacer-chelating | Total | UDCA | Spacer-chelating | Total | UDCA | Spacer-chelating |
| XP GScore | -3.9 | -0.7 | -1.2 | -4.2 | -0.2 | -5.0 | -9.4 | -3.3 | -6.1 | -4.7 | -0.3 | -4.9 |
| Lipophilic EvdW | -2.9 | -1.61 | -1.41 | -2.95 | -1.05 | -1.97 | -4.8 | -1.53 | -3.3 | -2.85 | -0.74 | -1.7 |
| PhobEn | 0 | 0 | -0.18 | 0 | 0 | -0.13 | -0.61 | 0 | -0.61 | -0.5 | 0 | -0.53 |
| PhobEnHB | 0 | 0 | 0 | 0 | 0 | 0 | 0 | 0 | 0 | 0 | 0 | 0 |
| PhobEnPairHB | 0 | 0 | 0 | 0 | 0 | 0 | 0 | 0 | 0 | 0 | 0 | 0 |
| HBond | -1.33 | -0.35 | -1.03 | -2.17 | -0.96 | -1.59 | -3.34 | -2.04 | -1.6 | -2.17 | -0.96 | -1.86 |
| Electro | -1.5 | -0.41 | -1.1 | -1.13 | -0.39 | -0.81 | -1.6 | -0.56 | -1.11 | -1.12 | -0.33 | -0.82 |
| Sitemap | -0.17 | -0.17 | 0 | 0 | 0 | 0 | -0.04 | 0 | -0.04 | -0.02 | -0.02 | 0 |
| PiCat | 0 | 0 | 0 | 0 | 0 | 0 | 0 | 0 | 0 | 0 | 0 | 0 |
| CIBr | 0 | 0 | 0 | 0 | 0 | 0 | 0 | 0 | 0 | 0 | 0 | 0 |
| LowMW | 0 | 0 | 0 | 0 | 0 | 0 | 0 | 0 | 0 | 0 | 0 | 0 |
| Penalties | 0 | 0 | 0 | 0 | 0 | 0 | 0 | 0 | 0 | 0 | 0 | 0 |
| HBPenal | 0 | 0 | 0 | 0 | 0 | 0 | 0 | 0 | 0 | 0 | 0 | 0 |
| ExposPenal | 1.99 | 1.85 | 0 | 2.03 | 2.16 | 0 | 0.79 | 0.79 | 0 | 1.68 | 1.69 | 0 |
| RotPenal | 0 | 0.22 | 0 | 0 | 0.22 | 0 | 0.19 | 0.22 | 0 | 0.28 | 0.22 | 0 |
| EpikState Penalty | 0 | 0 | 0 | 0 | 0 | 0 | 0.01 | 0.01 | 0.01 | 0.16 | 0.16 | 0.16 |
| Corrected Gscore | -4.19 | -0.47 | -3.72 | -4.52 | -0.02 | -4.5 | -9.76 | -3.11 | -6.65 | -4.73 | 0.02 | -4.75 |

Supplementary Table S3. IC50 values of UDCA-HDAC6i#1, #2, #6, #9 and #8, (8) and UDCA on HDACs 1-11.

| Enzyme | | UDCA-HDAC6i | | | | | | UDCA |
|-------------|-------------|-------------|----------|----------|----------|----------|----------|------|
| | | #1 | #2 | #6 | #9 | #8 | (8) | |
| HDAC1 | | 1.01E-05 | 9.01E-06 | 2.57E-06 | 1.52E-05 | 1.40E-07 | ND | ND |
| HDAC2 | | 1.88E-05 | 1.32E-05 | - | - | 5.16E-07 | ND | ND |
| HDAC3 | | 8.37E-06 | 9.99E-06 | - | - | - | ND | ND |
| HDAC4 | | 1.65E-05 | ND | - | - | - | ND | ND |
| HDAC5 | | 1.41E-05 | ND | - | - | - | 4.35E-04 | ND |
| HDAC6 | IC50 (M) | 5.80E-08 | 5.61E-08 | 8.21E-08 | 4.26E-09 | 8.08E-06 | 6.89E-07 | ND |
| HDAC7 | | 7.47E-06 | 1.76E-05 | - | - | - | 1.47E-05 | ND |
| HDAC8 | | 8.94E-07 | 6.15E-07 | - | - | - | 1.36E-05 | ND |
| HDAC9 | | 1.34E-05 | 1.16E-05 | - | - | - | ND | ND |
| HDAC10 | | 2.45E-05 | 2.18E-05 | - | - | - | ND | ND |
| HDAC11 | | 2.33E-06 | 2.56E-06 | - | - | - | ND | ND |
| Selectivity | HDAC6/HDAC1 | 174 | 160 | 31 | 3574 | - | - | - |
| | HDAC1/HDAC6 | - | - | - | - | 58 | - | - |

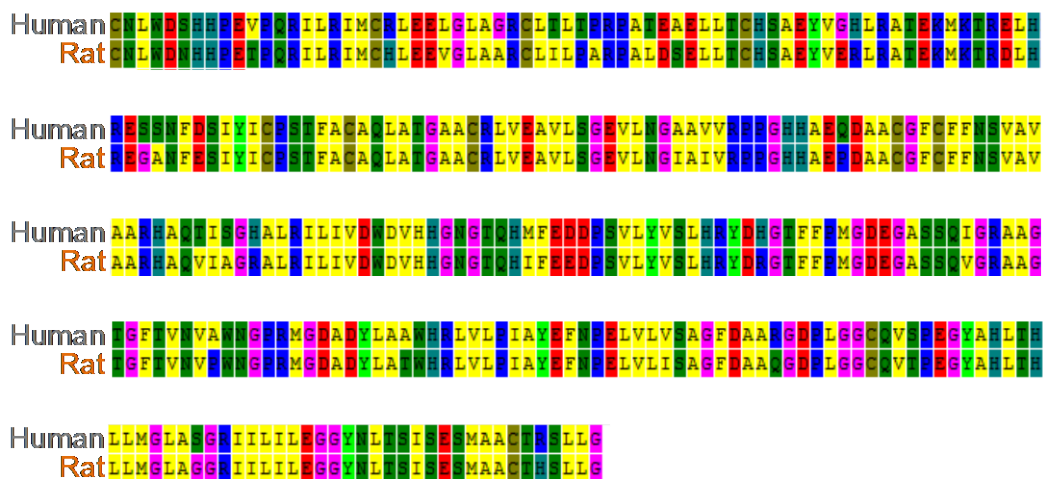
ND: non-determined
 (-), not analyzed

Supplementary Figure S1. Graphical 2D representation of the main interactions taking place in the binding of UDCA-HDAC6i #1 to the catalytic domain 2 of HDAC6.



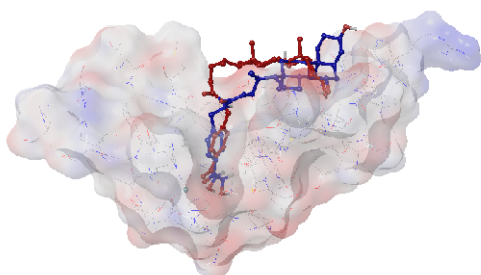
Supplementary Figure S3. Docking studies on a homology model of the catalytic domain 2 of rat HDAC6 based on the experimentally resolved three-dimensional structure of human HDAC6 catalytic domain 2. (A) Sequence alignment of human and rat HDAC6 catalytic domain 2. (B) Graphical representation of the binding modes of UDCA-HDAC6i #1, #2 and #9 with the active sites of human and rat HDAC6 catalytic domain 2, and table depicting the XP Gscores of the different UDCA-HDAC6is on both proteins.

A

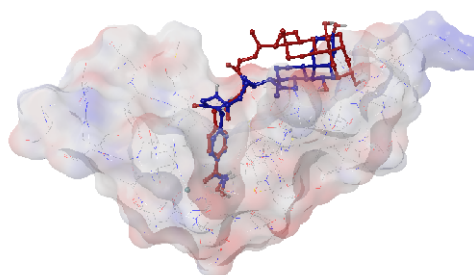


B

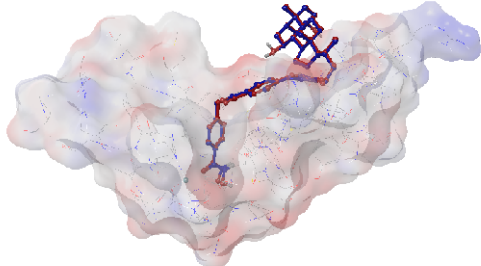
UDCA-HDAC6i #1



UDCA-HDAC6i #2



UDCA-HDAC6i #9



■ UDCA-HDAC6i docked in human HDAC6
■ UDCA-HDAC6i docked in rat HDAC6 homology model

| UDCA-HDAC6i | XP Gscore (kcal/mol) | |
|-------------|----------------------|------|
| | Human | Rat |
| #9 | -9.4 | -9.1 |
| #1 | -8.3 | -6.2 |
| #2 | -7.9 | -7.7 |
| #4 | -4.8 | -6 |
| #10 | -4.7 | -5.7 |
| #6 | -4.2 | -3 |
| #5 | -3.9 | -3.8 |
| #3 | -3.9 | -4.4 |

Supplementary Table S4A. QikProp predicted values.

| | Oral Absorption (%) | # stars | # rotor | mol_MW | Dipole | SASA | FOSA | FISA | PISA | WPSA | Vol. | donorHB | Accpt. HB |
|-----------------------------|---------------------|---------|---------|-----------|----------|------------|---------|---------|---------|---------|------------|---------|-----------|
| Range of recommended values | >80% is high | 0 – 5 | 0 – 15 | 130 – 725 | 1 – 12.5 | 300 – 1000 | 0 – 750 | 7 – 330 | 0 – 450 | 0 – 175 | 500 – 2000 | 0 – 6 | 2 – 20 |
| UDCA-HDAC6i#1 | 55.096 | 1 | 10 | 540.742 | 12.567 | 895.896 | 513.134 | 254.444 | 128.318 | 0 | 1695.439 | 5 | 10.1 |
| UDCA-HDAC6i#2 | 25.888 | 4 | 12 | 597.793 | 10.673 | 993.687 | 554.6 | 301.385 | 137.702 | 0 | 1868.260 | 5.25 | 11.85 |
| UDCA-HDAC6i#3 | 58.683 | 0 | 9 | 478.671 | 5.66 | 805.261 | 567.414 | 237.846 | 0 | 0 | 1517.723 | 4.25 | 9.35 |
| UDCA-HDAC6i#4 | 54.419 | 0 | 10 | 478.671 | 6.297 | 808.996 | 547.512 | 261.484 | 0 | 0 | 1519.515 | 4 | 9.1 |
| UDCA-HDAC6i#5 | 53.201 | 0 | 11 | 492.698 | 6.26 | 842.124 | 580.464 | 261.66 | 0 | 0 | 1580.373 | 5 | 10.1 |
| UDCA-HDAC6i#6 | 44.379 | 1 | 13 | 520.751 | 6.403 | 908.181 | 646.416 | 261.765 | 0 | 0 | 1701.654 | 5 | 10.1 |
| UDCA-HDAC6i#7 | 57.305 | 9 | 12 | 691.952 | 3.537 | 1148.244 | 506.819 | 214.417 | 427.008 | 0 | 2182.651 | 5.5 | 9.4 |
| UDCA-HDAC6i#8 | 60.241 | 5 | 11 | 615.854 | 11.349 | 1020.96 | 513.268 | 219.116 | 288.576 | 0 | 1941.437 | 5.5 | 9.4 |
| UDCA-HDAC6i#9 | 38.677 | 8 | 13 | 673.891 | 8.13 | 1111.053 | 544.626 | 307.514 | 258.914 | 0 | 2101.897 | 6 | 12.6 |
| UDCA-HDAC6i#10 | 47.858 | 1 | 10 | 530.703 | 9.067 | 882.103 | 511.824 | 272.196 | 98.082 | 0 | 1649.046 | 5 | 10.6 |

Percent Human Oral Absorption, predicted human oral absorption on 0 to 100% scale, based on a quantitative multiple linear regression model. #stars, number of property or descriptor values that fall outside the 95% range of similar values for known drugs. A large number of stars suggests that a molecule is less drug-like than molecules with few stars. #rotor, number of non-trivial (not CX3), non-hindered (not alkene, amide, small ring) rotatable bonds. MW, molecular weight of the molecule. Dipole, computed dipole moment of the molecule. SASA, total solvent accessible surface area (SASA) in square angstroms using a probe with a 1.4 Å radius. FOSA, hydrophobic component of the SASA (saturated carbon and attached hydrogen). FISA, hydrophilic component of the SASA (SASA on N, O, and H on heteroatoms). PISA, (carbon and attached hydrogen) component of the SASA. WPSA, weakly polar component of the SASA (halogens, P, and S). Volume, total solvent-accessible volume in cubic angstroms using a probe with a 1.4 Å radius. donorHB, estimated number of hydrogen bonds that would be donated by the solute to water molecules in an aqueous solution. accptHB, estimated number of hydrogen bonds that would be accepted by the solute from water molecules in an aqueous solution. For donorHB and accptHB, values are averages taken over a number of configurations, so they can be non-integer.

Supplementary Table S4B. QikProp predicted values

| | glob | QPpolrz | QPlogPC16 | QPlogPoct | QPlogPw | QPlogPo/w | QPlogS | QPlogBB | IPV | EA(eV) | #metab | QPlogKhsa | PSA |
|-----------------------------|-------------|---------|-----------|-----------|---------|-----------|------------|----------|------------|------------|--------|------------|---------|
| Range of recommended values | 0.75 – 0.95 | 13 – 70 | 4 – 18 | 8 – 35 | 4 – 45 | -2 – 6.5 | -6.5 – 0.5 | -3 – 1.2 | 7.9 – 10.5 | -0.9 – 1.7 | 1 – 8 | -1.5 – 1.5 | 7 – 200 |
| UDCA-HDAC6i#1 | 0.767 | 56.502 | 17.989 | 33.117 | 21.484 | 2.82 | -5.922 | -2.919 | 9.606 | 0.411 | 4 | 0.261 | 142.804 |
| UDCA-HDAC6i#2 | 0.738 | 62.224 | 20.339 | 36.056 | 26.091 | 2.174 | -5.598 | -3.846 | 9.699 | 0.652 | 5 | -0.066 | 181.227 |
| UDCA-HDAC6i#3 | 0.793 | 48.806 | 15.008 | 27.749 | 21.081 | 1.533 | -3.853 | -2.5 | 9.644 | -0.6 | 4 | -0.25 | 140.838 |
| UDCA-HDAC6i#4 | 0.790 | 48.236 | 15.152 | 27.188 | 20.491 | 1.514 | -3.816 | -2.832 | 9.798 | -0.684 | 4 | -0.237 | 145.127 |
| UDCA-HDAC6i#5 | 0.779 | 50.029 | 16.002 | 29.726 | 22.812 | 1.315 | -3.783 | -2.973 | 9.738 | -0.657 | 4 | -0.367 | 145.084 |
| UDCA-HDAC6i#6 | 0.759 | 53.599 | 17.276 | 30.834 | 22.514 | 2.019 | -4.521 | -3.249 | 9.7 | -0.745 | 4 | -0.185 | 145.14 |
| UDCA-HDAC6i#7 | 0.709 | 77.568 | 25.155 | 39.66 | 23.716 | 6.55 | -9.826 | -3.006 | 8.164 | 0.682 | 5 | 1.425 | 137.107 |
| UDCA-HDAC6i#8 | 0.737 | 67.235 | 21.551 | 36.817 | 22.457 | 4.887 | -7.934 | -2.788 | 8.219 | 0.452 | 7 | 0.871 | 138.016 |
| UDCA-HDAC6i#9 | 0.714 | 72.089 | 23.906 | 40.715 | 26.78 | 3.854 | -7.94 | -4.239 | 9.711 | 0.732 | 5 | 0.572 | 179.752 |
| UDCA-HDAC6i#10 | 0.765 | 54.356 | 17.504 | 32.049 | 22.135 | 2.189 | -5.442 | -3.138 | 9.542 | 0.514 | 5 | 0.065 | 153.405 |

Glob, globularity descriptor, where r is the radius of a sphere with a volume equal to the molecular volume. Globularity is 1.0 for a spherical molecule. QPpolrz, predicted polarizability in cubic angstroms. QPlogPC16, predicted hexadecane/gas partition coefficient. QPlogPoct, predicted octanol/gas partition coefficient. QPlogPw, predicted water/gas partition coefficient. QPlogPo/w, predicted octanol/water partition coefficient. QPlogS, predicted aqueous solubility, $\log S$. S in mol dm^{-3} is the concentration of the solute in a saturated solution that is in equilibrium with the crystalline solid. QPlogBB, predicted brain/blood partition coefficient. IPV, PM3 calculated ionization potential. EA(eV), PM3 calculated electron affinity. #metab, number of likely metabolic reactions. QPlogKhsa, prediction of binding to human serum albumin. PSA, Van der Waals surface area of polar nitrogen and oxygen atoms.

Supplementary Table S5. Relative abundancy of individual bile acids and conjugation types in portal blood. Statistical analysis, two-tailed unpaired t test

| | Portal blood (%) | | |
|--------------------|------------------|-------------------|---------------------------|
| | PCK | | p |
| | Control (a) | UDCA-HDAC6i#1 (b) | a (n=12) vs b (n=8) |
| TUDCA | 5.34 | 5.15 | 0.7112 |
| TCA | 25.57 | 18.53 | 0.1320 |
| Ta/bMCA | 9.33 | 6.92 | 0.1736 |
| TQDCA | 2.72 | 2.47 | 0.6640 |
| Tauro-conj. | 42.96 | 33.06 | 0.2140 |
| GUDCA | 1.20 | 1.72 | 0.1151 |
| GCA | 6.23 | 8.76 | 0.1194 |
| GQDCA | 0.30 | 0.40 | 0.7293 |
| Glyco-conj. | 7.73 | 10.87 | 0.1055 |
| UDCA | 0.40 | 1.68 | 0.0065 |
| CA | 39.50 | 43.39 | 0.5226 |
| a/bMCA | 3.64 | 3.11 | 0.4689 |
| HyoDCA | 5.76 | 7.83 | 0.2642 |
| SLCA | 0.017 | 0.055 | 0.0169 |
| Unconj. | 49.3 | 56.1 | 0.3628 |

Supplementary Table S6. Relative abundancy of individual bile acids and conjugation types in liver. Statistical analysis, two-tailed unpaired t test.

| | Liver (%) | | | | | |
|--------------------|--------------|--------------|-------------------|----------------|---------------|---------------|
| | SD | PCK | | | p | |
| | Control (a) | Control (b) | UDCA-HDAC6i#1 (C) | a (n=12) | a (n=12) | b (n=12) |
| | | | | vs b (n=12) | vs c (n=8) | vs c (n=8) |
| TUDCA | 13.78 | 10.58 | 8.84 | 0.0827 | 0.0144 | 0.2794 |
| TCA | 51.62 | 50.49 | 49.67 | 0.7584 | 0.5420 | 0.8412 |
| Ta/bMCA | 9.09 | 23.47 | 13.04 | 0.0010 | 0.1556 | 0.0564 |
| TQDCA | 7.23 | 5.33 | 5.08 | 0.0936 | 0.0830 | 0.7811 |
| Tauro-conj. | 80.52 | 85.66 | 76.63 | 0.1038 | 0.4078 | 0.0530 |
| GUDCA | 1.80 | 1.49 | 3.10 | 0.3599 | 0.0575 | 0.0234 |
| GCA | 9.79 | 10.81 | 16.93 | 0.6968 | 0.0834 | 0.1193 |
| GQDCA | 0.65 | 0.51 | 0.81 | 0.4986 | 0.4938 | 0.1229 |
| Glyco-conj. | 12.09 | 12.65 | 20.85 | 0.8426 | 0.0652 | 0.0678 |
| UDCA | 2.14 | 0.12 | 0.21 | 0.0022 | 0.0157 | 0.0088 |
| CA | 3.23 | 1.03 | 1.88 | 0.0004 | 0.0638 | 0.0283 |
| a/bMCA | 0.54 | 0.22 | 0.31 | 0.0038 | 0.0590 | 0.2551 |
| HyoDCA | 1.96 | 0.32 | 0.33 | 0.0001 | 0.0008 | 0.8963 |
| SLCA | 0.0965 | 0.0041 | 0.0199 | 0.0002 | 0.0613 | 0.0330 |
| Unconj. | 7.40 | 1.69 | 2.53 | 0.0002 | 0.0075 | 0.1042 |

Supplementary Table S7. Relative abundancy of individual bile acids and conjugation types in bile. Statistical analysis, two-tailed unpaired t test.

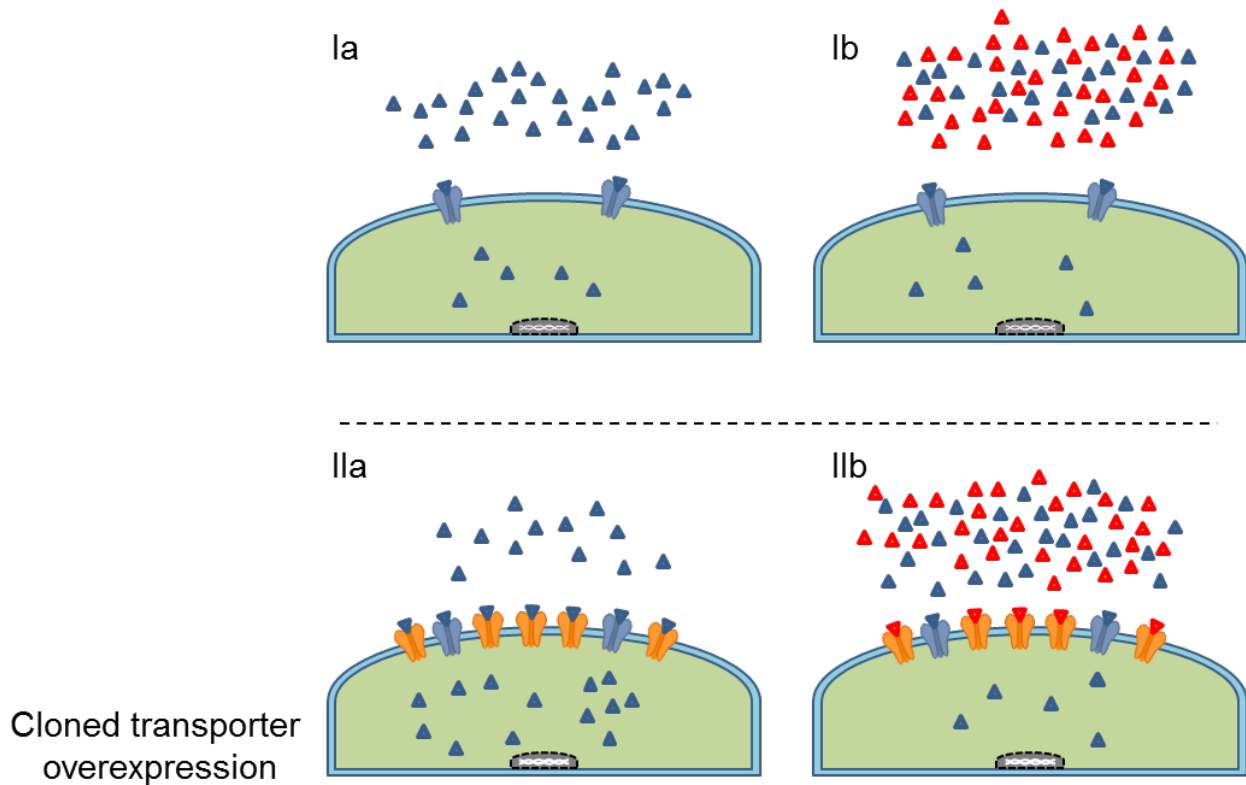
| | Bile (%) | | | | | |
|--------------------|--------------|--------------|-----------------------|---------------------------|--------------------------|--------------------------|
| | SD | PCK | | | p | |
| | Control (a) | Control (b) | UDCA- HDAC6i#1 (c) | a (n=8) vs b (n=10) | a (n=8) vs c (n=8) | b (n=8) vs c (n=8) |
| TUDCA | 7.63 | 8.35 | 10.32 | 0.5827 | 0.1845 | 0.3464 |
| TCA | 54.78 | 58.89 | 54.58 | 0.3998 | 0.9739 | 0.4033 |
| Ta/bMCA | 14.88 | 15.86 | 9.79 | 0.8296 | 0.0401 | 0.0328 |
| TQDCA | 5.71 | 3.91 | 7.15 | 0.0070 | 0.3302 | 0.0161 |
| Tauro-conj. | 82.99 | 87.01 | 80.62 | 0.2921 | 0.6884 | 0.1749 |
| GUDCA | 2.79 | 1.61 | 2.18 | 0.5001 | 0.4945 | 0.8144 |
| GCA | 9.80 | 9.50 | 11.90 | 0.9150 | 0.6672 | 0.5083 |
| GQDCA | 0.50 | 0.49 | 0.60 | 0.8410 | 0.6388 | 0.8130 |
| Glyco-conj. | 13.09 | 11.59 | 14.68 | 0.6937 | 0.7902 | 0.4883 |
| UDCA | 0.02 | 0.01 | 0.05 | 0.1858 | 0.0200 | 0.0009 |
| CA | 3.72 | 1.31 | 5.14 | 0.0196 | 0.5080 | 0.0202 |
| a/bMCA | 0.09 | 0.06 | 0.10 | 0.1739 | 0.9337 | 0.1283 |
| HyoDCA | 0.08 | 0.02 | 0.07 | 0.0386 | 0.9411 | 0.0310 |
| SLCA | 0.0091 | 0.0020 | 0.0046 | 0.0721 | 0.3101 | 0.0205 |
| Unconj. | 3.91 | 1.40 | 4.71 | 0.0199 | 0.7039 | 0.0516 |

Supplementary Table S8. Relative abundancy of individual bile acids and conjugation types in peripheral blood. Statistical analysis, two-tailed unpaired t test.

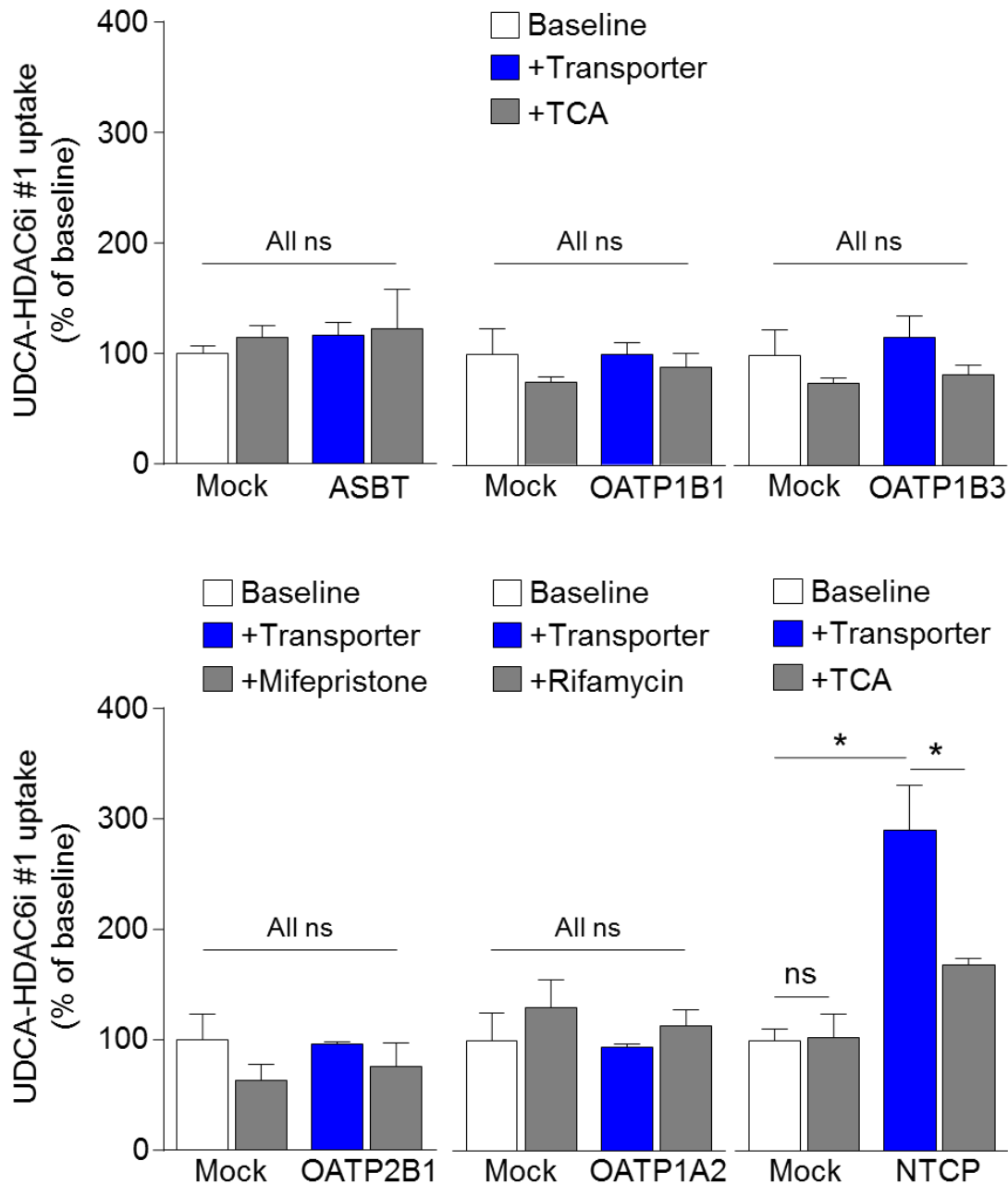
| | Peripheral blood (%) | | | | | |
|--------------------|----------------------|--------------|-----------------------|----------------------------|---------------------------|---------------------------|
| | SD | PCK | | | p | |
| | Control (a) | Control (b) | UDCA- HDAC6i#1 (c) | a (n=12) vs b (n=12) | a (n=12) vs c (n=8) | b (n=12) vs c (n=8) |
| TUDCA | 2.30 | 7.21 | 4.77 | 0.0007 | 0.0234 | 0.1380 |
| TCA | 13.01 | 31.77 | 24.53 | 0.0005 | 0.0099 | 0.1381 |
| Ta/bMCA | 1.82 | 12.40 | 8.01 | < 0.0001 | 0.0012 | 0.1266 |
| TQDCA | 1.98 | 2.89 | 2.21 | 0.0509 | 0.1802 | 0.3404 |
| Tauro-conj. | 19.10 | 54.27 | 38.96 | < 0.0001 | 0.0062 | 0.0357 |
| GUDCA | 0.71 | 0.84 | 2.21 | 0.0841 | 0.0025 | 0.0065 |
| GCA | 4.79 | 7.30 | 11.29 | 0.0925 | 0.0107 | 0.0574 |
| GQDCA | 0.52 | 0.42 | 0.54 | 0.5691 | 0.4872 | 0.2370 |
| Glyco-conj. | 6.02 | 8.56 | 14.04 | 0.1557 | 0.0089 | 0.0232 |
| UDCA | 1.03 | 0.22 | 1.77 | 0.8924 | 0.1732 | 0.0073 |
| CA | 56.70 | 29.88 | 35.18 | 0.0001 | 0.0011 | 0.2973 |
| a/bMCA | 3.08 | 2.75 | 3.22 | 0.6473 | 0.8618 | 0.5314 |
| HyoDCA | 13.63 | 4.30 | 6.72 | 0.0001 | 0.0101 | 0.0855 |
| SLCA | 0.44 | 0.02 | 0.11 | 0.1031 | 0.3223 | 0.0215 |
| Unconj. | 74.88 | 37.17 | 46.99 | < 0.0001 | 0.0007 | 0.1096 |

Supplementary Figure S4. Schematic example of a substrate competition transport experiment. Ia Incubation of cells with 100 μM UDCA-HDAC6i#1 in basal conditions. Ib Incubation of cells with 100 μM UDCA-HDAC6i#1 in the presence of transporter inhibitor. Ic Incubation of cells with 100 μM UDCA-HDAC6i#1 in after induced transporter overexpression. Id Incubation of cells with 100 μM UDCA-HDAC6i#1 in the presence of transporter inhibitor after induced transporter overexpression.

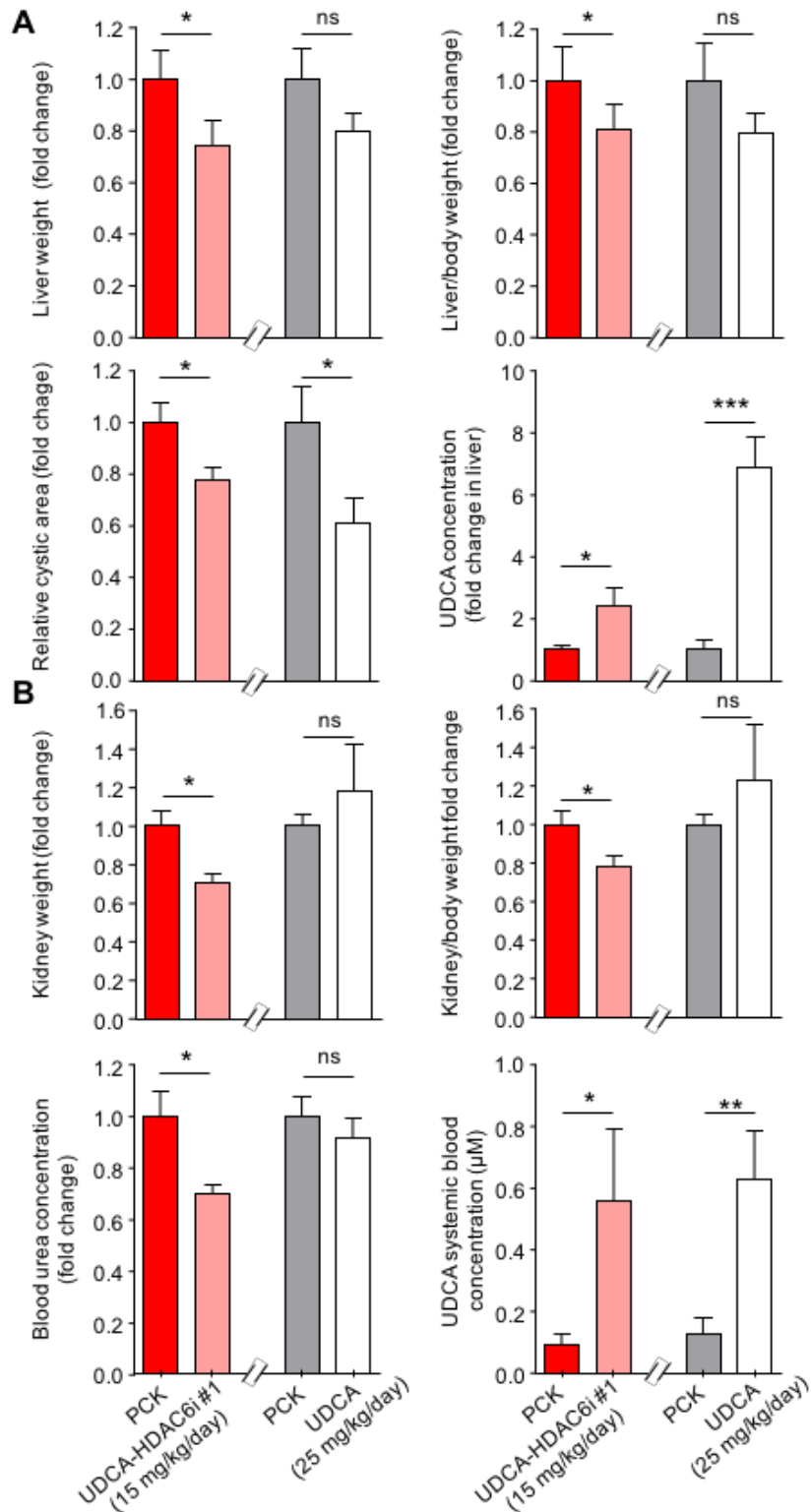
▲ UDCA-HDAC6i#1
 ▲ Inhibitor

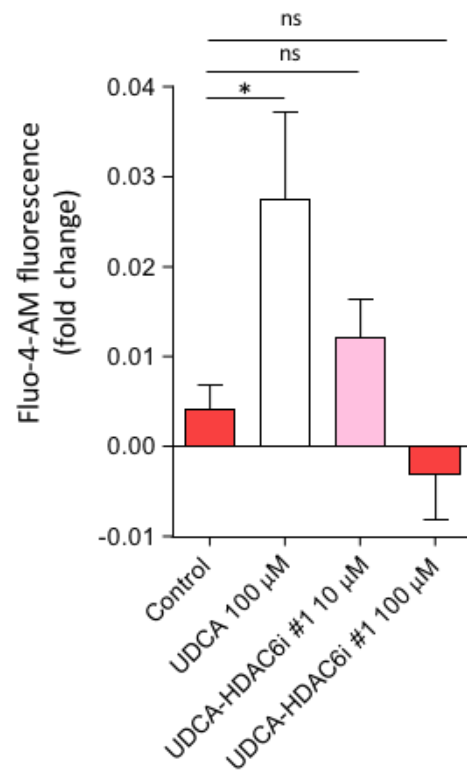


Supplementary Figure S5. Bar graphs representing UDCA-HDAC6i#1 uptake under baseline and transporter overexpressing conditions in the presence or absence of a transporter inhibitor/competitor. Transporter overexpression was carried out on CHO cells for OATP1B1 (n=7), OATP1B3 (n=7), OATP1A2 (n=3), OATP2B1 (n=3) and NTCP (n=4) transporters, and in TFK-1 cells for ASBT (n=3) transporter. Paired two-tailed *t*-test was used to assess statistical significance.



Supplementary Figure S6. Graphical comparisons between results previously reported by Munoz-Garrido *et al.*(7) or the treatment of PCK rats with UDCA and results obtained upon treatment of PCK rats with UDCA-HDAC6i #1. (A) Bar graphs representing liver weight, liver to body weight fold change, relative cystic area fold change and UDCA concentration fold change in liver. (B) Bar graphs representing kidney weight, kidney to body weight fold change, blood urea concentration and UDCA concentration in peripheral blood. In all cases statistical unpaired two-tailed t test was applied to determine significance, except in the case of liver to body weight ratio in which in both cases unpaired one-tailed t test was applied.



Supplementary Figure S7. Calcium mobilization assay in cystic cholangiocytes.

Supplementary Table S9. Enzymes and substrates used for HDAC inhibitory activity assays.

| Enzyme | | Accession Number | Mw (kDa) | Expression system | Concentration (nM) | Substrate |
|---------------|---|---|-----------------------------|-----------------------------|--------------------|---|
| HDAC1 | Full length with C-terminal GST tag | NM_004964 | 79.9 | Baculovirus in Sf9 cells | 75 | acetylated fluorogenic peptide from residues of p53, 379-382 (RHKKAc) |
| HDAC2 | Full length with C-terminal His marker | Q92769 | 60 | Baculovirus in Sf9 cells | 5 | acetylated fluorogenic peptide from residues of p53, 379-382 (RHKKAc) |
| HDAC3 / NcoR2 | Full length with C-terminal His marker (HDAC3) and N-terminal GST label (NCOR2) | NM_003883 (HDAC3) and NM_006312 (NcoR2) | 49.7 (HDAC3) and 39 (NCOR2) | Co-expressed in baculovirus | 2.3 | acetylated fluorogenic peptide from residues of p53, 379-382 (RHKKAc) |
| HDAC4 | Amino acids 627-1085 with N-terminal GST label | NM_006037 | 75.2 | Baculovirus | 266 | Fluorogenic Boc-L-Lys (s-trifluoroacetyl)-AMC |
| HDAC5 | Full length with N-terminal GST tag | NM_001015053 | 150 | Baculovirus in Sf9 cells | 588 | Fluorogenic Boc-L-Lys (s-trifluoroacetyl)-AMC |
| HDAC6 | Full length with N-terminal GST tag | BC069243 | 159 | Baculovirus in Sf9 cells | 13 | acetylated fluorogenic peptide from residues of p53, 379-382 (RHKKAc) |
| HDAC7 | End of 518 amino acids with N-terminal GST label | AY302468 | 78 | Baculovirus | 962 | Fluorogenic Boc-L-Lys (s-trifluoroacetyl)-AMC |
| HDAC8 | Full length | NM018486 | 42 | E. coli | 19 | acetylated fluorogenic peptide of p53 residues, 379-382 (RHKAckAc) |
| HDAC9 | Amino acids 604-1066 with C-terminal His marker | NM178423 | 50.7 | Baculovirus | 986 | Fluorogenic Boc-L-Lys (s-trifluoroacetyl)-AMC |
| HDAC10 | Amino acids 1-631 with N-terminal GST tag | NM_032019 | 96 | Baculovirus in Sf9 cells | 781 | acetylated fluorogenic peptide from residues of p53, 379-382 (RHKKAc) |
| HDAC11 | Full lenght N-terminal GST tag | NM_BC009676 | 66 | Baculovirus | 781 | acetylated fluorogenic peptide from residues of p53, 379-382 (RHKKAc) |

Supplementary Table S10. Oligonucleotide sequence of primers used to clone the ORF of human transporters.

| Gene | Protein | Forward (5'-3') | Reverse (5'-3') | Amplicon size (bp) | Accession Number |
|----------------|---------|--|--|--------------------|------------------|
| <i>SLC10A2</i> | ASBT | ATGAATGATCCGAACAGCTGTGT | CTACTTTTCGTCAGGTTGAAATCCTCC | 1047 | NM_000452 |
| <i>SLC10A1</i> | NTCP | ATGGAGGCCCAACACGC | GGCTGTGCAAGGGGAGC | 1047 | NM_003049 |
| <i>SLC10A2</i> | OATP1A2 | ATGGGAGAAACTGAGAAAAGAA TTGAAACCCATA | CAATTTAGTTTTCAATTCATCATCTTT CAAAACCGTCGTGGA | 2010 | NM_134431 |
| <i>SLC10B1</i> | OATP1B1 | ATGGACCAAAATCAACATTTGAA TAAACAGCAG | ACAATGTGTTTCACTATCTGCCCCAG | 2073 | NM_006446 |
| <i>SLC10B3</i> | OATP1B3 | ATGGACCAACATCAACATTTGAA TAAACAG | GTTGGCAGCAGCATTGTCTTGC | 2106 | NM_019844 |
| <i>SLC20B1</i> | OATP2B1 | ATGGGACCCAGGATAGGGC | CACTCGGGAATCCTCTGGCTTC | 2127 | NM_007256 |
| <i>SLC22A1</i> | OCT1 | ATGCCACCGTGGAT | GGTGCCCGAGGGTTCTGA | 1662 | NM_003057 |
| <i>SLC22A3</i> | OCT3 | ATGCCCTCCTTCGACG | AAGGTGAGAGCGGAAACTGG | 1668 | NM_021977 |

At the 5'-end of the primers an adapter was added containing the sequence of a restriction site for the enzymes MluI (Forward) and SpeI (Reverse).

Supplementary Table S11. Oligonucleotide sequence of primers used for RT-qPCR.

| Gene | Protein | Forward (5'-3') | Reverse (5'-3') | Amplicon size (bp) | Accession Number |
|----------------|---------------------------|-----------------------|-----------------------|--------------------|------------------|
| <i>SLC22A1</i> | OCT1 | GTCGCTTTGCCAGAGACCAT | CTTCATCCCTCCAACACGACA | 151 | NM_003057 |
| <i>SLC22A3</i> | OCT3 | ATCGTCAGCGAGTTTGACCTT | ACCTGTCTGCTGCATAGCCTA | 118 | NM_021977 |
| <i>RPL22</i> | 60S ribosomal protein L22 | AAAGTGAACGGAAAAGCTGGG | TCACGGTGATCTTGCTCTTGC | 76 | NM_000983 |

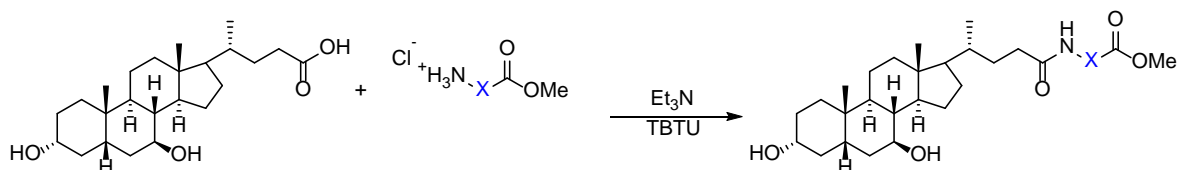
Supplementary Table S12. Antibodies used for immunoblot.

| Antigen | Source | Dilution | Reference | Provider |
|-----------------------|--------|----------|-----------|-----------------|
| Ac- α -tubulin | Mouse | 1:1000 | T6793 | Sigma |
| α -tubulin | Rabbit | 1:2000 | ab52866 | Abcam |
| Ac-H3K9 | Rabbit | 1:500 | C5B11 | Cell Signalling |
| β -actin | Mouse | 1:2000 | a5316 | Sigma |
| GAPDH | Rabbit | 1:1000 | ab22555 | Abcam |
| p-ERK1/2 | Rabbit | 1:1000 | 4370S | Cell Signalling |
| ERK1/2 | Rabbit | 1:1000 | 4695S | Cell Signalling |

Synthesis UDCA-derivates

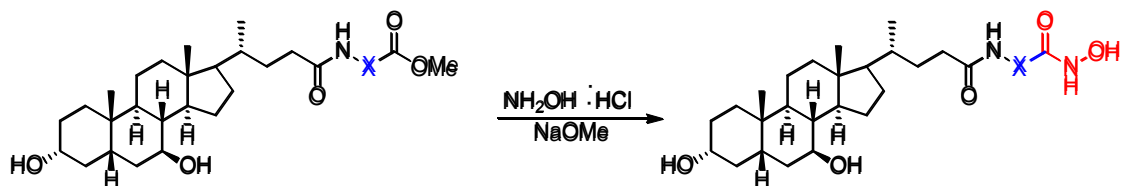
Method A

a.1) Coupling of ursodeoxycholic acid with spacers



To a solution of ursodeoxycholic acid (1 mmol) in DMF (2.5 ml) were added the hydrochloride of the corresponding methyl or ethyl amino ester (1 mmol) and TBTU (1.2 mmol). The solution was brought to 0 °C in an inert atmosphere and a solution of Et₃N (0.5 ml) in DMF (0.6 ml) was added dropwise. Reaction was followed by thin layer chromatography. The reaction mixture was kept under stirring for 3 hours. The solvent was then evaporated under reduced pressure, and the residue was dissolved in ethyl acetate (20 ml) and washed successively with 1N HCl (3 × 10 ml), saturated NaHCO₃ (2 × 10 ml) and saturated NaCl (1 × 10 ml). The organic phase was dried over MgSO₄ and evaporated under reduced pressure. The solid obtained was purified by chromatography obtaining the desired product.

a.2) Synthesis of hydroxamic acids

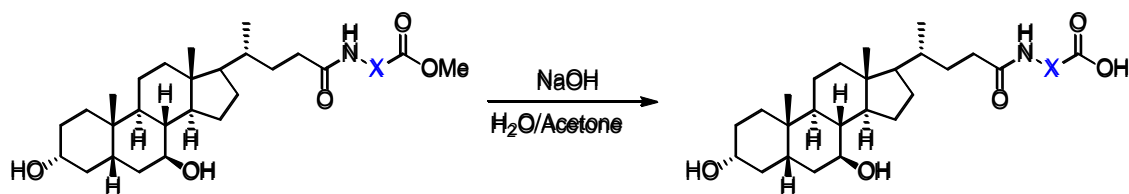


To a solution of hydroxylamine hydrochloride (10 mmol) and phenolphthalein (1 mg) in dry methanol (5 ml) at 0 °C under inert atmosphere, an aliquot of previously prepared suspension of sodium methoxide in methanol (37 mmol) was added dropwise until a permanent color switch to intense pink color was observed. Then

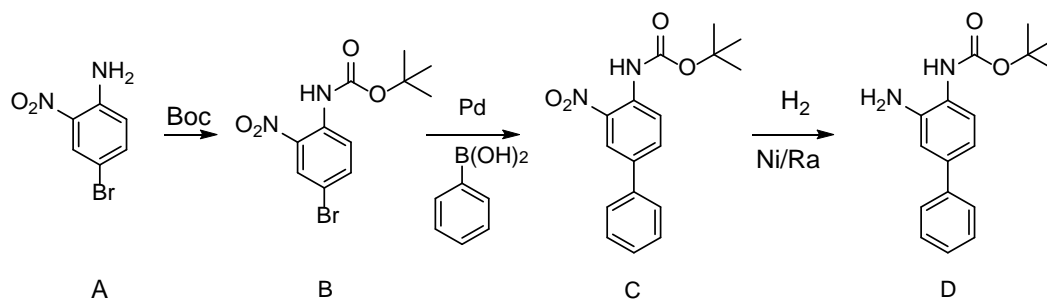
the corresponding methyl or ethyl ester (1 mmol) dissolved in dry methanol (1 ml) was added followed by addition of 1 ml of the previously prepared methoxide sodium methoxide suspension. Reaction was followed by thin layer chromatography. The reaction mixture was kept under stirring for 90 hours. Subsequently, distilled water (10 ml) was added and the reaction medium was acidified with glacial acetic acid. The product was then extracted with diethyl ether (3 × 20 ml) and the combined organic fractions were dried over MgSO₄ and evaporated under reduced pressure. The product thus obtained was redissolved in methanol (1 ml) and precipitated with water. This precipitate was filtered and washed with water and diethyl ether to obtain the desired product.

Method B

b.1) Hydrolysis of the methyl ester



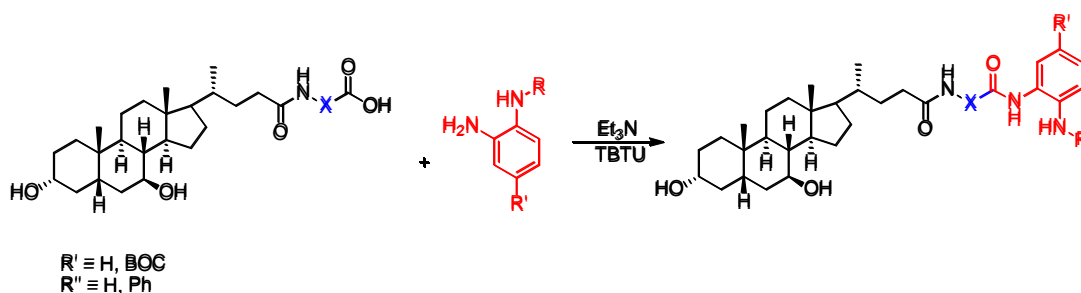
A solution of NaOH (0.5 M) in distilled water (4.35 ml) was slowly added to a solution of ester (1 mmol) in acetone (4.35 ml). The mixture was stirred for 5 hours. The reaction medium was then acidified with 1N HCl and kept under stirring for 15 minutes at 0 °C. The formed precipitate was filtered and washed successively with cold water, thereby obtaining the desired product.

Synthesis of tert-butyl (3-amino- [1,1'-biphenyl] -4-yl) carbamate

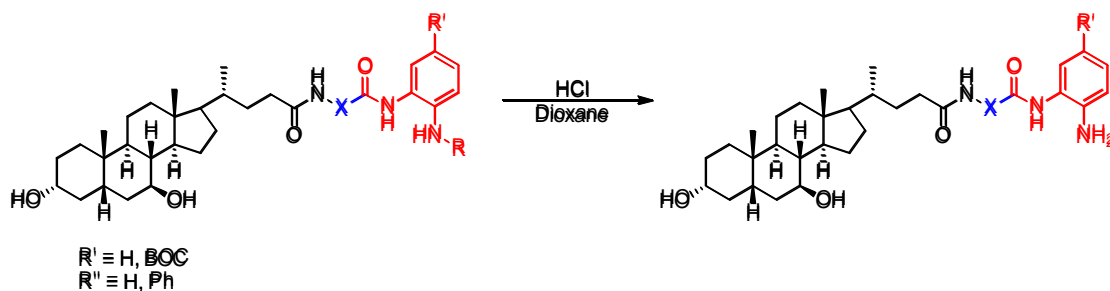
To a solution of 4-bromo-2-nitroaniline (A) (11.05 mmol) and Boc-anhydride (di-tert-butyl dicarbonate) (22.11 mmol) in THF (20 mL) a catalytic amount of DMAP (4-dimethylamino pyridine) was added. The reaction was maintained under stirring for 90 minutes at room temperature. The solvent was evaporated at low pressure and the oil obtained was dissolved in THF (10 ml). NaOH (10 ml, from a 2N solution) was added and the reaction was maintained under stirring for 18 hours at 65 °C. After that, NaOH (10 mmol) was added and the mixture reaction was maintained under stirring for an additional 4 hours at 65 °C. The progress of the reaction was followed by thin layer chromatography. The solvent was removed in vacuo, yielding a solid residue, which was filtered and washed with distilled water (2 x 20 ml) obtaining the desired product as a yellow solid (B), which was used directly for the next reaction step to obtain (C). For this purpose, Pd(PPh₃)₄ (10%, 0.346 mmol) was added to a reaction mixture in DME/H₂O (2:1,5 ml) containing the corresponding tert-butyl carbamate (B) (1 g, 3.15 mmol), obtained above, phenylboronic acid (422.91 mg 3.46 mmol) and sodium carbonate (491.8 mg, 4.73 mmol). The solution was kept under stirring for 20 hours at 110 °C and inert atmosphere. After this reaction time, water was added, and the product was extracted with ethyl acetate (3 x 20 ml). The organic phases were combined and washed with water (2 x 10 ml), dried over magnesium sulfate, filtered and the solvent was evaporated under reduced pressure. The yellow solid thus obtained was purified by chromatography obtaining the desired product (C). The last step of the reaction consisted in the reduction of the NO₂ group to NH₂, which was carried out using a modular catalytic hydrogenator (H-Cube Pro

of THALESNano) and a CatCart or cartridge catalyst system, which in this case has Ni/Ra supported. To carry out the reaction compound (C) was dissolved in 500 ml of MeOH and passed through the catalyst system at a flow rate of 1 ml / min, 50 °C and a pressure of 10 bar. The solvent was removed in vacuo giving a white solid corresponding to the desired product D.

b.2) Coupling of benzamide chelating groups



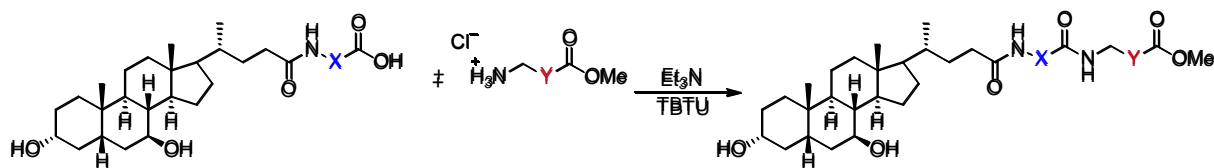
To a solution of the carboxylic acid obtained in (b.1) (205.7 mg, 0.38 mmol) in DMF (2.5 ml) were added the corresponding *o*-phenylenediamine (0.38 mmol) and TBTU (0.46 mmol). The solution was brought to 0 °C in an inert atmosphere and a solution of Et₃N (0.2 ml) in DMF (0.24 ml) was added dropwise. The mixture was kept under stirring for 3 hours. Reaction was followed by thin layer chromatography. The reaction mixture was kept under stirring for 3 hours. The solvent was then evaporated under reduced pressure, and the residue was dissolved in ethyl acetate (7.5 ml) and washed successively with 1N HCl (3 × 5 ml), saturated NaHCO₃ (2 × 5 ml) and saturated NaCl (1 × 5 ml). The organic phase was dried over MgSO₄ and evaporated under reduced pressure. The solid obtained was purified by chromatography obtaining the desired product.



To a suspension of the N-BOC protected compound (0.067 mmol) in a mixture of CH_2Cl_2 (0.63 ml) and dioxane (0.63 ml) was slowly added 4M HCl in dioxane (0.3 ml). Reaction was followed by TLC. The mixture was kept under stirring for 3 hours. The solvent was evaporated under reduced pressure. The solid obtained was suspended in AcOEt (10 ml) and washed with saturated NaHCO_3 solutions (3x5ml) and NaCl (3x5ml), then dried over magnesium sulfate, filtered and evaporated. Finally, it was dissolved in MeOH and precipitated in Et_2O , obtaining the desired product.

Method C

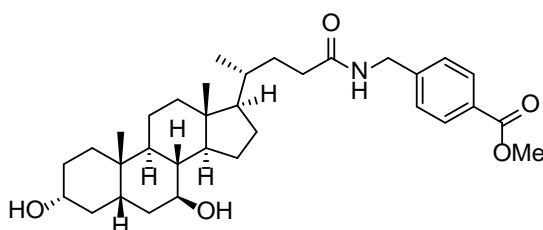
c.1) Coupling of the spacer



To a solution of the carboxylic acid obtained in (b.1) (205.7 mg, 0.38 mmol) in DMF (2.5 ml) were added hydrochloride of the corresponding methyl ester (76.4 mg, 0.38 mmol) and TBTU (0.46 mmol). The solution was brought to 0 °C in an inert atmosphere and a solution of Et_3N (0.2 ml) in DMF (0.24 ml) was added dropwise. Reaction was followed by thin layer chromatography. The mixture was kept under stirring for 3 hours. The solvent was then evaporated under reduced pressure, and the residue was dissolved in ethyl acetate (7.5 ml) and washed successively with 1N HCl (3 x 5 ml), saturated NaHCO_3 (2 x 5 ml) and saturated NaCl (1 x 5 ml). The

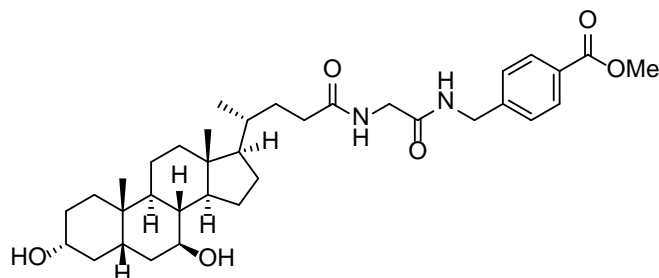
organic phase was dried over MgSO₄ and evaporated under reduced pressure. The solid obtained was purified by chromatography obtaining the desired product.

Synthesis of methyl 4-(((R)-4-((3R,5S,7S,8R,9S,10S,13R,14S,17R)-3,7-dihydroxy-10,13-dimethylhexadecahydro-1H-cyclopenta[a]phenanthren-17-yl)pentanamido)methyl)benzoate (3a).



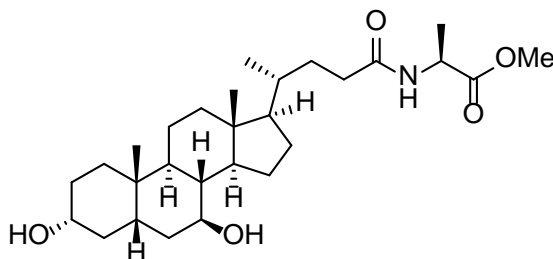
This compound was prepared following the **method A**. Ursodeoxycholic acid (392.6 mg, 1 mmol) methyl 4-(aminomethyl) benzoate hydrochloride (201.7 mg, 1 mmol), TBTU (385.3 mg, 1.2 mmol), Et₃N in DMF (1.1 ml, 3.26 M). White solid. Yield 84%; m.p.. 114-116 °C; IR 3293, 2927, 2862, 1720, 1650, 1277, 1106 cm⁻¹; ¹H NMR (400 MHz, DMSO-*d*₆) δ: 8.39 (t, *J* = 6.0 Hz, 1H), 7.90 (d, *J* = 8.2 Hz, 2H), 7.37 (d, *J* = 8.1 Hz, 2H), 4.49 (d, *J* = 4.4 Hz, 1H), 4.32 (dd, *J* = 6.0, 2.7 Hz, 2H), 3.88 (d, *J* = 6.7 Hz, 1H), 3.83 (s, 3H), 3.29 (s, 2H), 2.28 – 2.02 (m, 2H), 1.96 – 1.61 (m, 6H), 1.55 – 1.25 (m, 10H), 1.25 – 0.93 (m, 7H), 0.93 – 0.83 (m, 7H), 0.60 (s, 3H); ¹³C NMR (101 MHz, DMSO-*d*₆) δ 172.77, 166.06, 145.50, 129.16, 128.06, 127.26, 69.77, 69.48, 55.89, 54.77, 52.01, 43.10, 43.01, 42.22, 41.80, 39.86, 38.78, 37.74, 37.28, 34.93, 34.86, 33.76, 32.42, 31.67, 30.25, 28.20, 26.71, 23.32, 20.89, 18.44, 12.00; HRMS (ESI) for C₃₃H₄₉NO₅Na calculated [M + Na]⁺: 562.3509. Obtained: 562.3515.

Synthesis of methyl 4-((2-((R)-4-((3R,5S,7S,8R,9S,10S,13R,14S,17R)-3,7-dihydroxy-10,13-dimethylhexadecahydro-1H-cyclopenta[a]phenanthren-17-yl)pentanamido)acetamido) methyl)benzoate (3b).



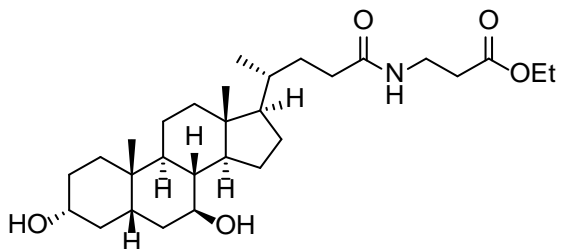
This compound was prepared following the **method A**. Glycoursodeoxycholic acid (121.4 mg, 0.27 mmol) methyl 4-(aminomethyl) benzoate hydrochloride (53.8 mg, 0.27) TBTU (104 mg, 0.32 mmol) Et₃N (0.3 ml, 3.26 M). White solid. Yield 63%; m.p. 145-147 °C; IR 3354, 2932, 2861, 1720, 1654, 1281, 1111, 847 cm⁻¹; ¹H NMR (400 MHz, DMSO-*d*₆) δ 8.41 (t, *J* = 6.1 Hz, 1H), 8.09 (t, *J* = 5.9 Hz, 1H), 7.90 (d, *J* = 8.2 Hz, 2H), 7.38 (d, *J* = 8.1 Hz, 2H), 4.45 (d, *J* = 4.5 Hz, 1H), 4.35 (d, *J* = 6.0 Hz, 2H), 3.87 (d, *J* = 6.8 Hz, 1H), 3.84 (s, 3H), 3.71 (d, *J* = 5.8 Hz, 2H), 3.29 (2H), 2.25 – 1.96 (m, 2H), 1.95 – 1.59 (m, 5H), 1.55 – 1.25 (m, 9H), 1.25 – 0.93 (m, 7H), 0.93 – 0.85 (m, 7H), 0.60 (s, 3H); ¹³C NMR (101 MHz, DMSO-*d*₆) δ 173.14, 169.42, 166.12, 145.21, 129.17, 128.09, 127.31, 69.75, 69.49, 55.89, 54.79, 52.11, 43.11, 43.04, 42.19, 41.78, 38.75, 38.28, 37.76, 37.29, 35.02, 34.86, 33.79, 32.21, 31.46, 30.27, 28.22, 26.76, 23.35, 20.88, 18.53, 12.08. HRMS (ESI) for C₂₈H₄₇NO₄ calculated [[M + H] + [-H₂O]]⁺: 579.3798. Obtained: 579.3783.

Synthesis of methyl ((R)-4-((3R,5S,7S,8R,9S,10S,13R,14S,17R)-3,7-dihydroxy-10,13-dimethylhexadecahydro-1H-cyclopenta[a]phenanthren-17-yl)pentanoyl)-L-alaninate (3c).



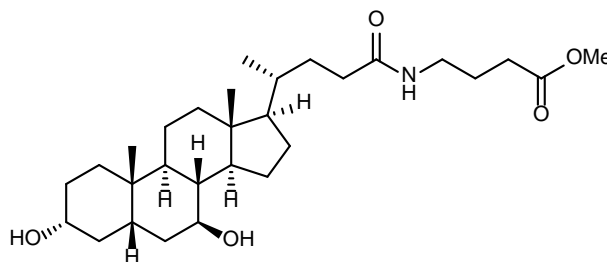
This compound was prepared following the **method A**. Ursodeoxycholic acid (392.6 mg, 1 mmol) L-Alanine methyl ester hydrochloride (139.6 mg, 1 mmol) TBTU (385.3 mg, 1.2 mmol), Et₃N (1.1 ml, 3.26 M) White solid. Yield 45%; m.p. 103-105 °C; IR 3296, 2928, 2863, 1739, 1650, 1209, 1049 cm⁻¹; ¹H NMR (400 MHz, DMSO-*d*₆) δ 8.19 (d, *J* = 7.0 Hz, 1H), 4.44 (d, *J* = 4.5 Hz, 1H), 4.23 (p, *J* = 7.2 Hz, 1H), 3.87 (d, *J* = 6.8 Hz, 1H), 3.60 (s, 3H), signal corresponding to 2H overlapped with broad signal of water at 3.29 ppm (confirmed by COSY), 2.19 – 1.88 (m, 3H), 1.88 – 1.57 (m, 4H), 1.56 – 1.27 (m, 9H), 1.27 – 0.93 (m, 12H), 0.93 – 0.82 (m, 7H), 0.61 (s, 3H); ¹³C NMR (101 MHz, DMSO-*d*₆) δ 173.26, 172.52, 69.71, 69.45, 55.87, 54.71, 51.72, 47.41, 43.07, 43.01, 42.16, 38.71, 37.72, 37.27, 34.87, 34.82, 33.75, 31.94, 31.47, 30.24, 28.16, 26.71, 23.31, 20.84, 18.47, 16.93, 12.03; HRMS (ESI) for C₂₈H₄₈NO₅ calculated [M + H]⁺: 478.3532. Obtained: 478.3531.

Synthesis of methyl 3-((R)-4-((3R,5S,7S,8R,9S,10S,13R,14S,17R)-3,7-dihydroxy-10,13-dimethylhexadecahydro-1H-cyclopenta[a]phenanthren-17-yl)pentanamido)propanoate (3d).



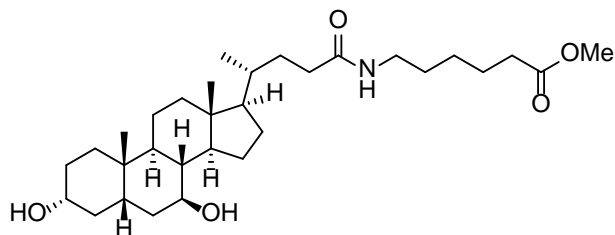
This compound was prepared following the **method A**. Ursodeoxycholic acid (392.6 mg, 1 mmol) β -Alanine ethyl ester hydrochloride (153.6 mg, 1 mmol), TBTU (385.3 mg, 1.2 mmol) Et_3N (1.1 ml 3.26 M). White solid. Yield 66%; m.p. 84-86 °C; IR 3292, 2927, 2862, 1734, 1647, 1180, 1049 cm^{-1} ; ^1H NMR (400 MHz, $\text{DMSO-}d_6$) δ 7.85 (t, $J = 5.7$ Hz, 1H), 4.43 (d, $J = 4.6$ Hz, 1H), 4.05 (q, $J = 7.1$ Hz, 2H), 3.86 (d, $J = 6.8$ Hz, 1H), 3.29 (2H), 3.24 (q, $J = 6.5$ Hz, 2H), 2.41 (t, $J = 6.8$ Hz, 2H), 2.12 – 1.89 (m, 4H), 1.89 – 1.59 (m, 4H), 1.53 – 1.25 (m, 9H), 1.24 – 0.90 (m, 11H), 0.87 (t, $J = 3.3$ Hz, 7H), 0.61 (s, 3H); ^{13}C NMR (101 MHz, $\text{DMSO-}d_6$) δ 172.63, 171.30, 69.70, 69.45, 59.86, 55.86, 54.69, 43.06, 43.00, 42.16, 38.71, 37.72, 37.26, 34.90, 34.82, 34.65, 33.90, 33.75, 32.29, 31.60, 30.24, 28.15, 26.70, 23.31, 20.84, 18.45, 14.08, 12.01; HRMS (ESI) for $\text{C}_{29}\text{H}_{50}\text{NO}_5$ calculated $[\text{M} + \text{H}]^+$: 492.3689. Obtained: 492.3684.

Synthesis of methyl 4-((R)-4-((3R,5S,7S,8R,9S,10S,13R,14S,17R)-3,7-dihydroxy-10,13-dimethylhexadecahydro-1H-cyclopenta[a]phenanthren-17-yl)pentanamido)butanoate (3e).



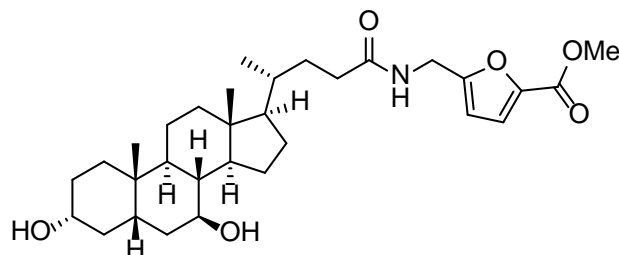
This compound was prepared following the **method A**. Ursodeoxycholic acid (392.6 mg, 1 mmol) 4-aminobutirate methyl ester hydrochloride (153.6 mg, 1 mmol) TBTU (385.3 mg, 1.2 mmol) Et₃N (1.1 ml 3.26 M). White solid. Yield 37 %; m.p. 92-94 °C; IR 3295, 2927, 2862, 1736, 1646, 1170, 1050 cm⁻¹; ¹H NMR (400 MHz, DMSO-*d*₆) δ 7.77 (t, *J* = 5.7 Hz, 1H), 4.42 (d, *J* = 4.6 Hz, 1H), 3.85 (d, *J* = 6.8 Hz, 1H), 3.58 (s, 3H), 3.02 (q, *J* = 6.5 Hz, 2H), 2.29 (t, *J* = 7.5 Hz, 2H), 2.15 – 2.00 (m, 1H), 2.01 – 1.53 (m, 9H), 1.54 – 1.24 (m, 8H), 1.24 – 0.90 (m, 7H), 0.88 (d, *J* = 7.4 Hz, 7H), 0.60 (s, 3H); ¹³C NMR (101 MHz, DMSO-*d*₆) δ 173.04, 172.45, 69.67, 69.41, 55.83, 54.66, 51.20, 43.03, 42.97, 42.13, 38.68, 37.69, 37.60, 37.23, 34.87, 34.79, 33.72, 32.38, 31.63, 30.65, 30.21, 28.14, 26.67, 24.52, 23.28, 20.80, 18.42, 11.96; HRMS (ESI) for C₂₉H₅₀NO₅ calculated [M + H]⁺: 492.3689. Obtained: 492.3686.

Synthesis of methyl 6-((R)-4-((3R,5S,7S,8R,9S,10S,13R,14S,17R)-3,7-dihydroxy-10,13-dimethylhexadecahydro-1H-cyclopenta[a]phenanthren-17-yl)pentanamido)hexanoate (3f).



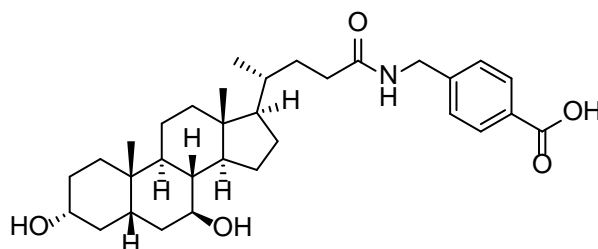
This compound was prepared following the **method A**. Ursodeoxycholic acid (392.6 mg, 1 mmol), 6-aminohexanoate methyl ester hydrochloride (181.7 mg, 1 mmol) TBTU (385.3 mg, 1.2 mmol) and Et₃N (1.1 ml 3.26 M). White solid. Yield 42%; m.p. 78-80 °C; IR 3299, 2926, 2861, 1736, 1644, 1165, 1050 cm⁻¹; ¹H NMR (400 MHz, DMSO-*d*₆) δ 7.71 (t, *J* = 5.7 Hz, 1H), 4.43 (d, *J* = 4.5 Hz, 1H), 3.86 (d, *J* = 6.7 Hz, 1H), 3.58 (s, 3H), 3.29 (2H), 2.99 (q, *J* = 7.1 Hz, 2H), 2.28 (t, *J* = 7.4 Hz, 2H), 2.14 – 1.56 (m, 10H), 1.56 – 0.91 (m, 20H), 0.88 (d, *J* = 7.2 Hz, 8H), 0.60 (s, 3H); ¹³C NMR (101 MHz, DMSO-*d*₆) δ 173.26, 172.28, 69.70, 69.45, 55.87, 54.70, 51.15, 43.06, 43.00, 42.16, 38.71, 38.12, 37.71, 37.26, 34.90, 34.82, 33.75, 33.22, 32.44, 31.69, 30.24, 28.82, 28.16, 26.70, 25.84, 24.15, 23.30, 20.83, 18.45, 12.00; HRMS (ESI) for C₃₁H₅₄NO₅ calculated [M + H]⁺: 520.4002. Obtained: 520.3997.

Synthesis of methyl 5-(((R)-4-((3R,5S,7S,8R,9S,10S,13R,14S,17R)-3,7-dihydroxy-10,13-dimethylhexadecahydro-1H-cyclopenta[a]phenanthren-17-yl)pentanamido)methyl)furan-2-carboxylate (3g).



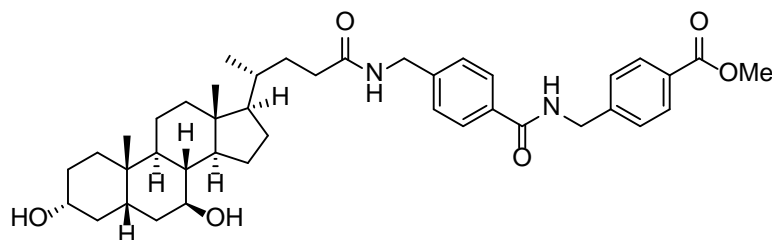
This compound was prepared following the **method A**. Ursodeoxycholic acid (145 mg, 0.37 mmol), 5-(aminomethyl)furan-2-carboxylate methyl ester hydrochloride (70.9 mg, 0.37) TBTU (146.4 mg, 0.46 mmol) Et₃N (0.41 ml 3.26 M). White solid. Yield 52%; m.p. 240-242 °C; IR 3463, 3285, 2935, 1705, 1683, 1518, 1210, 763 cm⁻¹; ¹H NMR (400 MHz, DMSO-*d*₆) δ 8.38 (t, *J* = 5.8 Hz, 1H), 7.23 (d, *J* = 3.5 Hz, 1H), 6.40 (d, *J* = 3.4 Hz, 1H), 4.42 (d, *J* = 4.5 Hz, 1H), 4.29 (d, *J* = 5.7 Hz, 2H), 3.85 (d, *J* = 6.8 Hz, 1H), 3.79 (s, 3H), signal corresponding to 2H overlapped with broad signal of water at 3.29 ppm (confirmed by COSY), 2.09 (m, *J* = 39.5, 14.2, 7.9 Hz, 2H), 1.96 – 1.58 (m, 5H), 1.54 – 1.24 (m, 10H), 1.24 – 0.90 (m, 8H), 0.87 (d, *J* = 6.5 Hz, 7H), 0.58 (s, 3H); ¹³C NMR (101 MHz, DMSO-*d*₆) δ 172.63, 158.23, 157.68, 142.62, 119.31, 109.11, 69.71, 69.45, 55.85, 54.69, 51.65, 43.06, 43.00, 42.16, 39.99, 38.71, 37.72, 37.27, 35.57, 34.86, 34.82, 33.75, 32.20, 31.54, 30.24, 28.15, 26.70, 23.30, 20.83, 18.42, 11.99; HRMS (ESI) for C₃₁H₅₁N₂O₆ calculated [M + NH₄]⁺: 547.3745. Obtained: 547.3738.

Synthesis of 4-(((4R)-4-((3R,5S,7S,8R,9S,10S,13R,14S)-3,7-dihydroxy-10,13-dimethylhexadecahydro-1H-cyclopenta[a]phenanthren-17-yl)pentanamido)methyl)benzoic acid (4a).



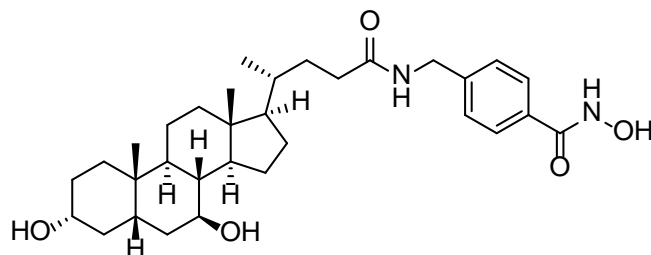
This compound was prepared following the **method B**. 4-(((4R)-4-((3R,5S,7S,8R,9S,10S,13R,14S)-3,7-dihydroxy-10,13-dimethylhexadecahydro-1H-cyclopenta[a]phenanthren-17-yl)pentanamido)methyl) benzoate (1079 mg, 2 mmol), NaOH (8.7 ml 0.5M). White solid. Yield 90%; m.p. 155-157 °C; IR 3288, 2922, 2851, 1638, 1542, 1281, 1015 cm^{-1} ; ^1H NMR (400 MHz, $\text{DMSO-}d_6$) δ 12.85 (s, 1H), 8.37 (t, $J = 6.0$ Hz, 1H), 7.88 (d, $J = 8.2$ Hz, 2H), 7.34 (d, $J = 8.1$ Hz, 2H), 4.48 – 4.39 (m, 1H), 4.34 – 4.28 (m, 2H), 3.86 (d, $J = 6.8$ Hz, 1H), signal corresponding to 2H overlapped with broad signal of water at 3.29 ppm, 2.24 – 2.01 (m, 2H), 1.98 – 1.60 (m, 6H), 1.53 – 1.26 (m, 10H), 1.26 – 0.93 (m, 7H), 0.93 – 0.85 (m, 7H), 0.61 (s, 3H); ^{13}C NMR (101 MHz, $\text{DMSO-}d_6$) δ 172.67, 167.15, 145.01, 129.30, 129.19, 127.10, 69.73, 69.47, 55.88, 54.76, 43.09, 43.01, 42.18, 41.77, 39.84, 38.74, 37.73, 37.27, 34.89, 34.83, 33.76, 32.38, 31.65, 30.25, 28.19, 26.72, 23.32, 20.85, 18.44, 12.01; HRMS (ESI) para $\text{C}_{32}\text{H}_{48}\text{NO}_5$ calculated $[\text{M} + \text{H}]^+$: 525.3532. Obtained: 525.3538.

Synthesis of methyl 4-(((4R)-4-((3R,5S,7S,8R,9S,10S,13R,14S)-3,7-dihydroxy-10,13-dimethylhexadecahydro-1H-cyclopenta[a]phenanthren-17-yl)pentanamido)methyl)benzamido)methyl)benzoate (6a).



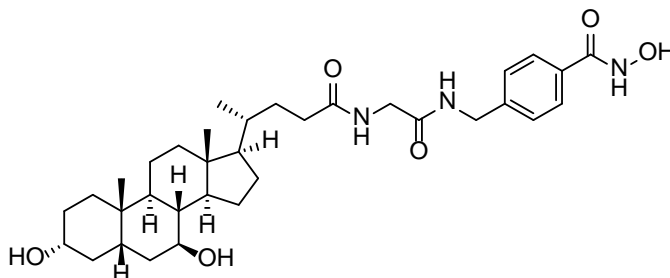
This compound was prepared following the **method A**. 4-(((4R)-4-((3R,5S,7S,8R,9S,10S,13R,14S)-3,7-dihydroxy-10,13-dimethylhexadecahydro-1H-cyclopenta[a]phenanthren-17-yl)pentanamido)methyl) benzoic acid (200 mg, 0.38 mmol) methyl 4-(aminomethyl) benzoate hydrochloride (76.6 mg 0.38 mmol) TBTU (146.4 mg 0.46 mmol) Et₃N (0.42 ml 3.26 M). White solid. Yield 60%; m.p.139-141 °C; IR 3301, 2926, 2861, 1719, 1638, 1276, 1107, 1047 cm⁻¹; ¹H NMR (400 MHz, DMSO-*d*₆) δ 9.08 (t, *J* = 6.0 Hz, 1H), 8.36 (t, *J* = 6.0 Hz, 1H), 7.92 (d, *J* = 8.1 Hz, 2H), 7.85 (d, *J* = 8.1 Hz, 2H), 7.44 (d, *J* = 8.1 Hz, 2H), 7.32 (d, *J* = 8.1 Hz, 2H), 4.55 (d, *J* = 5.9 Hz, 2H), 4.45 (d, *J* = 4.5 Hz, 1H), 4.36 – 4.15 (m, 2H), 3.87 (d, *J* = 6.8 Hz, 1H), 3.83 (s, 3H), 3.29 (2H), 2.23 – 2.01 (m, 2H), 1.97 – 1.59 (m, 6H), 1.55 – 1.25 (m, 10H), 1.25 – 0.93 (m, 7H), 0.93 – 0.82 (m, 7H), 0.61 (s, 3H); ¹³C NMR (101 MHz, DMSO-*d*₆) δ 172.67, 166.11, 145.41, 143.37, 132.52, 129.25, 128.10, 127.29, 126.95, 69.73, 69.48, 55.88, 54.77, 52.06, 43.10, 43.02, 42.40, 42.18, 41.71, 38.73, 37.73, 37.28, 34.91, 34.84, 33.77, 32.41, 31.68, 30.25, 28.20, 26.73, 23.32, 20.86, 18.46, 12.04; HRMS (ESI) for C₄₁H₅₇N₂O₆ calculated [M + H]⁺: 673.4216. Obtained: 673.4214.

Synthesis of 4-(((4R)-4-((3R,5S,7S,8R,9S,10S,13R,14S)-3,7-dihydroxy-10,13-dimethylhexadecahydro-1H-cyclopenta[a]phenanthren-17-yl)pentanamido)methyl)-N-hydroxybenzamide. UDCA-HDAC6i #1.



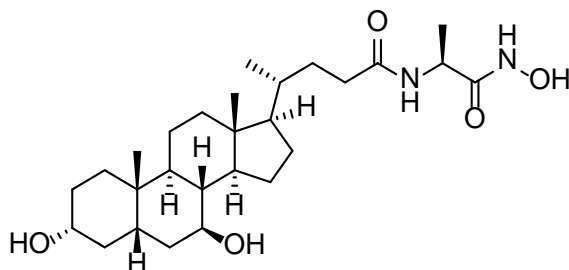
This compound was prepared following the method A. Methyl 4-(((4R)-4-((3R,5S,7S,8R,9S,10S,13R,14S)-3,7-dihydroxy-10,13-dimethylhexadecahydro-1H-cyclopenta[a]phenanthren-17-yl)pentanamido)methyl) benzoate (539.4 mg, 1 mmol), hydroxylamine hydrochloride (694.9 mg, 10 mmol), phenolphthalein (1 mg), sodium methoxide (2000 mg, 37 mmol). White solid. Yield 61 %; m.p. 170-172 °C; IR 3275, 2927, 2862, 1638, 1535, 1012 cm^{-1} ; ^1H NMR (400 MHz, $\text{DMSO-}d_6$) δ 11.17 (s, 1H), 9.01 (s, 1H), 8.34 (t, $J = 6.0$ Hz, 1H), 7.69 (d, $J = 8.1$ Hz, 2H), 7.29 (d, $J = 8.1$ Hz, 2H), 4.44 (d, $J = 4.5$ Hz, 1H), 4.28 (dd, $J = 5.9, 3.6$ Hz, 2H), 3.87 (d, $J = 6.8$ Hz, 1H), 3.29 (2H). 2.24 – 2.01 (m, 2H), 1.99 – 1.59 (m, 6H), 1.56 – 1.26 (m, 10H), 1.26 – 0.94 (m, 7H), 0.94 – 0.84 (m, 7H), 0.62 (s, 3H); ^{13}C NMR (101 MHz, $\text{DMSO-}d_6$) δ 172.63, 163.99, 143.06, 131.18, 126.92, 126.83, 69.73, 69.47, 55.88, 54.76, 43.09, 43.02, 42.18, 41.71, 39.85, 38.73, 37.73, 37.27, 34.93, 34.84, 33.77, 32.38, 31.67, 30.25, 28.21, 26.73, 23.33, 20.86, 18.44, 12.04; HRMS (ESI) for $\text{C}_{32}\text{H}_{47}\text{N}_2\text{O}_4$ calculated $[[\text{M} + \text{H}] + [-\text{H}_2\text{O}]]^+$: 523.3536. Obtained: 523.3536.

Synthesis of 4-((2-((R)-4-((3R,5S,7S,8R,9S,10S,13R,14S,17R)-3,7-dihydroxy-10,13-dimethylhexadecahydro-1H-cyclopenta[a]phenanthren-17-yl)pentanamido)acetamido)methyl)-N-hydroxybenzamide. UDCA-HDAC6i #2.



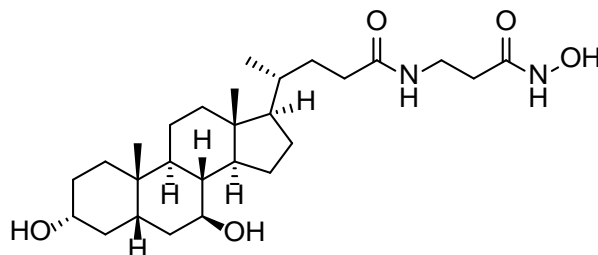
This compound was prepared following the **method A**. Methyl 4-((2-((4R)-4-((3R,5S,7S,8R,9S,10S,13R,14S)-3,7-dihydroxy-10,13-dimethylhexadecahydro-1H-cyclopenta[a]phenanthren-17-yl)pentanamido)acetamido) methyl)benzoate (83.9 mg, 0.14 mmol), hydroxylamine hydrochloride (97.3 mg, 1.4 mmol), phenolphthalein (1 mg), sodium methoxide (2000 mg, 37 mmol). White solid. Yield 42% m.p. 153-155 °C; IR 3217, 2928, 2864, 1641, 1534, 1013 cm^{-1} ; ^1H NMR (400 MHz, $\text{DMSO-}d_6$) δ 11.17 (s, 1H), 8.98 (s, 1H), 8.35 (t, $J = 6.0$ Hz, 1H), 8.05 (t, $J = 5.9$ Hz, 1H), 7.69 (d, $J = 8.1$ Hz, 2H), 7.30 (d, $J = 8.0$ Hz, 2H), 4.46 – 4.40 (m, 1H), 4.31 (d, $J = 6.0$ Hz, 2H), 3.86 (d, $J = 6.7$ Hz, 1H), 3.71 (d, $J = 5.9$ Hz, 2H), 3.29 (2H), 2.11 (m, $J = 57.0$, 14.2, 10.0, 5.6 Hz, 2H), 1.97 – 1.89 (m, 1H), 1.90 – 1.58 (m, 5H), 1.54 – 1.25 (m, 10H), 1.25 – 0.93 (m, 7H), 0.93 – 0.83 (m, 7H), 0.61 (s, 3H); ^{13}C NMR (101 MHz, $\text{DMSO-}d_6$) δ 173.04, 169.24, 164.03, 142.70, 131.21, 126.94, 126.81, 69.71, 69.46, 55.87, 54.73, 43.07, 43.01, 42.17, 42.10, 41.71, 38.72, 37.72, 37.27, 34.98, 34.83, 33.76, 32.18, 31.42, 30.25, 28.18, 26.72, 23.31, 20.85, 18.51, 12.05; HRMS (ESI) for $\text{C}_{34}\text{H}_{52}\text{N}_3\text{O}_6$ calculated $[\text{M} + \text{H}]^+$: 598.3856. Obtained: 598.3857.

Synthesis of (R)-4-((3R,5S,7S,8R,9S,10S,13R,14S,17R)-3,7-dihydroxy-10,13-dimethylhexadecahydro-1H-cyclopenta[a]phenanthren-17-yl)-N-((S)-1-(hydroxyamino)-1-oxopropan-2-yl) pentanamide. UDCA-HDAC6i #3.



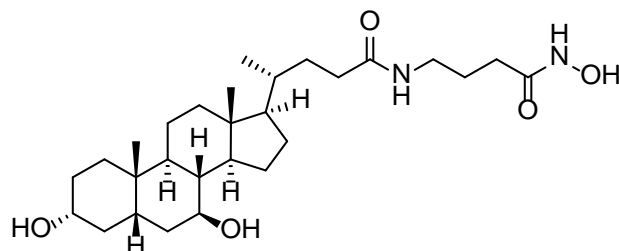
This compound was prepared following the **method A**. Methyl ((4R)-((3R,5S,7S,8R,9S,10S,13R,14S)-3,7-dihydroxy-10,13-dimethylhexadecahydro-1H-cyclopenta[a]phenanthren-17-yl)pentanoyl)-L-alaninate (193 mg, 0.4 mmol), hydroxylamine hydrochloride (278 mg, 4 mmol), phenolphthalein (1 mg), sodium methoxide (2000 mg, 37 mmol). White solid. Yield 22%. m.p. 170-172 °C; IR 3265, 2928, 2863, 1642, 1537, 1047 cm^{-1} ; ^1H NMR (400 MHz, $\text{DMSO}-d_6$) δ 7.96 (d, $J = 7.8$ Hz, 1H), 4.44 (s, 1H), 4.17 (p, $J = 7.1$ Hz, 1H), 3.86 (d, $J = 6.6$ Hz, 1H), 3.29 (2H), 2.13 (m, $J = 14.8, 10.2, 5.2$ Hz, 1H), 2.04 – 1.89 (m, 2H), 1.89 – 1.55 (m, 4H), 1.54 – 1.24 (m, 10H), 1.22 – 0.93 (m, 11H), 0.88 (d, $J = 6.1$ Hz, 7H), 0.61 (s, 3H); ^{13}C NMR (101 MHz, $\text{DMSO}-d_6$) δ 172.19, 169.09, 69.71, 69.45, 55.87, 54.71, 45.74, 43.07, 43.01, 42.16, 38.72, 37.72, 37.26, 35.03, 34.83, 33.75, 32.10, 31.48, 30.24, 28.18, 26.72, 23.31, 20.84, 18.49, 12.04. HRMS (ESI) for $\text{C}_{27}\text{H}_{47}\text{N}_2\text{O}_5$ calculated $[\text{M} + \text{H}]^+$: 479.3485. Obtained: 479.3483.

Synthesis of (R)-4-((3R,5S,7S,8R,9S,10S,13R,14S,17R)-3,7-dihydroxy-10,13-dimethylhexadecahydro-1H-cyclopenta[a]phenanthren-17-yl)-N-(3-(hydroxyamino)-3-oxopropyl)pentanamide. UDCA-HDAC6i #4.



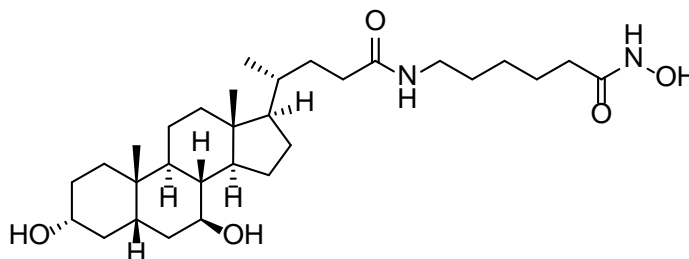
This compound was prepared following the **method A**. Ethyl 3-((4R)-4-((3R,5S,7S,8R,9S,10S,13R,14S)-3,7-dihydroxy-10,13-dimethylhexadecahydro-1H-cyclopenta[a]phenanthren-17-yl)pentanamido)propanoate (298 mg, 0.61 mmol), hydroxylamine hydrochloride (424.5 mg, 6.1 mmol), phenolphthalein (1 mg), sodium methoxide (2000 mg, 37 mmol). White solid. Yield 59%; m.p. 180-182 °C; IR 3271, 2927, 2862, 1638, 1542, 1047 cm^{-1} ; ^1H NMR (400 MHz, DMSO-d_6) δ 7.82 (t, $J = 5.7$ Hz, 1H), 4.43 (s, 1H), 3.86 (d, $J = 6.8$ Hz, 1H), 3.30 (s, 2H), 3.19 (q, $J = 6.8$ Hz, 2H), 2.11 (m, 2H), 1.99 – 1.56 (m, 8H), 1.54 – 1.24 (m, 8H), 1.23 – 0.90 (m, 9H), 0.87 (d, $J = 4.4$ Hz, 7H), 0.61 (s, 3H); ^{13}C NMR (101 MHz, DMSO-d_6) δ 172.53, 167.03, 69.71, 69.45, 55.86, 54.70, 43.07, 43.01, 42.16, 39.99, 38.71, 37.72, 37.27, 35.27, 34.98, 34.83, 33.75, 32.53, 32.35, 31.59, 30.24, 28.17, 26.71, 23.31, 20.84, 18.47, 12.04; HRMS (ESI) for $\text{C}_{27}\text{H}_{47}\text{N}_2\text{O}_5$ calculated $[\text{M} + \text{H}]^+$: 479.3485. Obtained: 479.3480.

Synthesis of (R)-4-((3R,5S,7S,8R,9S,10S,13R,14S,17R)-3,7-dihydroxy-10,13-dimethylhexadecahydro-1H-cyclopenta[a]phenanthren-17-yl)-N-(4-(hydroxyamino)-4-oxobutyl)pentanamide. UDCA-HDAC6i #5.



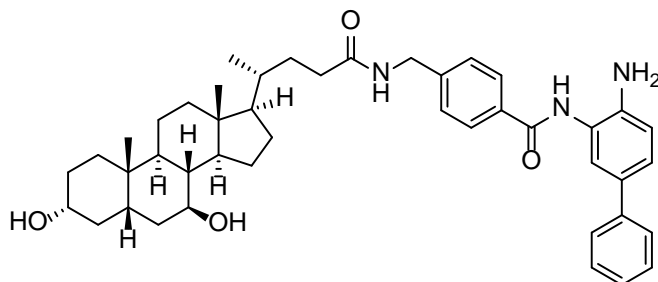
This compound was prepared following the **method A**. Methyl 4-((4R)-4-((3R,5S,7S,8R,9S,10S,13R,14S)-3,7-dihydroxy-10,13-dimethylhexadecahydro-1H-cyclopenta[a]phenanthren-17-yl)pentanamido)butanoate (165 mg, 0.34 mmol), hydroxylamine hydrochloride (236.6 mg, 3.4 mmol), phenolphthalein (1 mg), sodium methoxide (2000 mg, 37 mmol). White solid. Yield 54%. m.p. 165-167 °C; IR 3269, 2928, 2862, 1643, 1550, 1047 cm^{-1} ; ^1H NMR (400 MHz, $\text{DMSO-}d_6$) δ 7.81 (t, $J = 5.6$ Hz, 1H), 4.46 (s, 1H), 3.88 (d, $J = 6.6$ Hz, 1H), 3.29 ppm 3.00 (q, $J = 6.6$ Hz, 2H), 2.16 – 1.91 (m, 6H), 1.89 – 1.54 (m, 7H), 1.54 – 1.25 (m, 9H), 1.25 – 0.92 (m, 9H), 0.89 (d, $J = 7.8$ Hz, 7H), 0.62 (s, 3H); ^{13}C NMR (101 MHz, $\text{DMSO-}d_6$) δ 172.45, 168.69, 69.71, 69.45, 55.87, 54.70, 43.07, 43.01, 42.17, 38.72, 38.05, 37.72, 37.27, 34.97, 34.83, 33.76, 32.43, 31.67, 30.24, 29.91, 28.18, 26.72, 25.45, 23.31, 20.84, 18.48, 12.03; HRMS (ESI) for $\text{C}_{28}\text{H}_{49}\text{N}_2\text{O}_5$ calculated $[\text{M} + \text{H}]^+$: 493.3641. Obtained: 493.3642.

Synthesis of 6-((R)-4-((3R,5S,7S,8R,9S,10S,13R,14S, 17R)-3,7-dihydroxy-10,13-dimethylhexadecahydro-1H-cyclopenta[a]phenanthren-17-yl)pentanamido)-N-hydroxyhexanamide. UDCA-HDAC6i #6.



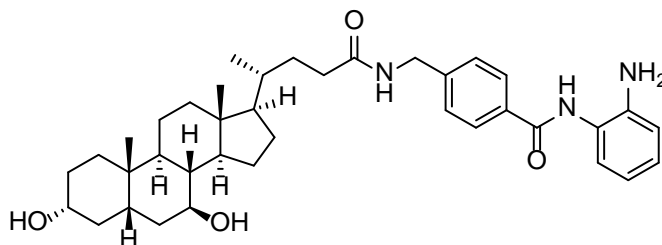
This compound was prepared following the **method A**. Methyl 6-((4R)-4-((3R,5S,7S,8R,9S,10S,13R,14S)-3,7-dihydroxy-10,13-dimethylhexadecahydro-1H-cyclopenta[a]phenanthren-17-yl)pentanamido)hexanoate (200 mg, 0.38 mmol), hydroxylamine hydrochloride (262.9, 3.8 mmol), phenolphthalein (1 mg), sodium methoxide (2000 mg, 37 mmol). White solid. Yield 43%; m.p. 125-127 °C; IR 3269, 2927, 2861, 1642, 1547, 1047 cm^{-1} ; ^1H NMR (400 MHz, $\text{DMSO-}d_6$) δ 10.32 (s, 1H), 8.64 (s, 1H), 7.71 (t, $J = 5.6$ Hz, 1H), 4.43 (d, $J = 4.5$ Hz, 1H), 3.86 (d, $J = 6.8$ Hz, 1H), 3.29 (2H), 2.98 (q, $J = 6.5$ Hz, 2H), 2.06 (m, $J = 14.5, 9.7, 5.2$ Hz, 1H), 2.00 – 1.53 (m, 9H), 1.55 – 1.26 (m, 14H), 1.26 – 0.90 (m, 9H), 0.88 (d, $J = 7.3$ Hz, 7H), 0.61 (s, 3H); ^{13}C NMR (101 MHz, $\text{DMSO-}d_6$) δ 172.28, 168.99, 69.71, 69.45, 55.87, 54.70, 43.07, 43.00, 42.16, 38.72, 38.27, 37.72, 37.26, 34.93, 34.82, 33.75, 32.43, 32.20, 31.69, 30.24, 28.93, 28.18, 26.71, 26.04, 24.88, 23.31, 20.84, 18.47, 12.02; HRMS (ESI) for $\text{C}_{30}\text{H}_{53}\text{N}_2\text{O}_5$ calculated $[\text{M} + \text{H}]^+$: 521.3954. Obtained: 521.3955.

Synthesis of N-(4-amino-[1,1'-biphenyl]-3-yl)-4-(((R)-4-((3R,5S,7S,8R,9S,10S,13R,14S,17R)-3,7-dihydroxy-10,13-dimethylhexadecahydro-1H-cyclopenta[a]phenanthren-17-yl)pentanamido)methyl)benzamide. UDCA-HDAC6i #7.



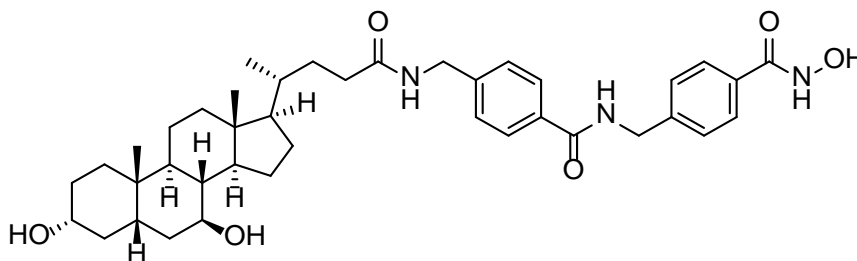
This compound was prepared following the **method B** Tert-butyl (3-(4-(((4R)-4-((3R,5S,7S,8R,9S,10S,13R,14S)-3,7-dihydroxy-10,13-dimethylhexadecahydro-1H-cyclopenta[a]phenanthren-17-yl)pentanamido)methyl) benzamido)-[1,1'-biphenyl]-4-yl)carbamate (53 mg, 0.07 mmol) HCl 4M in dioxane (0.3 ml). White solid. Yield 22%; m.p. 163-165 °C; IR 3321, 2927, 2862, 1649, 1489, 1048, 760, 698 cm⁻¹; ¹H NMR (400 MHz, DMSO-*d*₆) δ 9.70 (s, 1H), 8.39 (t, *J* = 6.0 Hz, 1H), 7.95 (d, *J* = 7.9 Hz, 2H), 7.59 – 7.49 (m, 3H), 7.45 – 7.29 (m, 5H), 7.25 (q, *J* = 7.3, 6.6 Hz, 1H), 6.87 (d, *J* = 8.3 Hz, 1H), 5.08 (s, 2H), 4.43 (d, *J* = 4.6 Hz, 1H), 4.33 (dd, *J* = 5.9, 3.8 Hz, 2H), 3.86 (d, *J* = 6.8 Hz, 1H), signal corresponding to 2H overlapped with broad signal of water at 3.29 ppm, 2.29 – 1.88 (m, 3H), 1.89 – 1.59 (m, 6H), 1.54 – 1.26 (m, 10H), 1.26 – 0.97 (m, 4H), 0.97 – 0.83 (m, 9H), 0.62 (s, 3H); ¹³C NMR (101 MHz, DMSO-*d*₆) δ 172.66, 165.23, 143.46, 142.74, 140.17, 132.98, 128.78, 128.13, 127.81, 126.83, 126.00, 125.49, 124.75, 124.65, 123.60, 116.52, 69.71, 69.46, 55.88, 54.75, 43.09, 43.01, 42.16, 41.73, 38.72, 37.72, 37.27, 34.93, 34.83, 33.76, 32.41, 31.70, 30.24, 28.20, 26.73, 23.31, 20.85, 18.46, 12.04; HRMS (ESI) for C₄₄H₅₈N₃O₄ calculated [M + H]⁺: 692.4427. Obtained: 692.4414.

Synthesis of N-(2-aminophenyl)-4-(((R)-4-(((3R,5S,7S,8R,9S,10S,13R,14S,17R)-3,7-dihydroxy-10,13-dimethylhexadecahydro-1H-cyclopenta[a]phenanthren-17-yl)pentanamido)methyl)benzamide. UDCA-HDAC6i #8.



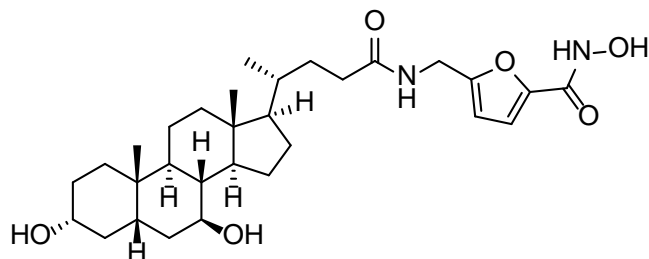
This compound was prepared following the method B. 4-(((4R)-4-(((3R,5S,7S,8R,9S,10S,13R,14S)-3,7-dihydroxy-10,13-dimethylhexadecahydro-1H-cyclopenta[a]phenanthren-17-yl)pentanamido)methyl)benzoic acid (200 mg, 0.38 mmol) *o*-Phenylenediamine (41.1 mg 0.38 mmol) TBTU (146.4 mg 0.46 mmol) Et₃N (0.42 ml 3.26 M). White solid. Yield 39 %; m.p. 168-170 °C; IR 3294, 2927, 2862, 1647, 1505, 1048, 745 cm⁻¹; ¹H NMR (400 MHz, DMSO-*d*₆) δ 9.61 (s, 1H), 8.38 (t, *J* = 6.0 Hz, 1H), 7.92 (d, *J* = 7.9 Hz, 2H), 7.35 (d, *J* = 7.9 Hz, 2H), 7.16 (d, *J* = 7.9 Hz, 1H), 7.04 – 6.92 (m, 1H), 6.78 (dd, *J* = 8.0, 1.4 Hz, 1H), 6.69 – 6.49 (m, 1H), 4.88 (s, 2H), 4.42 (d, *J* = 4.6 Hz, 1H), 4.37 – 4.25 (m, 2H), 3.86 (d, *J* = 6.8 Hz, 1H), 3.29 (2H), 2.25 – 2.01 (m, 2H), 1.98 – 1.58 (m, 6H), 1.56 – 1.27 (m, 9H), 1.27 – 0.94 (m, 5H), 0.94 – 0.82 (m, 10H), 0.62 (s, 3H); ¹³C NMR (101 MHz, DMSO-*d*₆) δ 172.63, 165.05, 143.38, 143.11, 132.99, 127.74, 126.81, 126.66, 126.43, 123.32, 116.23, 116.11, 69.70, 69.46, 55.87, 54.75, 43.08, 43.01, 42.15, 41.71, 38.71, 37.71, 37.26, 34.91, 34.82, 33.75, 32.39, 31.69, 30.24, 28.19, 26.72, 23.31, 20.84, 18.45, 12.03; HRMS (ESI) for C₃₈H₅₄N₃O₄ calculated [M + H]⁺: 616.4114. Obtained: 616.4110.

Synthesis of 4-(((R)-4-((3R,5S,7S,8R,9S,10S,13R,14S,17R)-3,7-dihydroxy-10,13-dimethylhexadecahydro-1H-cyclopenta[a]phenanthren-17-yl)pentanamido)methyl)-N-(4-(hydroxycarbonyl) benzyl)benzamide. UDCA-HDAC6i #9.



This compound was prepared following the **method C**. Methyl 4-(((4-(((4R)-4-((3R,5S,7S,8R,9S,10S,13R,14S)-3,7-dihydroxy-10,13-dimethylhexadecahydro-1H-cyclopenta[a]phenanthren-17-yl)pentanamido)methyl)benzamido)methyl)benzoate (133.7 mg, 0.2 mmol), hydroxylamine hydrochloride (139.2, 2 mmol), phenolphthalein (1 mg), sodium methoxide (2000 mg, 37 mmol). White solid. Yield 60 %; m.p. 187-189 °C; IR 3288, 2922, 2851, 1638, 1542, 1015 cm^{-1} ; ^1H NMR (400 MHz, $\text{DMSO-}d_6$) δ 9.03 (t, $J = 6.0$ Hz, 1H), 8.35 (t, $J = 6.0$ Hz, 1H), 7.84 (d, $J = 8.0$ Hz, 2H), 7.70 (d, $J = 7.9$ Hz, 2H), 7.33 (dd, $J = 10.4, 8.0$ Hz, 4H), 4.50 (d, $J = 5.9$ Hz, 2H), 4.46 – 4.40 (m, 1H), 4.36 – 4.22 (m, 2H), 3.88 (s, 1H), 3.92 (2H), 2.28 – 1.99 (m, 2H), 1.99 – 1.56 (m, 5H), 1.54 – 1.25 (m, 9H), 1.25 – 0.94 (m, 8H), 0.94 – 0.84 (m, 8H), 0.61 (s, 3H); ^{13}C NMR (101 MHz, $\text{DMSO-}d_6$) δ 172.63, 166.03, 164.08, 143.29, 142.96, 132.60, 131.26, 127.24, 126.99, 126.90, 69.71, 69.46, 55.86, 54.74, 43.08, 43.01, 42.35, 42.16, 41.69, 39.99, 38.71, 37.71, 37.27, 34.91, 34.82, 33.76, 32.38, 31.66, 30.24, 28.18, 26.72, 23.31, 20.84, 18.45, 12.03; HRMS (ESI) for $\text{C}_{40}\text{H}_{54}\text{N}_3\text{O}_5$ calculated $[[\text{M} + \text{H}] + [-\text{H}_2\text{O}]]^+$: 656.4064. Obtained: 656.4054.

Synthesis of 5-(((R)-4-((3R,5S,7S,8R,9S,10S,13R,14S,17R)-3,7-dihydroxy-10,13-dimethylhexadecahydro-1H-cyclopenta[a]phenanthren-17-yl)pentanamido)methyl)-N-hydroxyfuran-2-carboxamide. UDCA-HDAC6i#10.



This compound was prepared following the **method A**. Methyl 5-(((4R)-((3R,5S,7S,8R,9S,10S,13R,14S)-3,7-dihydroxy-10,13-dimethylhexadecahydro-1H-cyclopenta[a]phenanthren-17-yl)pentanamido)methyl) furan-2-carboxylate (79.4 mg, 0.15 mmol), hydroxylamine hydrochloride (104.4, 1.5 mmol), phenolphthalein (1 mg), sodium methoxide (2000 mg, 37 mmol). White solid. Yield 47%; m.p. 149-151 °C; IR 3272, 2929, 2864, 1644, 1540, 1016 cm^{-1} ; ^1H NMR (400 MHz, $\text{DMSO-}d_6$) δ 11.02 (s, 1H), 9.05 (s, 1H), 8.30 (t, $J = 5.6$ Hz, 1H), 6.95 (d, $J = 3.3$ Hz, 1H), 6.30 (d, $J = 3.4$ Hz, 1H), 4.43 (d, $J = 4.6$ Hz, 1H), 4.26 (d, $J = 5.5$ Hz, 2H), 3.86 (d, $J = 6.8$ Hz, 1H), 3.26 (d, $J = 5.2$ Hz, 0H), 2.24 – 1.97 (m, 2H), 1.97 – 1.56 (m, 6H), 1.56 – 1.25 (m, 9H), 1.25 – 0.93 (m, 7H), 0.93 – 0.83 (m, 8H), 0.60 (s, 3H); ^{13}C NMR (101 MHz, $\text{DMSO-}d_6$) δ 172.57, 156.39, 154.91, 144.99, 113.56, 108.14, 69.71, 69.45, 55.86, 54.69, 43.07, 43.01, 42.16, 38.71, 37.72, 37.27, 35.62, 34.93, 34.83, 33.76, 32.18, 31.52, 30.24, 28.16, 26.71, 23.31, 20.84, 18.45, 12.03; HRMS (ESI) for $\text{C}_{30}\text{H}_{45}\text{N}_2\text{O}_5$ calculated $[[\text{M} + \text{H}] + [-\text{H}_2\text{O}]]^+$: 513.3329. Obtained: 513.3327.

Supplementary Figure legends

Supplementary Table S1. Main protein-ligand interactions characterized in the docking model. (**UDCA**, ursodeoxycholic acid)

Supplementary Table S2. Contribution of different molecular descriptors to the total binding affinities. (ΔG in kcal/mol)

Supplementary Table S3. IC₅₀ values of UDCA-HDAC6i #1, #2, #6, #9 and #8, (8) and UDCA on different HDACs.

Supplementary Figure S1. Graphical 2D representation of the main interactions taking place in the binding of UDCA-HDAC6i #1 to the catalytic domain 2 of HDAC6.

Supplementary Figure S2. Superimposed view of protein surfaces in 3D structural alignment of different HDAC isoforms with docking model of human HDAC6 CD2, and sequence alignment of these HDAC isoforms with the sequence fragment of HDAC6 corresponding to the amino acids located in the surface area occupied by UDCA in the three most active and selective UDCA-HDAC6is for HDAC6.

Supplementary Figure S3. Docking studies on a homology model of the catalytic domain 2 of rat HDAC6 based on the experimentally resolved three-dimensional structure of human HDAC6 catalytic domain 2. (A) Sequence alignment of human and rat HDAC6 catalytic domain 2. (B) Graphical representation of the binding modes of UDCA-HDAC6i #1, #2 and #9 with the active sites of human and rat HDAC6 catalytic domain 2, and table depicting the XP Gscores of the different UDCA-HDAC6is on both proteins.

Supplementary Table S4. QikProp predicted values. Percent Human Oral Absorption, predicted human oral absorption on 0 to 100% scale, based on a quantitative multiple linear regression model. #stars, number of property or descriptor values that fall outside the 95% range of similar values for known drugs. A large number of stars suggests that a molecule is less drug-like than molecules

with few stars. #rotor, number of non-trivial (not CX3), non-hindered (not alkene, amide, small ring) rotatable bonds. MW, molecular weight of the molecule. Dipole, computed dipole moment of the molecule. SASA, total solvent accessible surface area (SASA) in square angstroms using a probe with a 1.4 Å radius. FOSA, hydrophobic component of the SASA (saturated carbon and attached hydrogen). FISA, hydrophilic component of the SASA (SASA on N, O, and H on heteroatoms). PISA, (carbon and attached hydrogen) component of the SASA. WPSA, weakly polar component of the SASA (halogens, P, and S). Volume, total solvent-accessible volume in cubic angstroms using a probe with a 1.4 Å radius. donorHB, estimated number of hydrogen bonds that would be donated by the solute to water molecules in an aqueous solution. accptHB, estimated number of hydrogen bonds that would be accepted by the solute from water molecules in an aqueous solution. For donorHB and accptHB, values are averages taken over a number of configurations, so they can be non-integer. glob, globularity descriptor, where r is the radius of a sphere with a volume equal to the molecular volume. Globularity is 1.0 for a spherical molecule. QPpolrz, predicted polarizability in cubic angstroms. QPlogPC16, predicted hexadecane/gas partition coefficient. QPlogPoct, predicted octanol/gas partition coefficient. QPlogPw, predicted water/gas partition coefficient. QPlogPo/w, predicted octanol/water partition coefficient. QPlogS, predicted aqueous solubility, $\log S$. S in mol dm^{-3} is the concentration of the solute in a saturated solution that is in equilibrium with the crystalline solid. QPlogBB, predicted brain/blood partition coefficient. IP(ev), PM3 calculated ionization potential. EA(eV), PM3 calculated electron affinity. #metab, number of likely metabolic reactions. QPlogKhsa, prediction of binding to human serum albumin. PSA, Van der Waals surface area of polar nitrogen and oxygen atoms.

Supplementary Table S5. Relative abundancy of individual bile acids and conjugation types in portal blood. Statistical analysis, two-tailed unpaired t test. TUDC is tauroursodeoxycholic, TC is taurocholic, Ta/bMC is tauro α/β murocholic, TQDC is taurochenodeoxycholic, GUDC is glycoursoxycholic, GC is glycocholic,

GQDC glycochenodeoxycholic, UDC is ursodeoxycholic, CA is cholic, a/bMC is α/β murocholic, HyoDC is hyodeoxycholic and SLC is sulpholithocholic .

Supplementary Table S6. Relative abundancy of individual bile acids and conjugation types in liver. Statistical analysis, two-tailed unpaired t test. TUDC is tauroursodeoxycholic, TC is taurocholic, Ta/bMC is tauro α/β murocholic, TQDC is taurochenodeoxycholic, GUDC is glyoursodeoxycholic, GC is glycocholic, GQDC glycochenodeoxycholic, UDC is ursodeoxycholic, CA is cholic, a/bMC is α/β murocholic, HyoDC is hyodeoxycholic and SLC is sulpholithocholic .

Supplementary Table S7. Relative abundancy of individual bile acids and conjugation types in bile. Statistical analysis, two-tailed unpaired t test. TUDC is tauroursodeoxycholic, TC is taurocholic, Ta/bMC is tauro α/β murocholic, TQDC is taurochenodeoxycholic, GUDC is glyoursodeoxycholic, GC is glycocholic, GQDC glycochenodeoxycholic, UDC is ursodeoxycholic, CA is cholic, a/bMC is α/β murocholic, HyoDC is hyodeoxycholic and SLC is sulpholithocholic .

Supplementary Table S8. Relative abundancy of individual bile acids and conjugation types in peripheral blood. Statistical analysis, two-tailed unpaired t test. TUDC is tauroursodeoxycholic, TC is taurocholic, Ta/bMC is tauro α/β murocholic, TQDC is taurochenodeoxycholic, GUDC is glyoursodeoxycholic, GC is glycocholic, GQDC glycochenodeoxycholic, UDC is ursodeoxycholic, CA is cholic, a/bMC is α/β murocholic, HyoDC is hyodeoxycholic and SLC is sulpholithocholic .

Supplementary Figure S4. Schematic example of a substrate competition transport experiment. Ia Incubation of cells with 100 μ M UDCA-HDAC6i #1 in basal conditions. Ib Incubation of cells with 100 μ M UDCA-HDAC6i #1 in the presence of transporter inhibitor. Ic Incubation of cells with 100 μ M UDCA-HDAC6i #1 in after induced transporter overexpression. Id Incubation of cells with 100 μ M UDCA-HDAC6i #1 in the presence of transporter inhibitor after induced transporter overexpression.

Supplementary Figure S5. Bar graphs representing UDCA-HDAC6i#1 uptake under baseline and transporter overexpressing conditions in the presence or

absence of a transporter inhibitor/competitor. Transporter overexpression was carried out on CHO cells for OATP1B1 (n=7), OATP1B3 (n=7), OATP1A2 (n=3), OATP2B1 (n=3) and NTCP (n=4) transporters, and in TFK-1 cells for ASBT (n=3) transporter. Paired two-tailed t-test was used to assess statistical significance.

Supplementary Figure S6. Graphical comparisons between results previously reported by *Munoz-Garrido et al.*(7) for the treatment of PCK rats with UDCA and results obtained upon treatment of PCK rats with UDCA-HDAC6i #1. (A) Bar graphs representing liver weight, liver to body weight fold change, relative cystic area fold change and UDCA concentration fold change in liver. (B) Bar graphs representing kidney weight, kidney to body weight fold change, blood urea concentration fold change, and UDCA concentration in peripheral blood. In all cases statistical unpaired two-tailed t test was applied to determine significance, except in the case of liver to body weight ratio in which in both cases unpaired one-tailed t test was applied.

Supplementary Figure S7. Calcium mobilization assay in polycystic cholangiocytes.

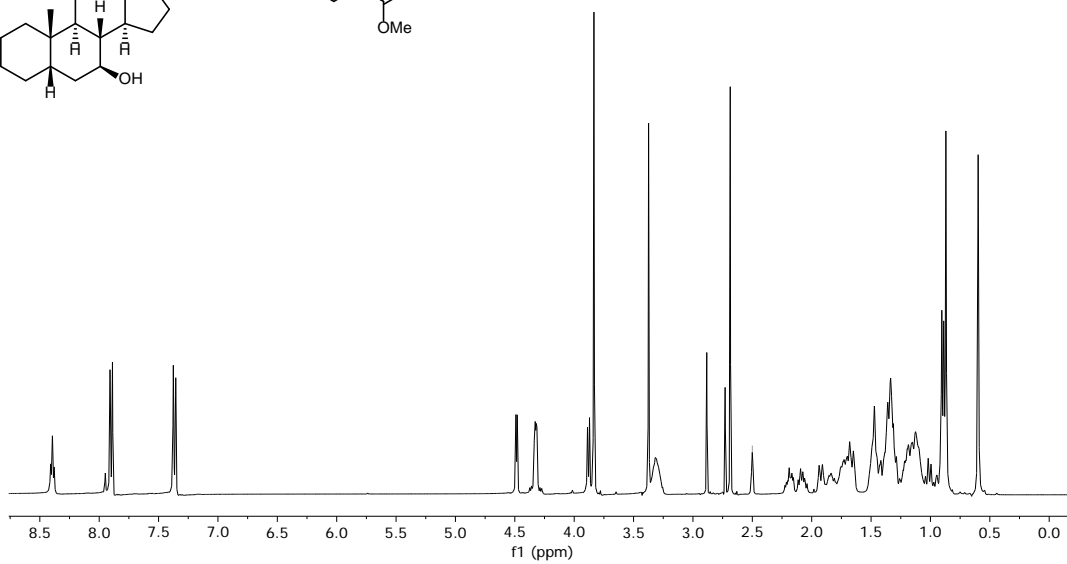
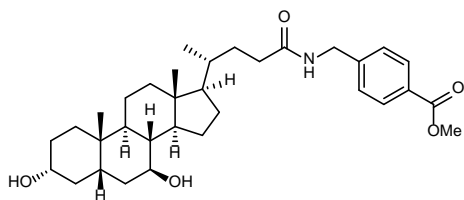
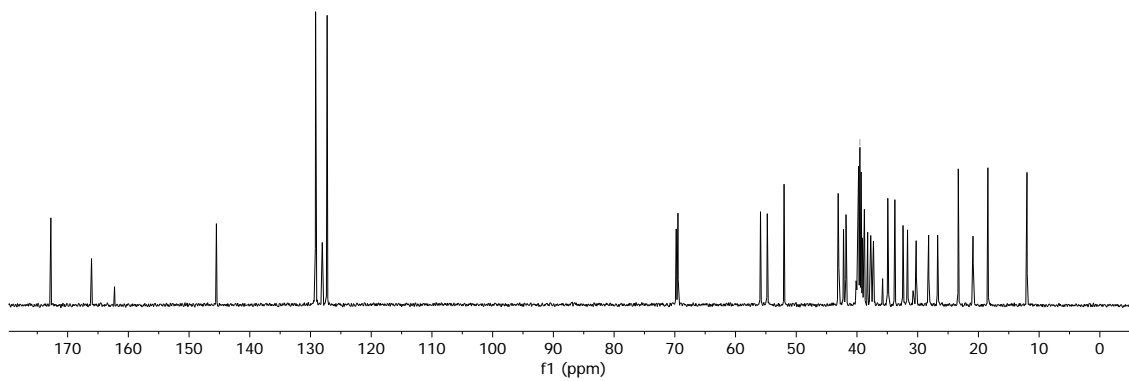
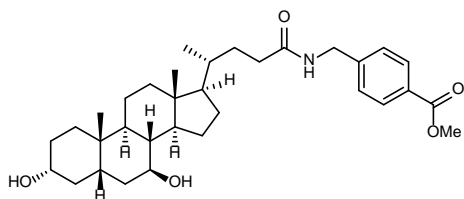
Supplementary Table S9. Enzymes and substrates used for HDAC inhibitory activity assays.

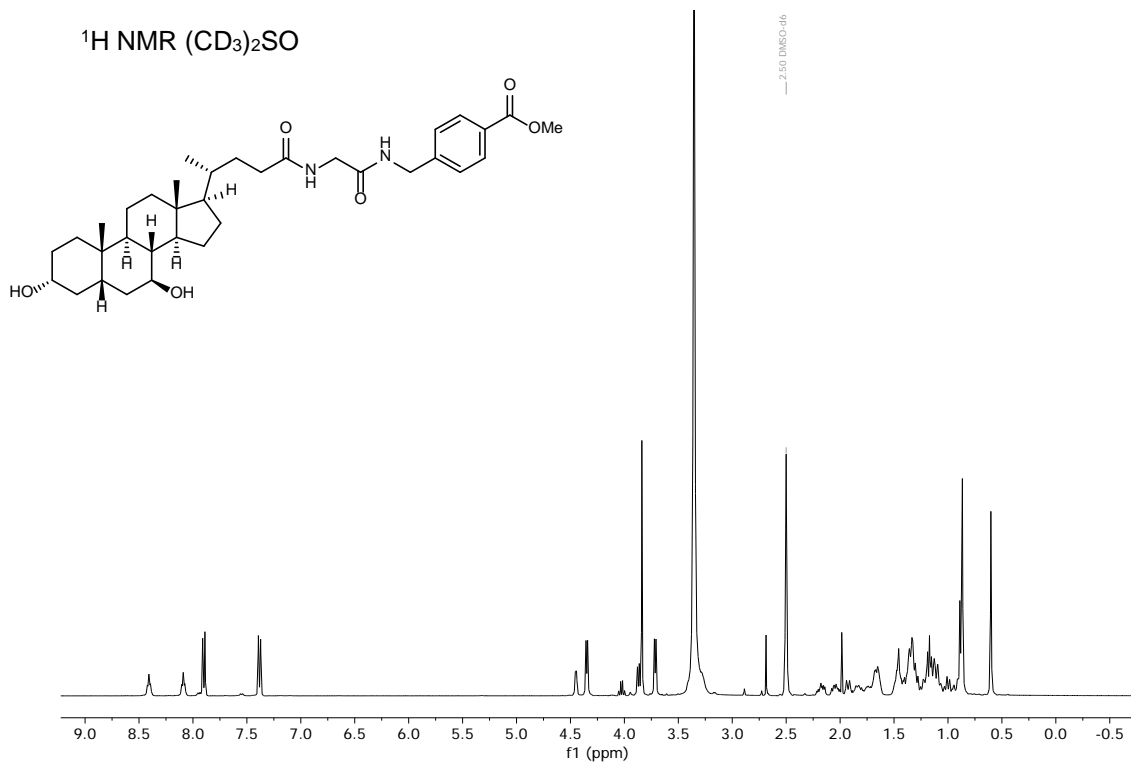
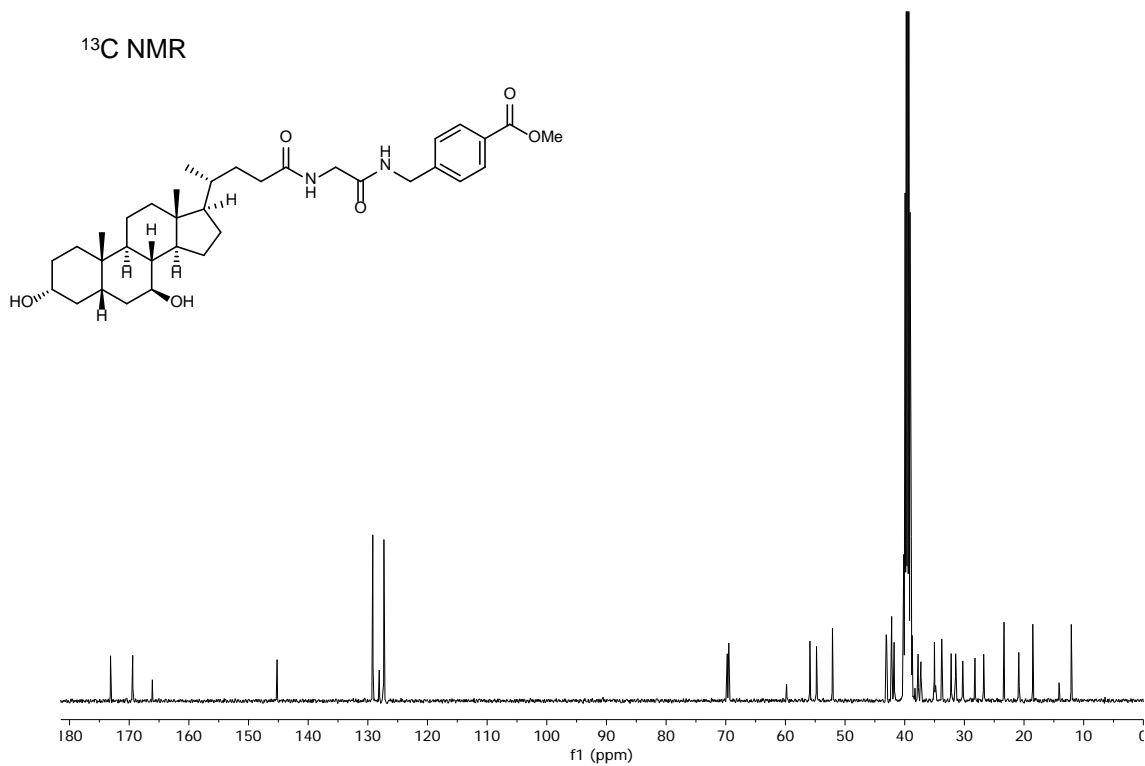
Supplementary Table S10. Oligonucleotide sequence of primers used to clone the ORF of human transporters.

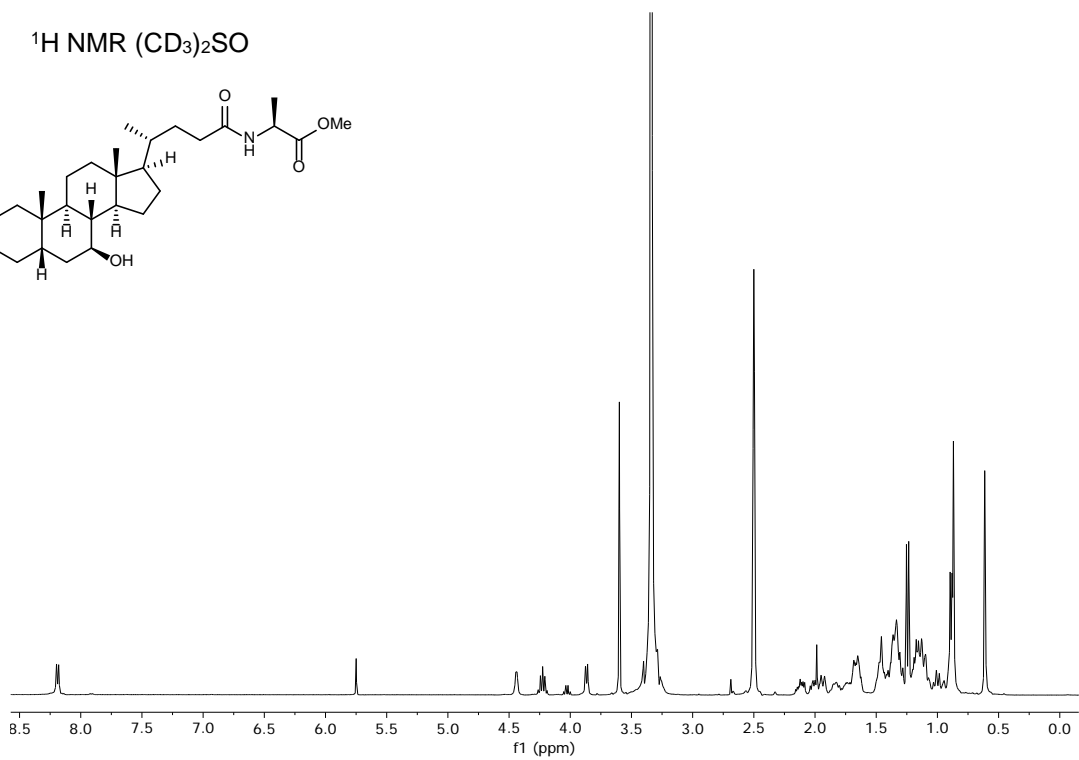
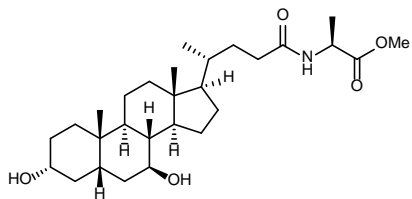
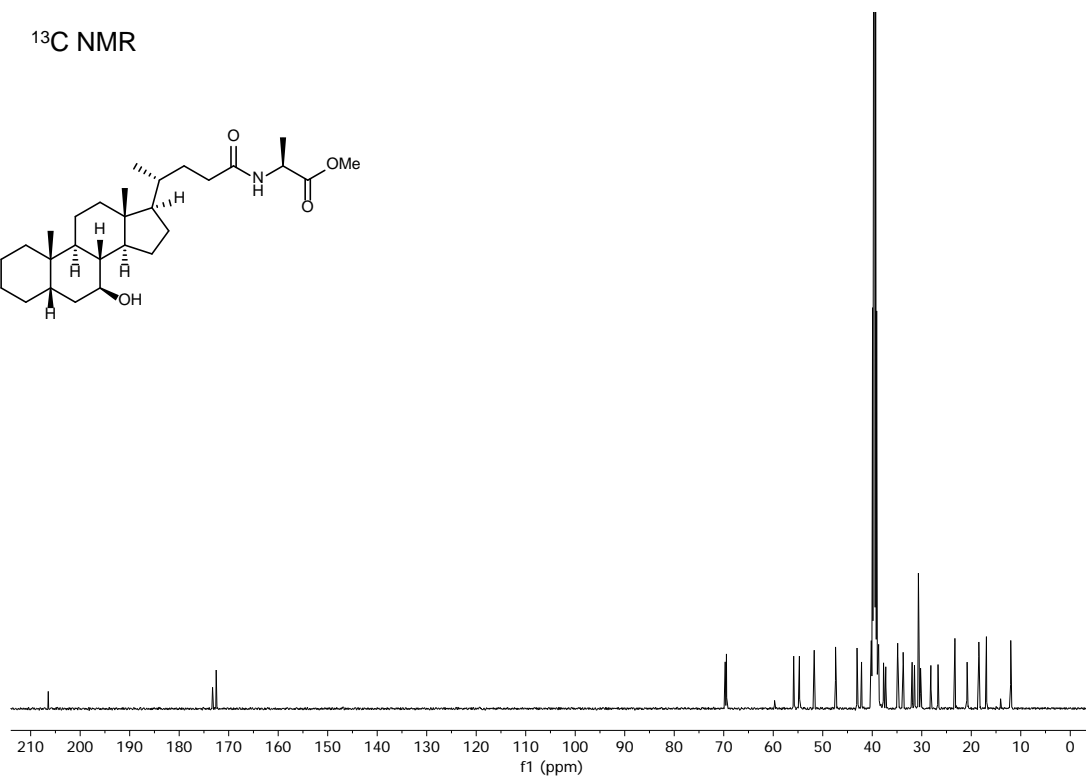
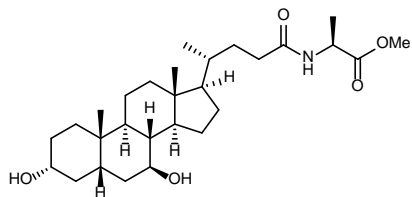
Supplementary Table S11. Oligonucleotide sequence of primers used for RT-qPCR.

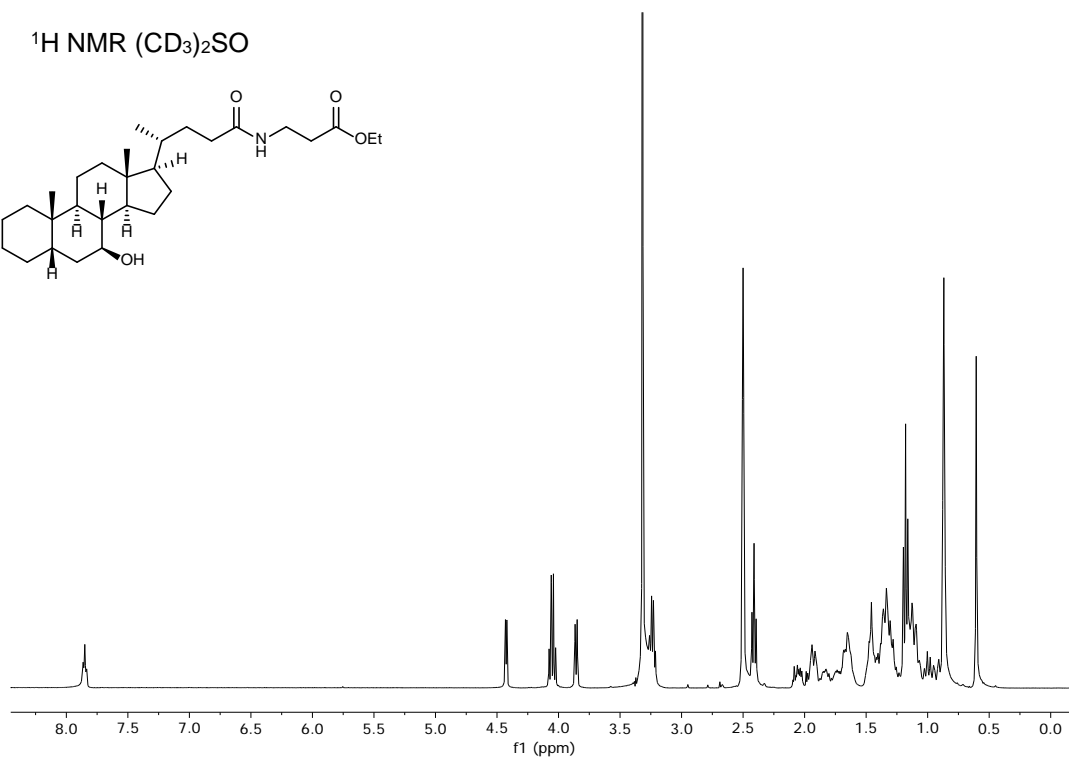
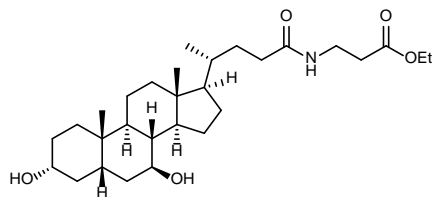
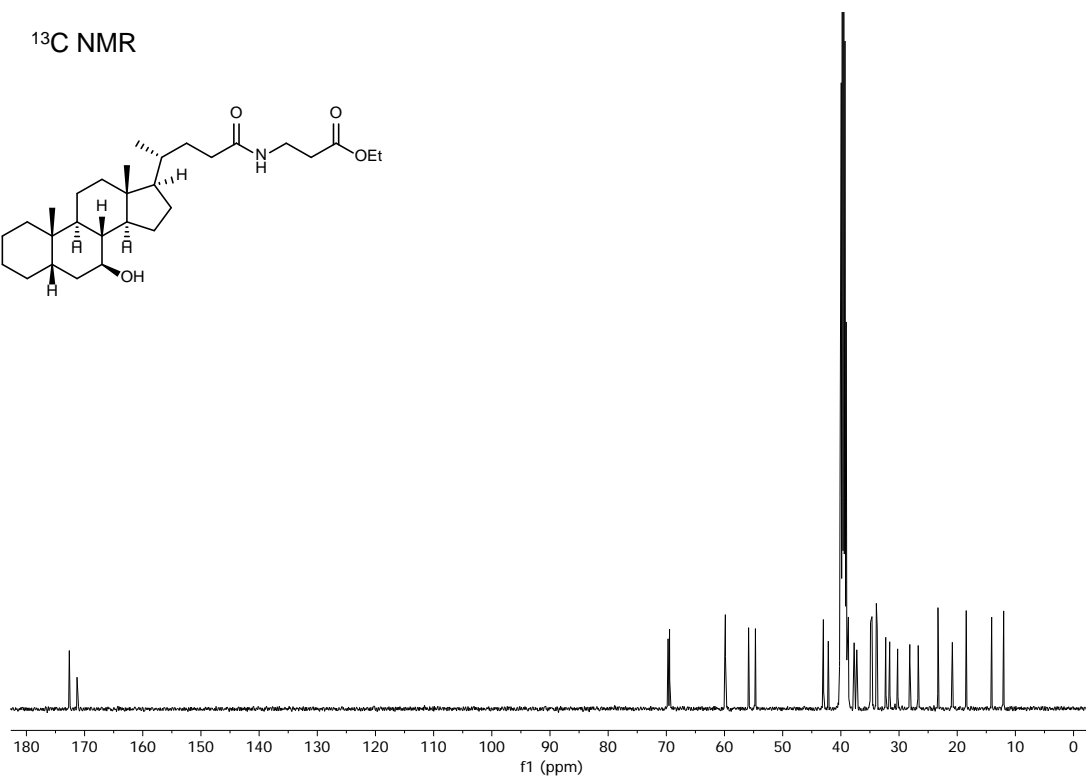
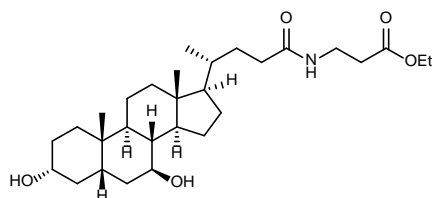
Supplementary Table S12. Antibodies used for immunoblot.

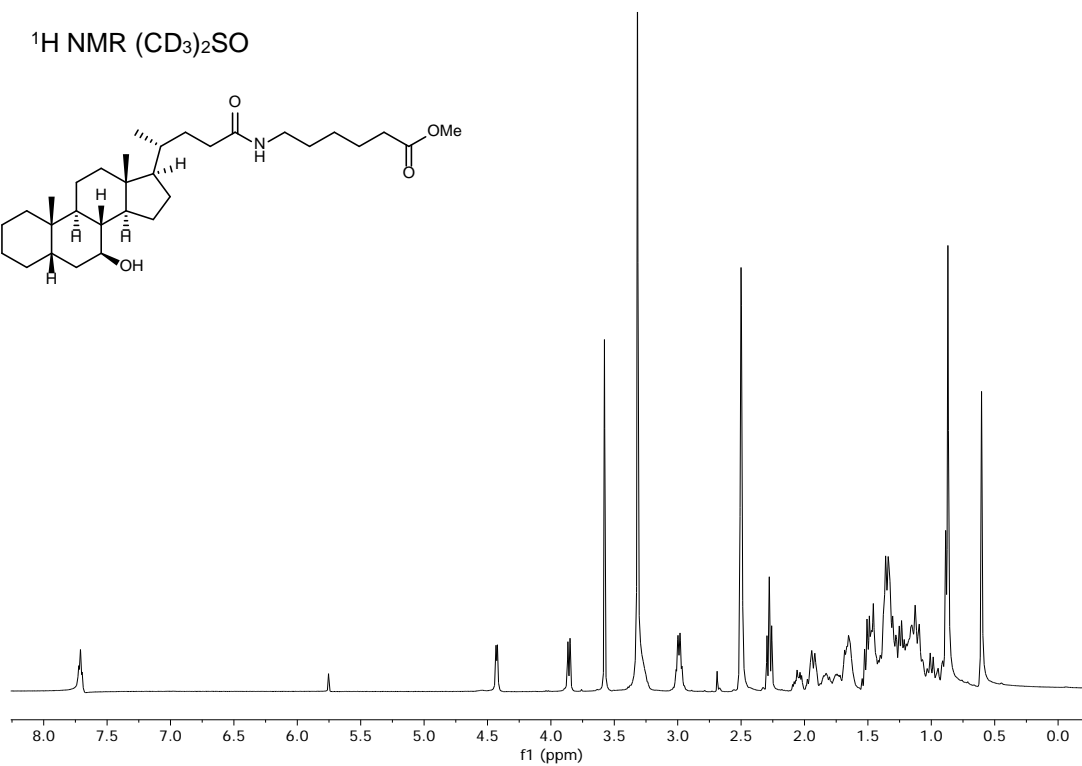
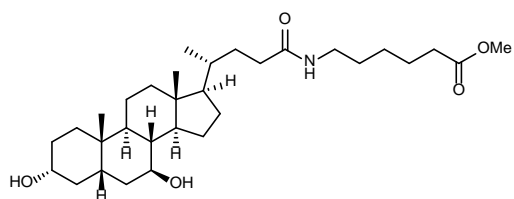
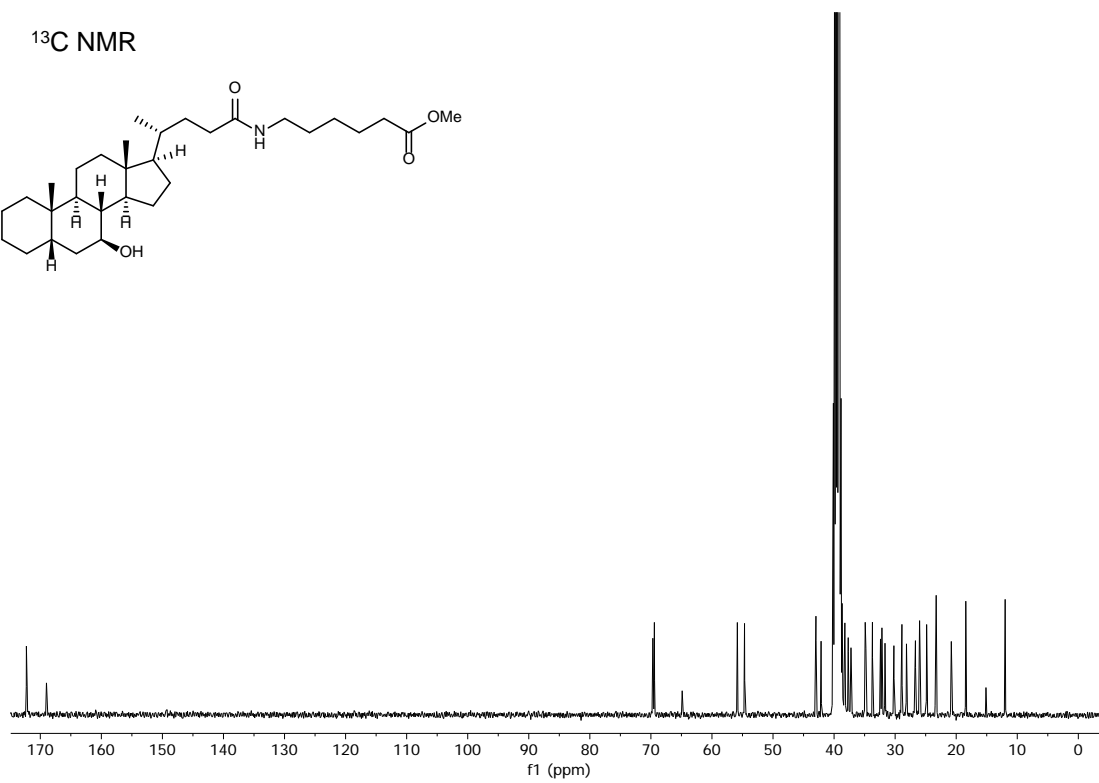
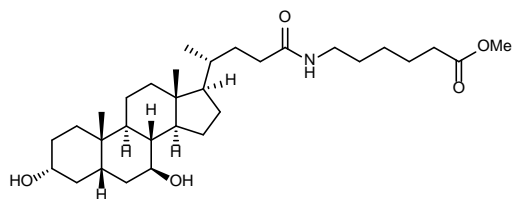
NMR spectra

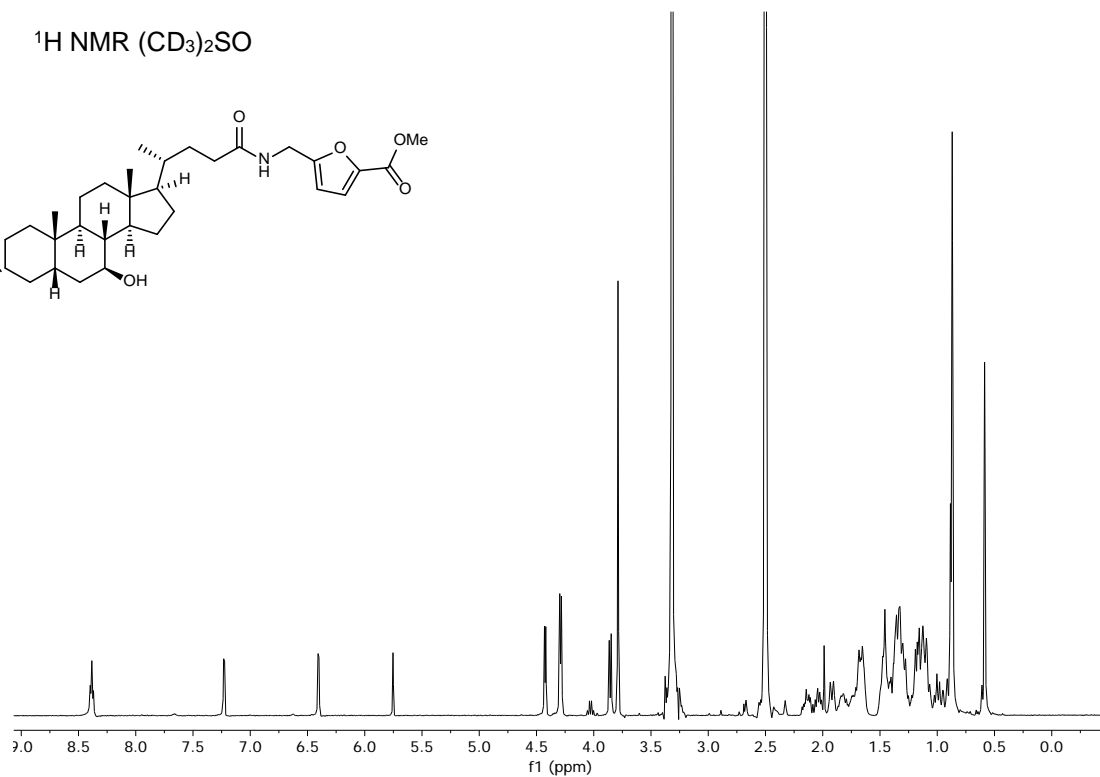
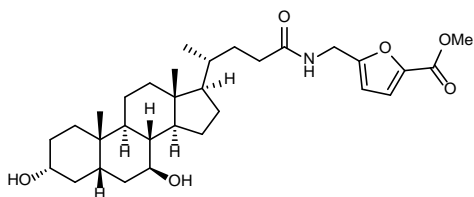
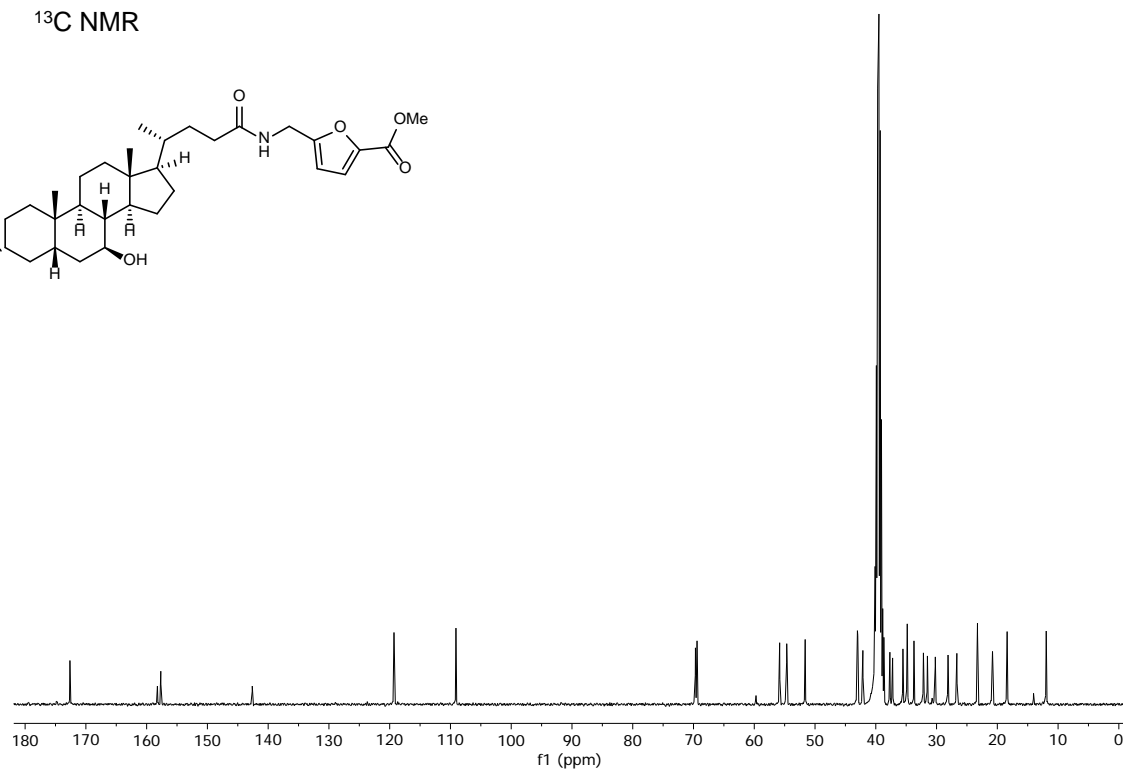
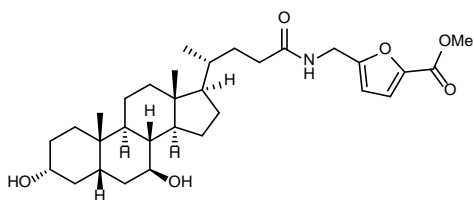
Compound 3a $^1\text{H NMR}$ ($\text{CD}_3)_2\text{SO}$  $^{13}\text{C NMR}$ 

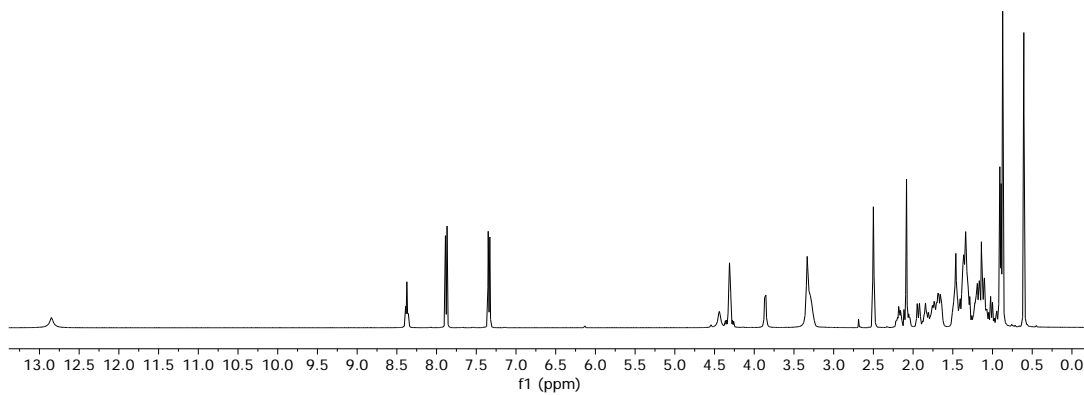
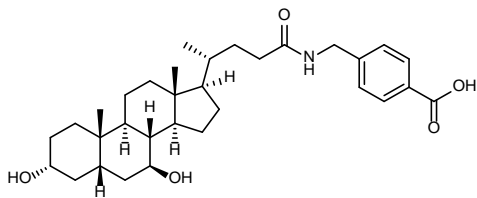
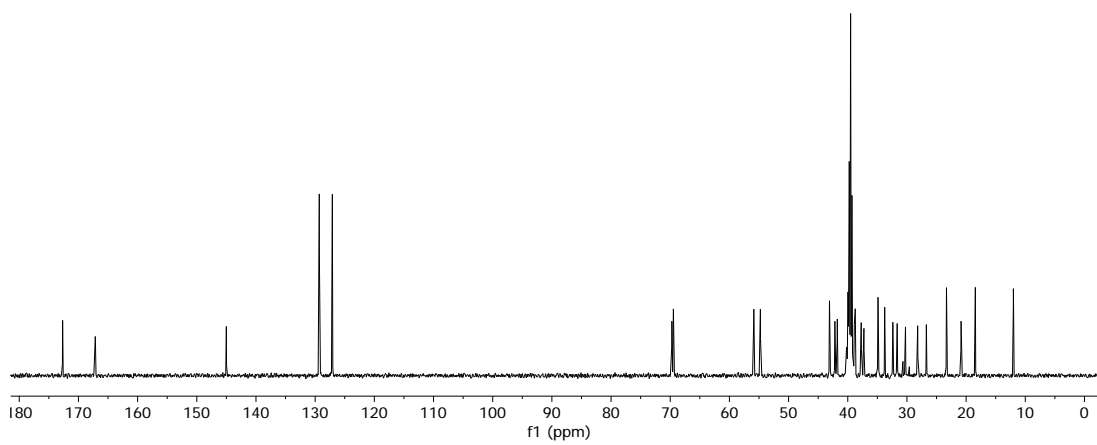
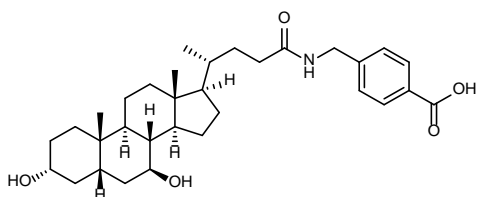
Compound 3b¹H NMR (CD₃)₂SO¹³C NMR

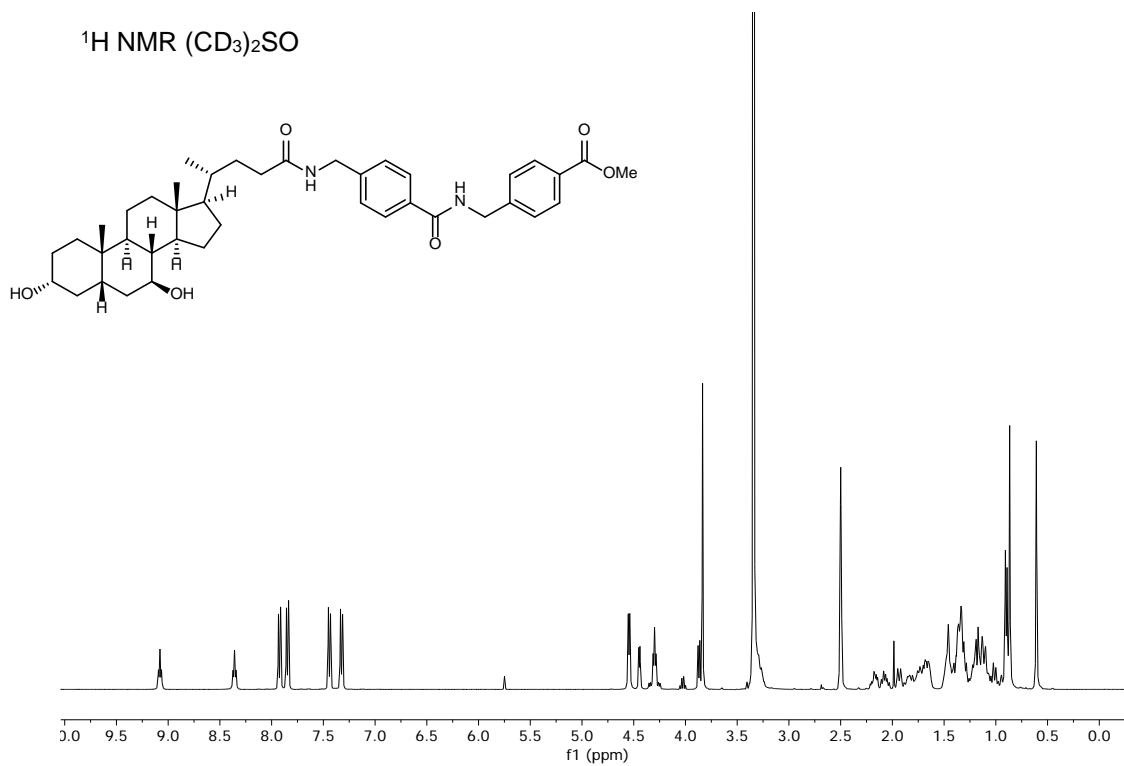
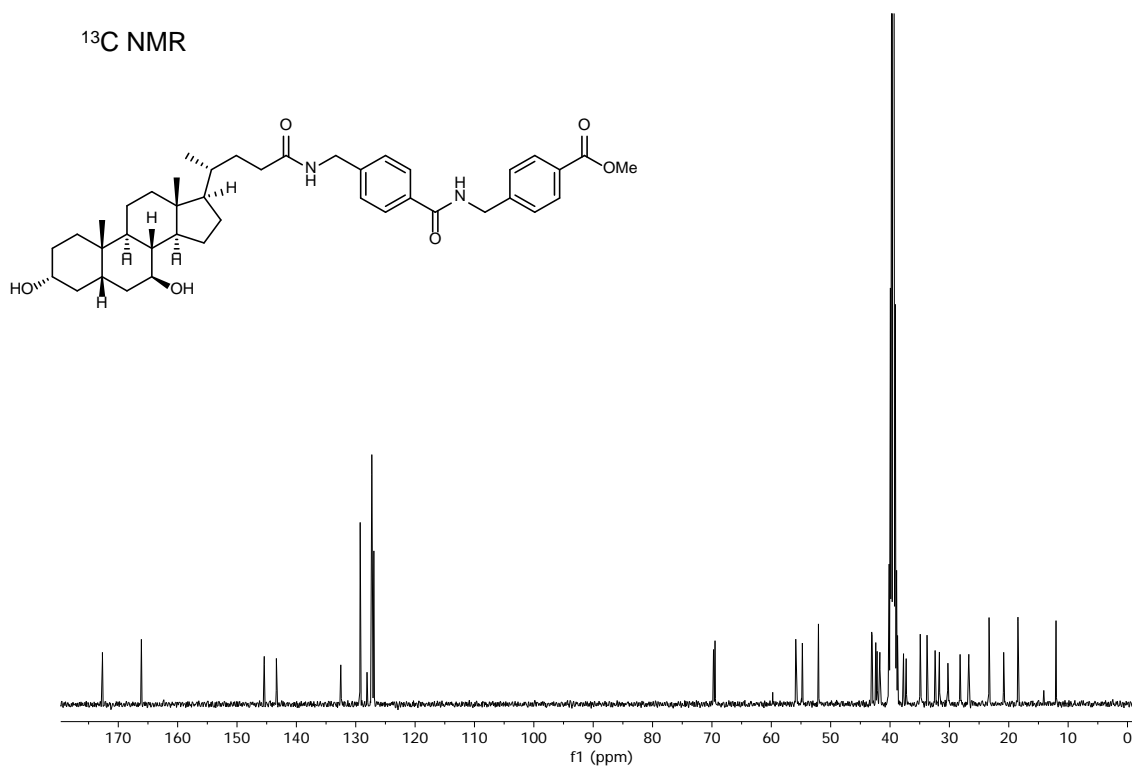
Compound 3c¹H NMR (CD₃)₂SO¹³C NMR

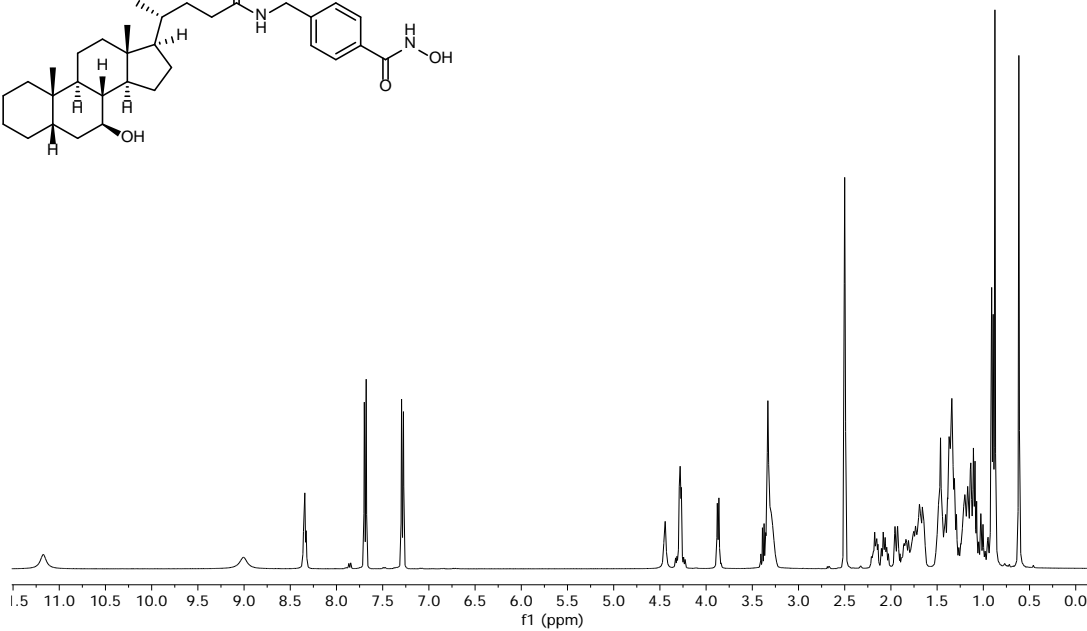
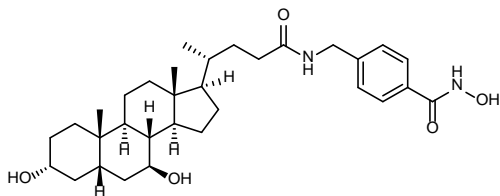
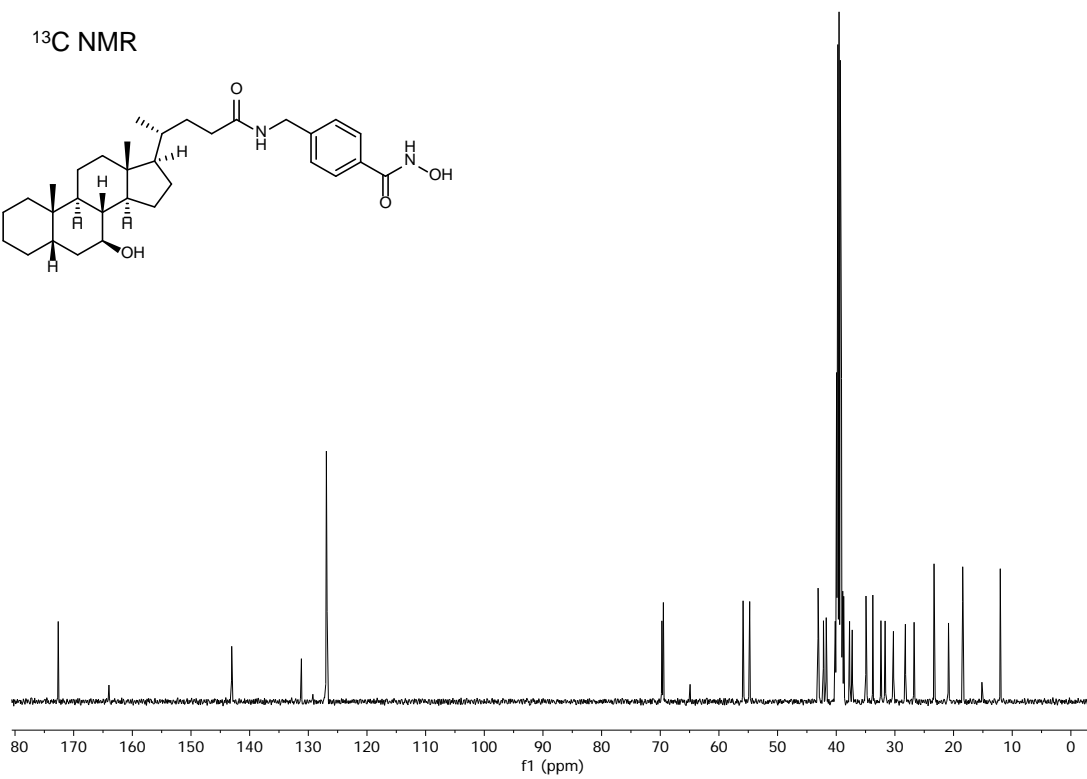
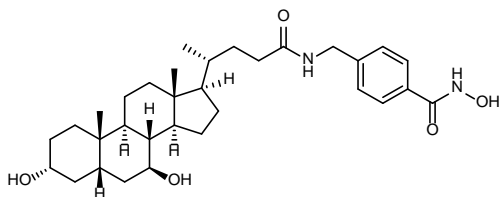
Compound 3d¹H NMR (CD₃)₂SO¹³C NMR

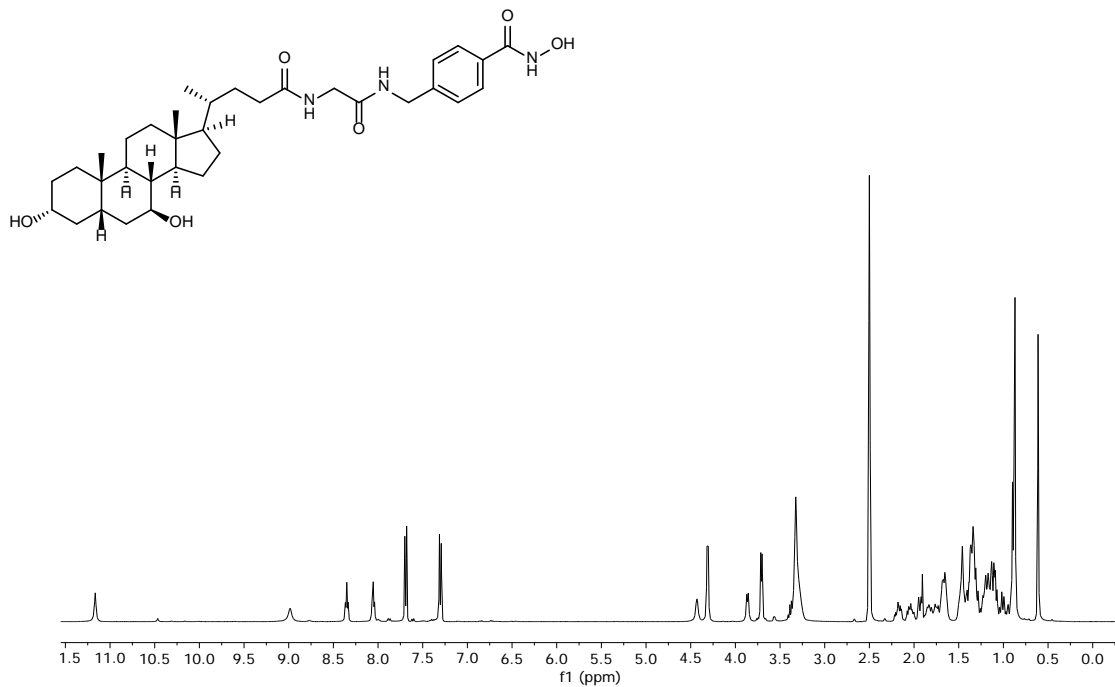
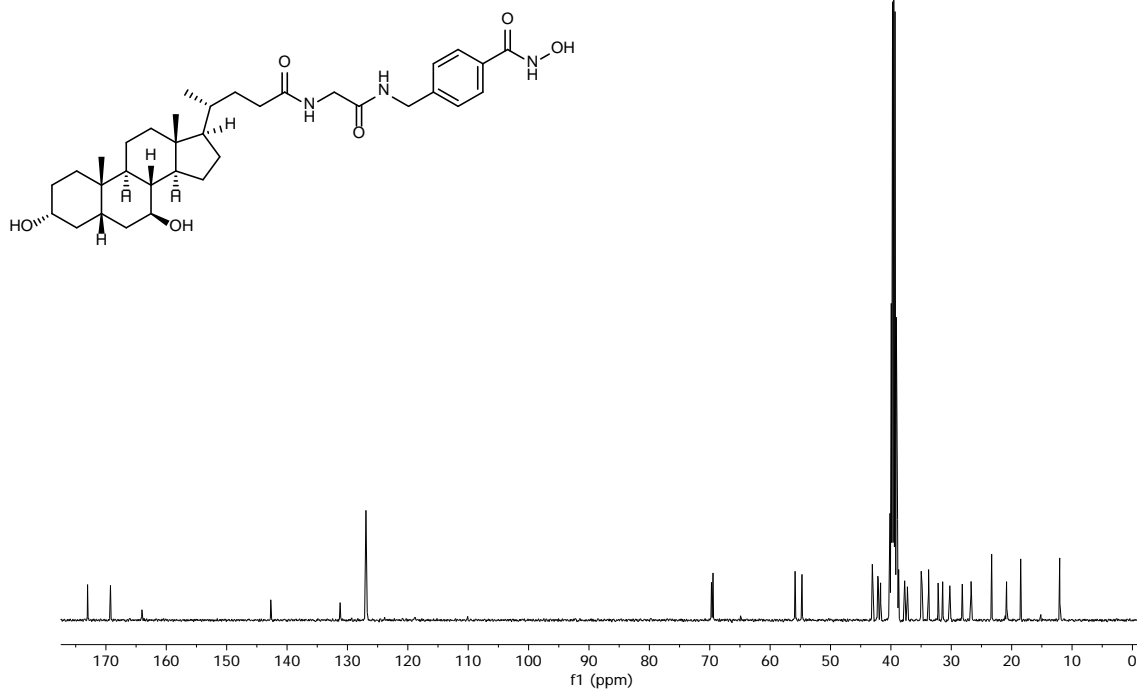
Compound 3f¹H NMR (CD₃)₂SO¹³C NMR

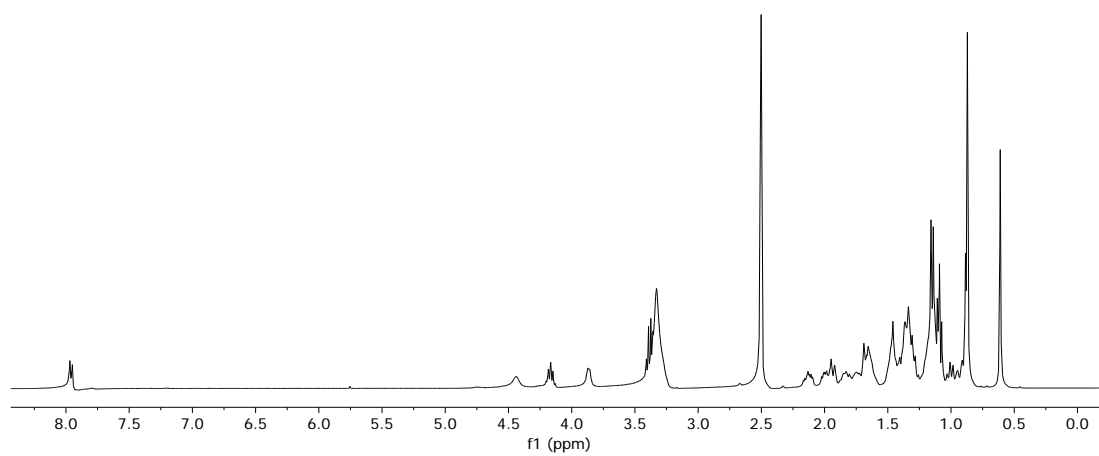
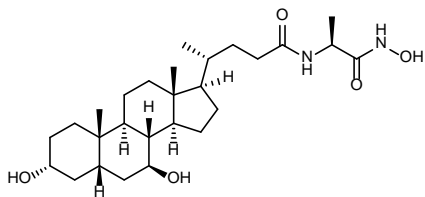
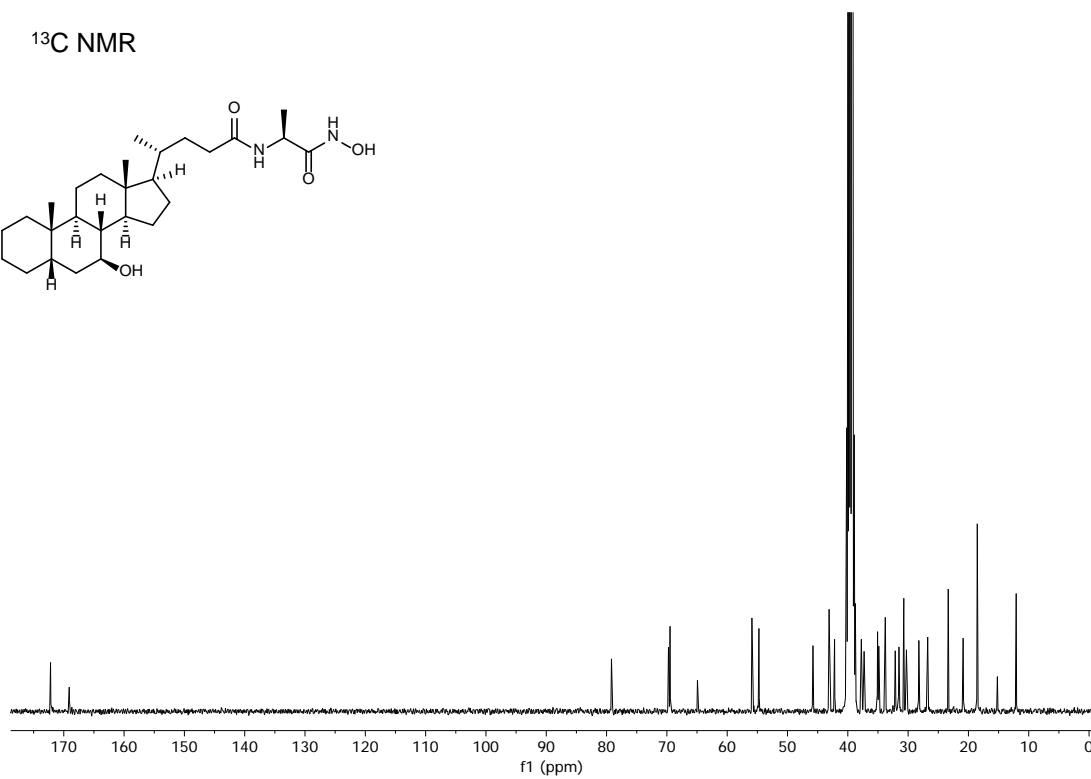
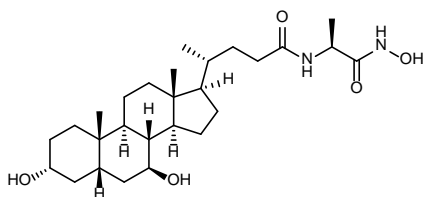
Compound 3g¹H NMR (CD₃)₂SO¹³C NMR

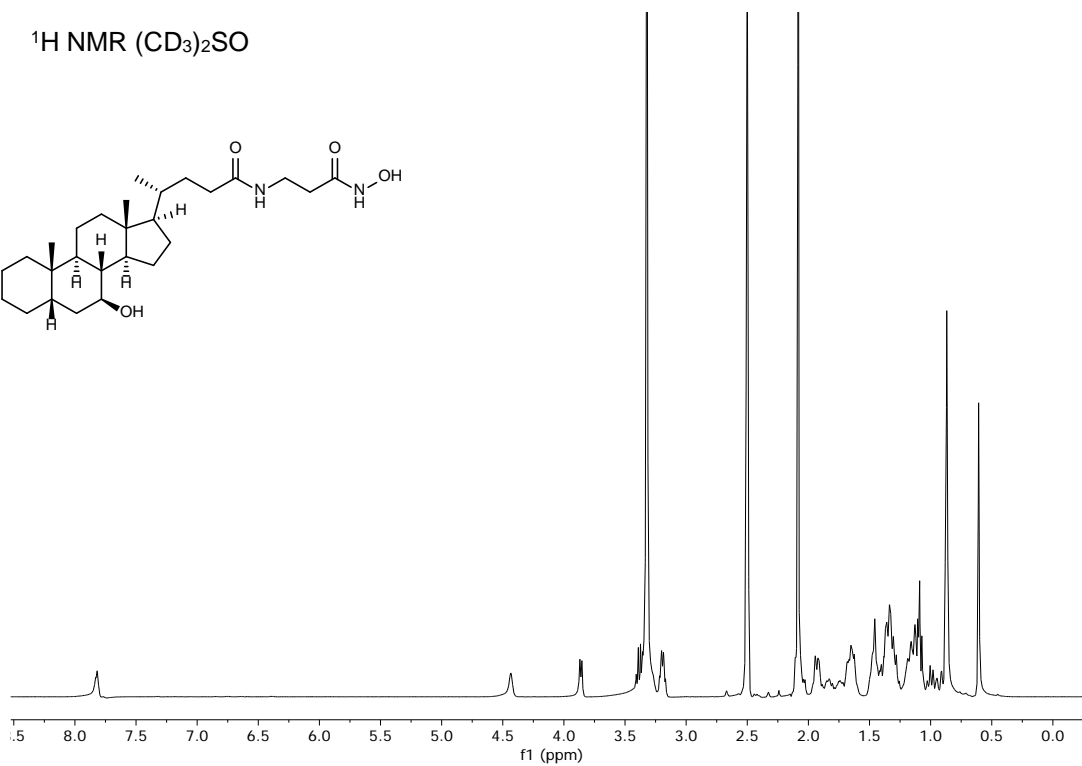
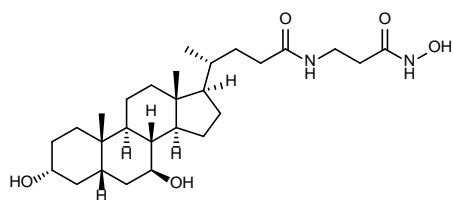
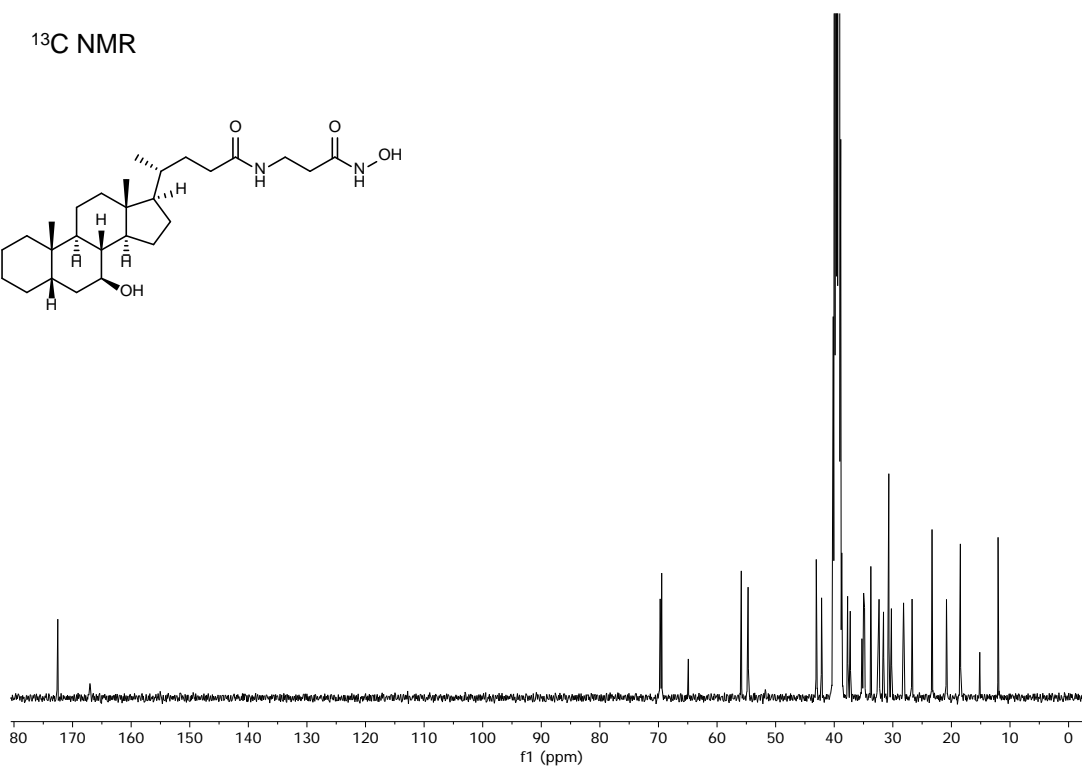
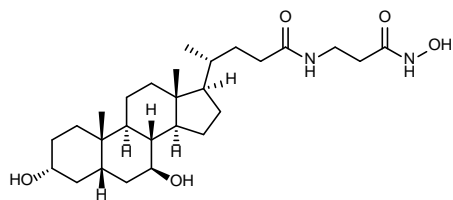
Compound 4a¹H NMR (CD₃)₂SO¹³C NMR

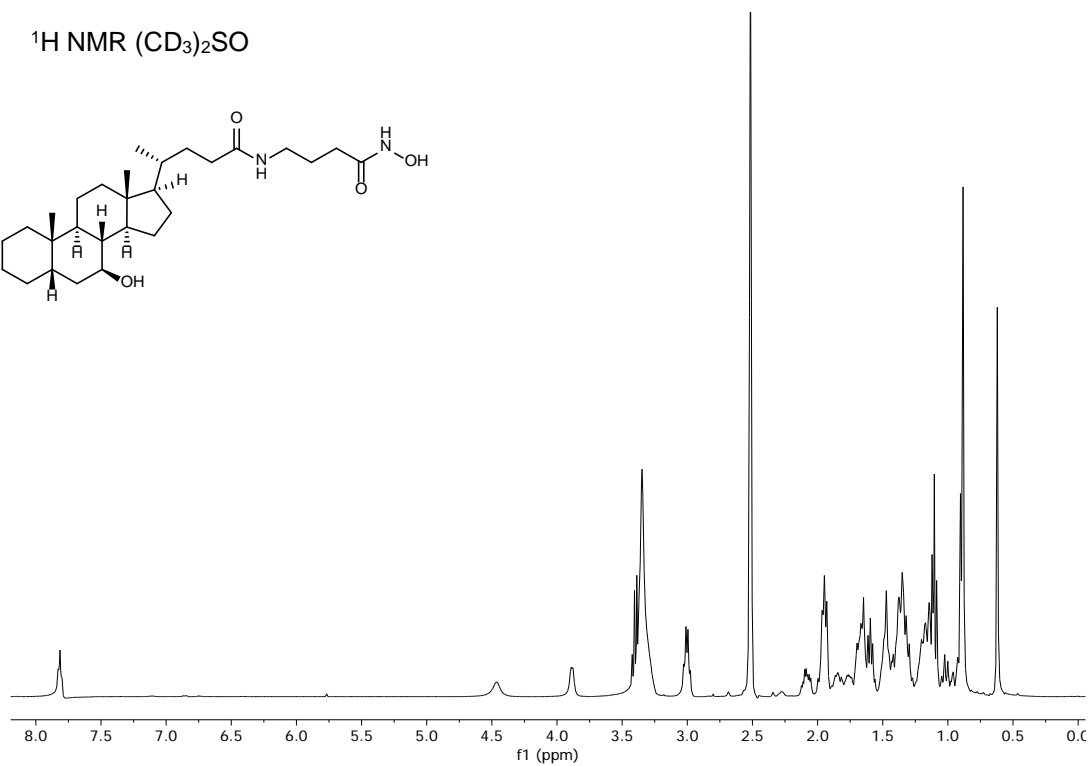
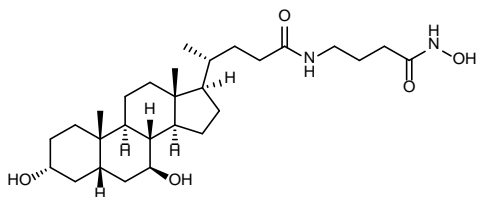
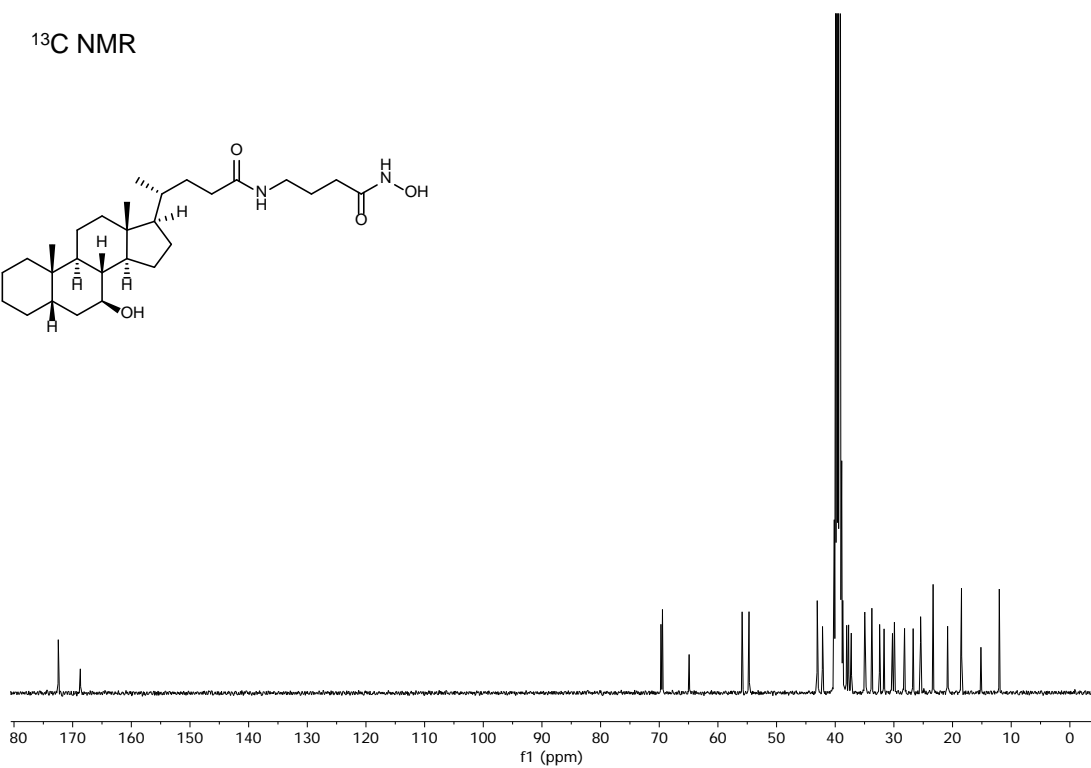
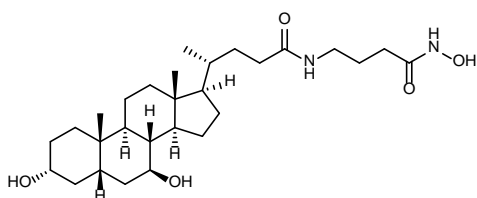
Compound 6a $^1\text{H NMR}$ ($\text{CD}_3)_2\text{SO}$  $^{13}\text{C NMR}$ 

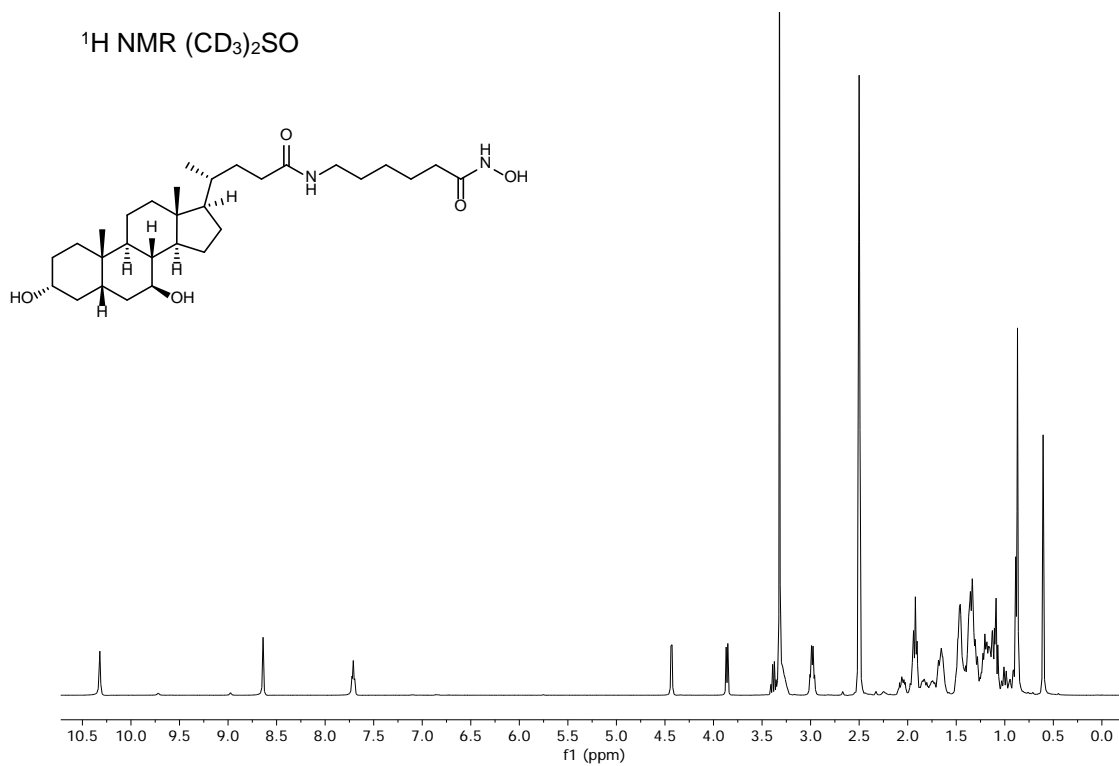
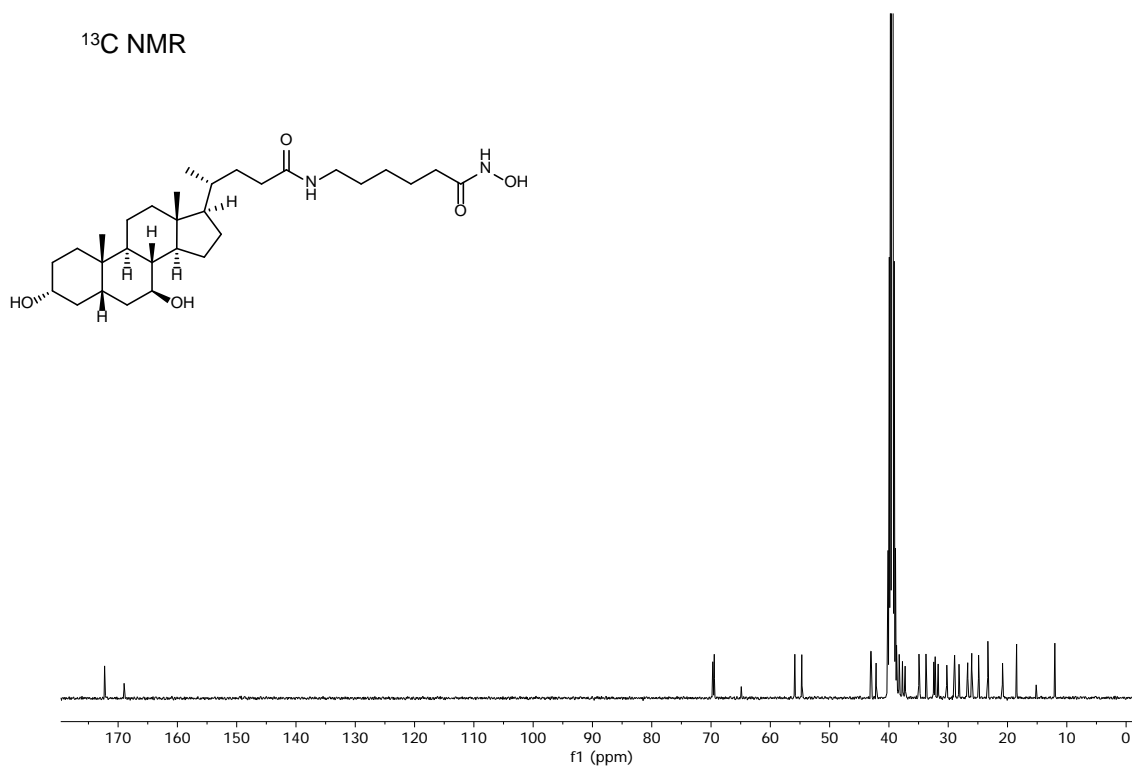
UDCA-HDAC6i#1¹H NMR (CD₃)₂SO¹³C NMR

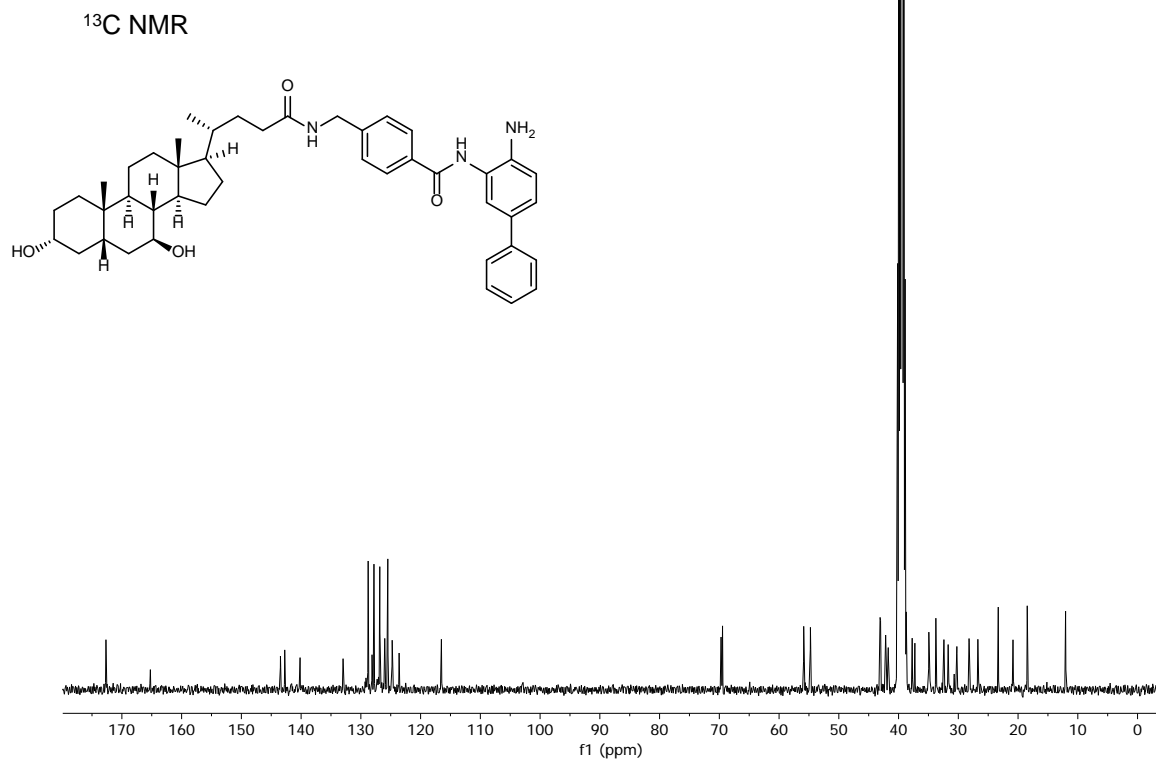
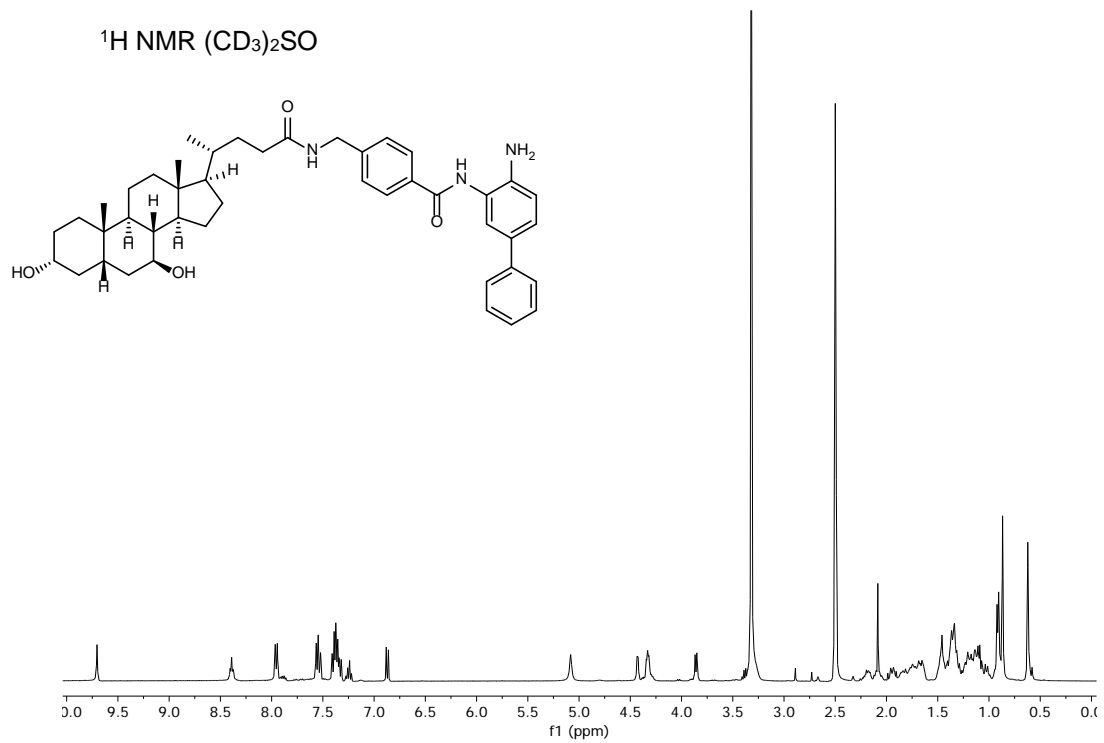
UDCA-HDAC6i#2¹H NMR (CD₃)₂SO¹³C NMR

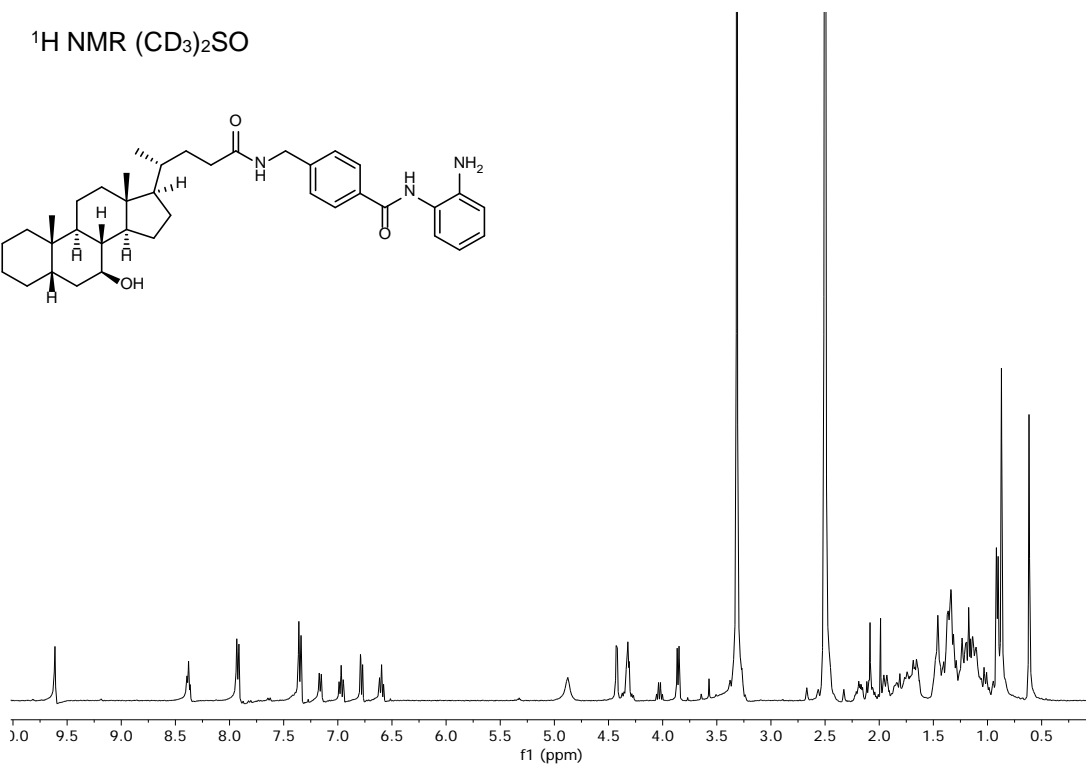
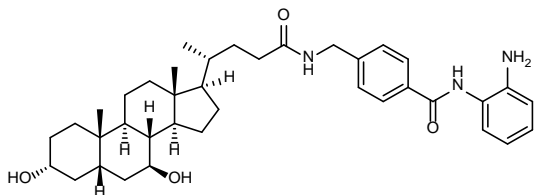
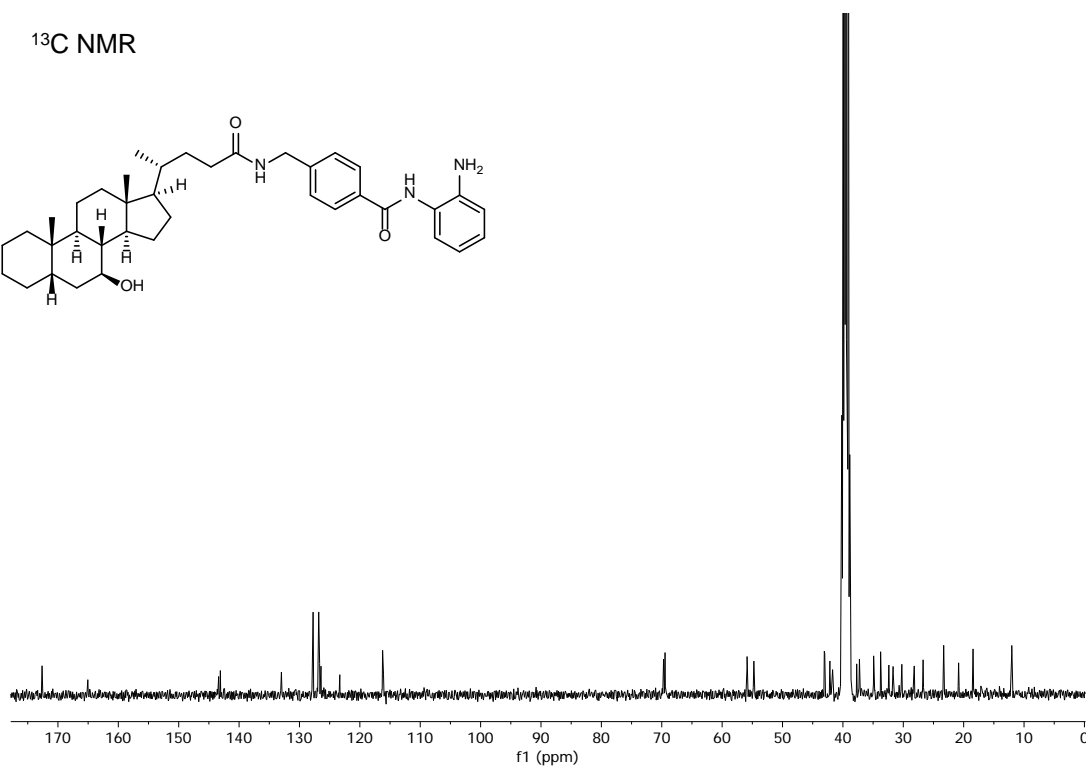
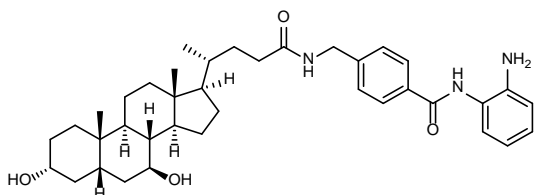
UDCA-HDAC6i#3¹H NMR (CD₃)₂SO¹³C NMR

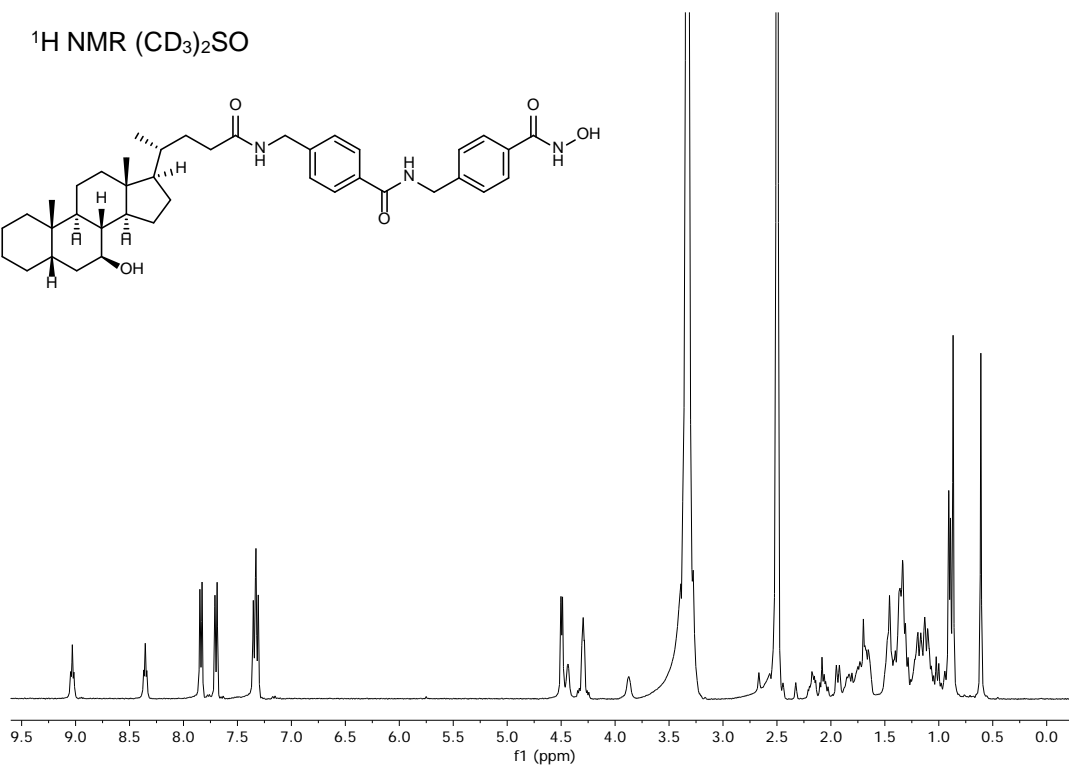
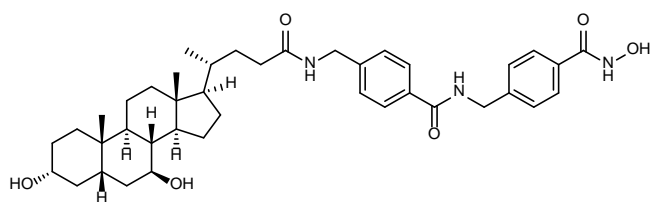
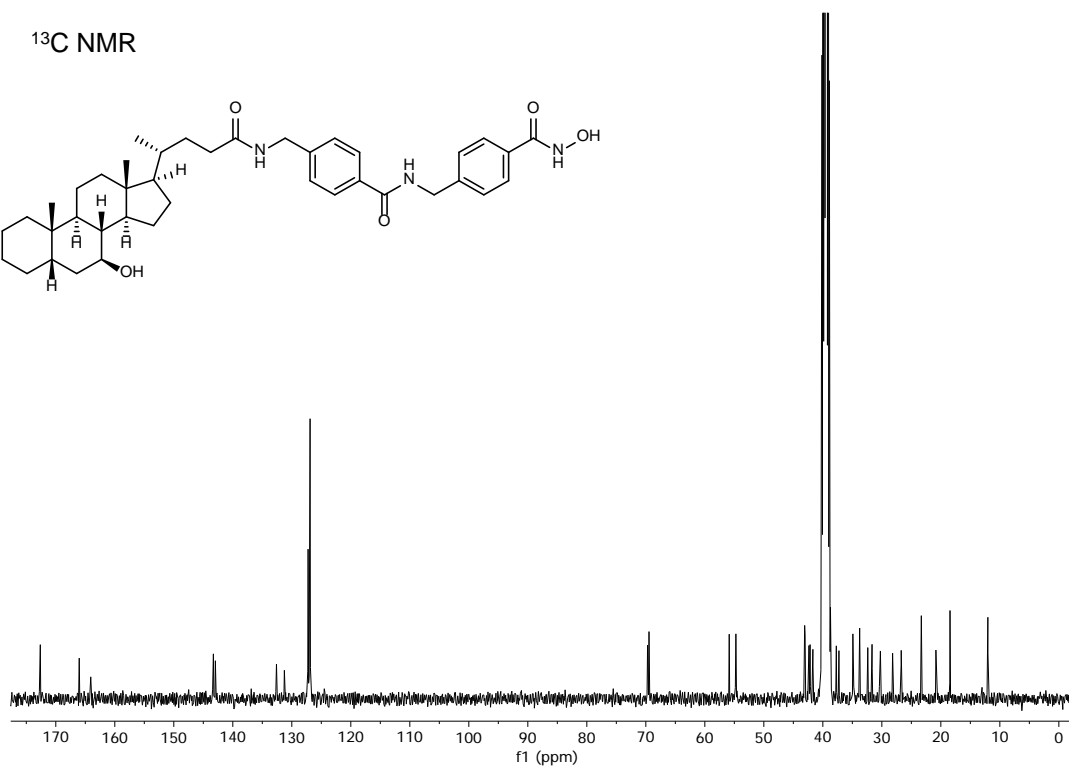
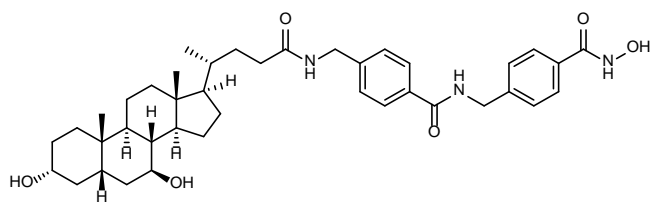
UDCA-HDAC6i#4¹H NMR (CD₃)₂SO¹³C NMR

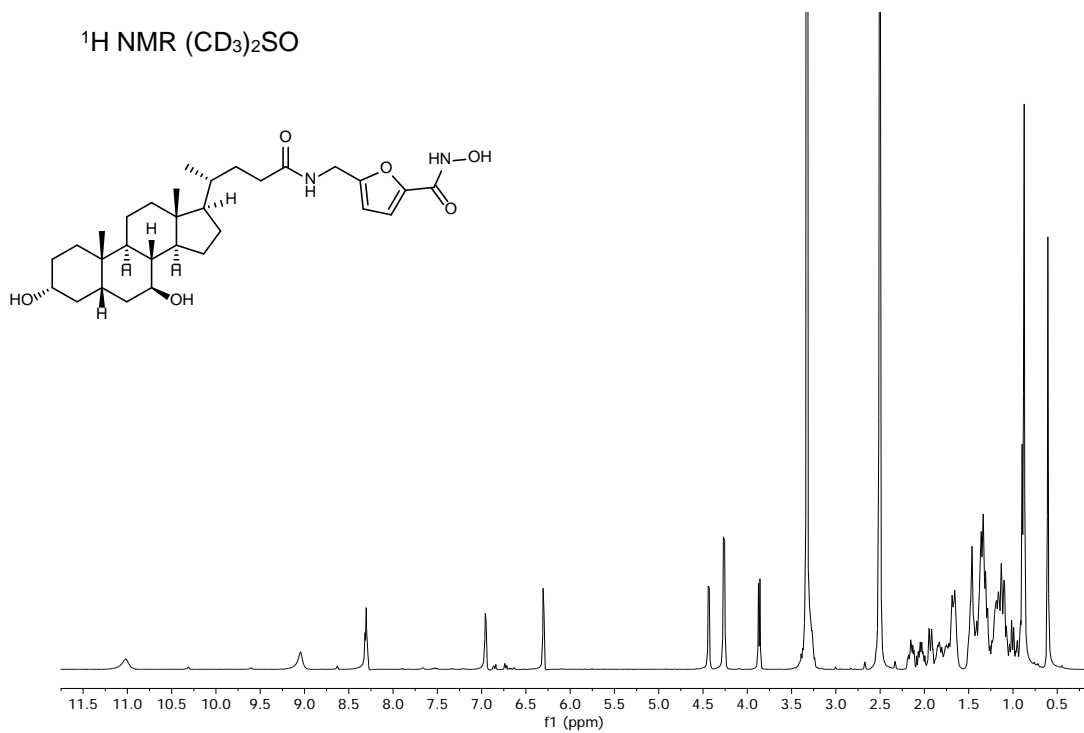
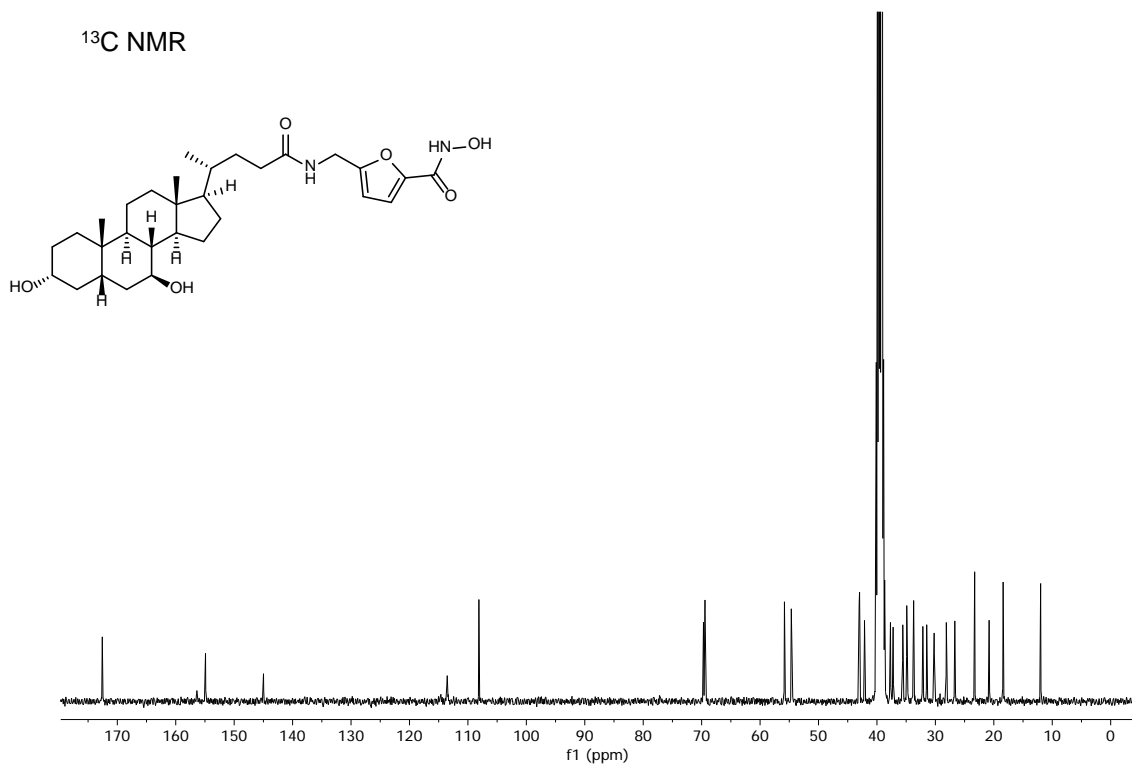
UDCA-HDAC6i#5¹H NMR (CD₃)₂SO¹³C NMR

UDCA-HDAC6i#6¹H NMR (CD₃)₂SO¹³C NMR

UDCA-HDAC6i#7

UDCA-HDAC6i#8¹H NMR (CD₃)₂SO¹³C NMR

UDCA-HDAC6i#9¹H NMR (CD₃)₂SO¹³C NMR

UDCA-HDAC6i#10¹H NMR (CD₃)₂SO¹³C NMR

References

1. **Urribarri AD, Munoz-Garrido P**, Perugorria MJ, Erice O, Merino-Azpitarte M, Arbelaiz A, Lozano E, *et al.* Inhibition of metalloprotease hyperactivity in cystic cholangiocytes halts the development of polycystic liver diseases. *Gut* 2014;63:1658-1667.
2. Masyuk TV, Masyuk AI, Torres VE, Harris PC, Larusso NF. Octreotide inhibits hepatic cystogenesis in a rodent model of polycystic liver disease by reducing cholangiocyte adenosine 3',5'-cyclic monophosphate. *Gastroenterology* 2007;132:1104-1116.
3. Lozano E, Monte MJ, Briz O, Hernandez-Hernandez A, Banales JM, Marin JJ, Macias RI. Enhanced antitumour drug delivery to cholangiocarcinoma through the apical sodium-dependent bile acid transporter (ASBT). *J Control Release* 2015;216:93-102.
4. Al-Abdulla R, Lozano E, Macias RIR, Monte MJ, Briz O, O'Rourke CJ, Serrano MA, *et al.* Epigenetic events involved in organic cation transporter 1-dependent impaired response of hepatocellular carcinoma to sorafenib. *Br J Pharmacol* 2019;176:787-800.
5. Markwell MA, Haas SM, Bieber LL, Tolbert NE. A modification of the Lowry procedure to simplify protein determination in membrane and lipoprotein samples. *Anal Biochem* 1978;87:206-210.
6. Gradilone SA, Radtke BN, Bogert PS, Huang BQ, Gajdos GB, LaRusso NF. HDAC6 inhibition restores ciliary expression and decreases tumor growth. *Cancer Res* 2013;73:2259-2270.
7. Munoz-Garrido P, Marin JJ, Perugorria MJ, Urribarri AD, Erice O, Saez E, Uriz M, *et al.* Ursodeoxycholic Acid Inhibits Hepatic Cystogenesis in Experimental Models of Polycystic Liver Disease. *J Hepatol* 2015.